



National Library
of Canada

Bibliothèque nationale
du Canada

Canadian Theses Service

Service des thèses canadiennes

Ottawa, Canada
K1A 0N4

NOTICE

The quality of this microform is heavily dependent upon the quality of the original thesis submitted for microfilming. Every effort has been made to ensure the highest quality of reproduction possible.

If pages are missing, contact the university which granted the degree.

Some pages may have indistinct print especially if the original pages were typed with a poor typewriter ribbon or if the university sent us an inferior photocopy.

Reproduction in full or in part of this microform is governed by the Canadian Copyright Act, R.S.C. 1970, c. C-30, and subsequent amendments.

AVIS

La qualité de cette microforme dépend grandement de la qualité de la thèse soumise au microfilmage. Nous avons tout fait pour assurer une qualité supérieure de reproduction.

S'il manque des pages, veuillez communiquer avec l'université qui a conféré le grade.

La qualité d'impression de certaines pages peut laisser à désirer, surtout si les pages originales ont été dactylographiées à l'aide d'un ruban usé ou si l'université nous a fait parvenir une photocopie de qualité inférieure.

La reproduction, même partielle, de cette microforme est soumise à la Loi canadienne sur le droit d'auteur, SRC 1970, c. C-30, et ses amendements subséquents.

An NMR Study of the Aggregation
and Alkylation Reactions
of Some Lithiated Imines

by

Philip A. Carson

Submitted in partial fulfilment
of the requirements for the degree of
Doctor of Philosophy
in the Department of Chemistry

Faculty of Graduate Studies
University of Ottawa



Philip A. Carson, Ottawa, Canada, 1990



National Library
of Canada

Bibliothèque nationale
du Canada

Canadian Theses Service Service des thèses canadiennes

Ottawa, Canada
K1A 0N4

The author has granted an irrevocable non-exclusive licence allowing the National Library of Canada to reproduce, loan, distribute or sell copies of his/her thesis by any means and in any form or format, making this thesis available to interested persons.

L'auteur a accordé une licence irrévocable et non exclusive permettant à la Bibliothèque nationale du Canada de reproduire, prêter, distribuer ou vendre des copies de sa thèse de quelque manière et sous quelque forme que ce soit pour mettre des exemplaires de cette thèse à la disposition des personnes intéressées.

The author retains ownership of the copyright in his/her thesis. Neither the thesis nor substantial extracts from it may be printed or otherwise reproduced without his/her permission.

L'auteur conserve la propriété du droit d'auteur qui protège sa thèse. Ni la thèse ni des extraits substantiels de celle-ci ne doivent être imprimés ou autrement reproduits sans son autorisation.

ISBN 0-315-60027-6

Canada



UNIVERSITÉ D'OTTAWA
UNIVERSITY OF OTTAWA

For my parents.

Abstract

The solution structure of lithiated N-*iso*-propylacetaldimine, **1**, was determined by a variety of NMR methods. ^{15}N - ^6Li Doubly labelled samples of **1** allowed the determination of lithium-nitrogen connectivities on the basis of ^{15}N - ^6Li NMR coupling patterns. The lithiated imine was found to exist as a rapidly exchanging mixture of two isomeric dimers and a triple ion, whose relative proportions were sensitive to THF concentration, and which exhibited discrete ^{13}C and ^{15}N NMR signals at -90°C . The NMR signals for each of these nuclei were found to coalesce at higher temperatures. Under conditions of increasing THF concentration the triple ion was favoured. Addition of HMPA or PMDETA resulted in solutions containing only triple ions and monomers, but no dimers. The triple ion was found to be solvated by only one more molecule of THF than was the dimer, and HMPA and PMDETA were demonstrated to have the effect of displacing THF from coordination to the lithiated imine.

The choice of solvent, and by inference, the nature of the dominant solution structures, was found not to alter the predominant selectivity for alkylation to yield $>90\%$ *syn* products.

A structurally similar compound, lithiated N-*iso*-propylpropionaldimine, **3**, was found to exhibit coalescence behaviour in the ^{13}C spectrum similar to that observed for **1**. Upon addition of HMPA, however, an apparently new species was observed. ^1H NMR evidence suggested that this new species had *anti* stereochemistry. Alkylation of solutions of **3** containing HMPA were found to give *anti* products in the same proportion as the new species introduced upon addition of HMPA, while in the absence of HMPA there was 93% *syn* selectivity.

Acknowledgements

My greatest thanks goes to my wife, Dee Brandes, for her inexhaustable support, encouragement and patience ♡xox .

During a portion of my Ph.D. research my supervisor, Professor Robert Fraser, was unavailable for consultation due to illness. That I was able to continue without his guidance does not mean that his advice was not needed, but rather is a testament to the quality of the advice he provided prior to his illness. I am grateful to Professor Fraser for his guidance and especially for the great interest in my thesis and effort to help me that he has shown over the past year. In the end, the most important comment is to simply say that I learned a great deal from Professor Fraser.

Thanks are due to Dr. Heather Dettman, Prof. Christian Detellier and Mr. Raj Capoor for lending their NMR expertise, and to Professor Edgar Anderson, Imperial College, London (UK), for his helpful comments.

Thanks are also due to NSERC for funding of this research and to the Department of Chemistry support staff, without whose willing assistance little can be accomplished.

Table of Contents

Certificate of Examination	ii
Abstract	iii
Acknowledgements	iv
Table of Contents	v
List of Tables	viii
List of Figures	ix
List of Abbreviations	xi
Claims to Original Research	xii
Chapter 1: Introduction	
1.1 An Overview	1
1.2 Aggregation of Lithiated Organo-nitrogen Compounds	3
1.3 The <i>Syn</i> -Effect	10
1.4 The Origin of the <i>Syn</i> -Effect	14
1.5 Purpose	18
1.6 Selected NMR Methods.....	19
Chapter 2: Results and Discussion	
2.1.1 Lithiated N- <i>iso</i> -propylacetaldimine (1): General Observations and Effect of Temperature	26

2.1.2	Exchange Phenomena.....	35
2.1.3	Is this an Aggregation Phenomenon? Effect of Mixed Lithiated Imines.....	38
2.1.4	Effect of Solvent and Concentration on 1.....	42
2.1.5	Effect of Strongly Coordinating Ligands on 1: Displacement of THF.....	47
2.1.6	Effect of PMDETA on 1: New Species.....	52
2.1.7	Effect of HMPA on 1: New Species.....	55
2.1.8	Is Di- <i>iso</i> -propylamine Coordinated to 1?.....	58
2.1.9	¹³ C T ₁ Measurements of 1a, 1c and 1d: Relative Sizes of these Species.....	59
2.1.10	¹⁵ N and ⁶ Li Double Labelling: Lithium-Nitrogen Connectivities in 1.....	63
2.1.11	Molecular Mechanics Calculations	78
2.1.12	Models for Inter-Aggregate Exchange.....	80
2.1.13	Alkylation Products of 1.....	84
2.2.1	Lithiated N- <i>iso</i> -propylpropionaldimine (3) : General Observations and Effect of Temperature	89
2.2.2	Lithiated N- <i>iso</i> -propylpropionaldimine (3) : Effect of HMPA	89
2.2.3	Alkylation Products of 3	96
2.3.1	Determination of <i>Syn/Anti</i> Stereochemistry	99
2.4.1	Effect of a Chelating Bis-Phosphine Oxide on 1.....	101

Chapter 3	Conclusions	
3.1	General Conclusions	104
3.2	Comparisons to Similar Molecules in the Literature.....	105
3.3	Solution Structures <i>vis a vis</i> the <i>Syn</i> -Effect.....	107
3.4	Proposals for Further Research.....	109
Chapter 4	Experimental	
4.1	General Procedures and Materials	110
4.2	Imine Synthesis	110
4.3	Preparation of Lithiated Imine NMR Samples	113
4.4	Preparation of ¹⁵ N/ ⁶ Li Doubly Labelled 1	114
4.5	Alkylation Reactions	116
4.6	General NMR Methods	116
4.7	Synthesis of "NIPA" Ligand	120
References		124
Vita		136

List of Tables

Table 1	^{13}C NMR shifts for 1-H and 1	26
Table 2	^{13}C NMR coalescence behaviour of 1	27
Table 3	Temperature dependent behaviour of 1	29
Table 4	Effect of [THF] on 1	46
Table 5	T_1 and NOE data for 1 at -80°C	60
Table 6	Models for aggregation and solvation	83
Table 7	Alkylation product <i>syn/anti</i> ratio for 1	87
Table 8	Effect of HMPA on the ratio of 3-E:3-Z	94
Table 9	Alkylation product <i>syn/anti</i> ratio for 3	98
Table 10	^1H and ^{13}C NMR Data for imines.....	112
Table 11	NMR Acquisition parameters	117

List of Figures

Figure 1	Lithiation of aldimines	2
Figure 2	Typical structural types of Li-N aggregates	6
Figure 3	HMPA as a bridging ligand	7
Figure 4	Literature examples of some lithiated imines	10
Figure 5	Structures isoelectronic to lithiated imines	16
Figure 6	Homoaromatic explanation of <i>syn</i> -effect	16
Figure 7	$n \rightarrow \sigma^*$ Interactions	17
Figure 8	The NOE effect	23
Figure 9	Variable temperature ^{13}C spectra of 1	28
Figure 10	^{13}C spectra of 1 at -60°C to -90°C (formyl carbon)...	30
Figure 11	Structures of species 1a , 1c and 1d	31
Figure 12	^1H spectrum of 1	33
Figure 13	^1H spectra of 1 : Coalescence of formyl proton.....	34
Figure 14	Mixed lithiated imines experiment.....	40
Figure 15	Effect of [THF] on 1	44
Figure 16	Plot of $1/T_1$ of THF vs. [HMPA] and [PMDETA].....	49
Figure 17	Plot of $1/T_1$ of THF vs. [HMPA] and 3X[PMDETA].....	51
Figure 18	Effect of PMDETA on 1	53
Figure 19	Effect of HMPA on 1	56
Figure 20	^{15}N - ^6Li - 1 in toluene/pentane with 2 eq. THF.....	65

Figure 21	Curve-fitting of ^{15}N spectra	67
Figure 22	Possible nitrogen-lithium connectivities	69
Figure 23	Possible isomeric trimers	70
Figure 24	<i>Trans</i> and <i>cis</i> dimers of 1	70
Figure 25	^{15}N - ^6Li - 1 in toluene/pentane with 4 eq. HMPA.....	72
Figure 26	Curve-fitting of ^6Li spectra	73
Figure 27	Triple ion and monomer of 1	73
Figure 28	^{15}N - ^6Li - 1 in toluene/pentane with 2 eq. THF and 1 eq. PMDETA	76
Figure 29	Optimal geometries for MM2 calculations	79
Figure 30	^{13}C NMR spectra of 3	90
Figure 31	^1H NMR spectra of 3 : Effect of HMPA	92
Figure 32	^1H - ^1H couplings for 3 : <i>E</i> and <i>Z</i> stereochemistry	93
Figure 33	Lithiated N-cyclohexylpropionaldimine: <i>Z-anti</i> and <i>E-syn</i> isomers	95
Figure 34	Possible origins of NOE-effect in 2	100
Figure 35	Apparatus for aldimine preparation	111

List of Abbreviations

1	Lithiated N- <i>iso</i> -propylacetaldimine
1-H	N- <i>iso</i> -propylacetaldimine
2	Lithiated N- <i>iso</i> -propylpropionaldimine
2-H	N- <i>iso</i> -propylpropionaldimine
3	Lithiated N- <i>tert</i> -butylacetaldimine
3-H	N- <i>tert</i> -butylacetaldimine
DIPA	Di- <i>iso</i> -propylamine
HMPA	Hexamethylphosphoramide
LDA	Lithium di- <i>iso</i> -propylamide
NIPA	Nonamethylimidodiphosphoramidate
NMR	Nuclear Magnetic Resonance
NOE	Nuclear Overhauser Effect
PMDETA	N,N,N',N'',N'''-Pentamethyldiethylenetriamine
T ₁	Spin-lattice relaxation time
THF	Tetrahydrofuran
TMEDA	N,N,N',N'-Tetramethylethylenediamine

Claims to Original Research

- 1) The structures attributable to signals observed in low temperature NMR spectra of THF solutions of lithiated N-*iso*-propylacetaldimine were established, primarily using ^6Li - ^{15}N doubly labelled samples. These results correct a previous claim in the literature.
- 2) The aforementioned lithiated imine was found to exist as a mixture of about 30% of each of two stereoisomeric dimers and 40% of a triple ion in 0.67 M THF/hexanes solutions at -80°C .
- 3) The relative proportions of each of the three species was found to be influenced by concentration, temperature, THF concentration and by additives such as HMPA or PMDETA which are known to coordinate strongly to lithium.
- 4) ^{13}C relaxation time were used as a tool for determining relative molecular sizes, and the results were consistent with the structural determinations.
- 5) Changes in the medium, and hence changes in the proportions of the various aggregate forms were found not to affect the proportion of *syn* methylation products.
- 6) NOE Difference measurements indicated the presence of an unknown, but substantial amount of the *anti* isomer of lithiated N-*tert*butylacetaldimine in THF solutions, providing firm support for previously published suggestions of such stereochemistry.

Chapter 1: Introduction

1.1 An Overview

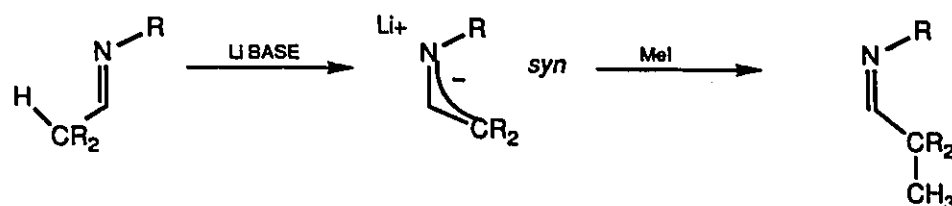
During the rise of carbanion chemistry to a position as the predominant general synthetic approach to carbon-carbon bond formation, enolate chemistry has maintained a leading role. Concurrent with the refinement of enolate chemistry has been the development of "enolate equivalents"¹⁻³, which can lend new reactivity and selectivity to the already versatile enolate. Among these enolate equivalents is a family derived from deprotonation of ketone and aldehyde equivalents, which include imines, N,N-dialkylhydrazones, oximes and oxime ethers and the structurally related nitrosamines^{2,4}.

When an unsymmetrical ketone is deprotonated, the kinetically favoured enolate tends to be that formed by deprotonation at the less substituted position, while the thermodynamically more stable enolate tends to be that which possesses the more substituted C-C partial double bond⁴⁻⁶. Imines and related C=N containing molecules, as ketone equivalents, offer the possibility of different regioselectivity and stereoselectivity in the kinetic and thermodynamic product of deprotonation, (also termed "lithiation" if a lithium base is used for deprotonation) and subsequent alkylation⁴.

Most aldimines and ketimines have a thermodynamic preference for the *anti* geometry, and *syn* imines readily isomerize

at room temperature to adopt the less hindered *anti* geometry⁷. The initial product of alkylation of the anion formed by deprotonation α to the C=N double bond of an aldimine has the more hindered *syn* geometry⁷ (Figure 1).

Figure 1: *Syn* lithiation and alkylation of aldimines



In the kinetic deprotonation of symmetrical ketimines where there are two possible sites for deprotonation there is often little regioselectivity in proton abstraction *syn* or *anti* to the alkyl group on nitrogen⁸⁻¹⁰, but the more stable anion at equilibrium tends to be the less substituted one and always has a *syn* stereochemistry. Alkylation always yields initially a product in which the substituent on nitrogen is *syn* to the newly introduced alkyl group^{7,11}. In ketimines this can allow for regioselective alkylation opposite to that obtained via alkylation of the thermodynamically more stable of the two possible ketone enolates. Should the substituent on nitrogen be an optically active chiral auxiliary, optical activity in the product may be induced^{1,2,12}, a result which would not be possible for lithium enolates of ketones or aldehydes.

This apparent preference for the more hindered *syn* geometry about the carbon-nitrogen partial double bond has been dubbed the "*syn-effect*". The terms *syn* and *anti* refer to geometries in which

the carbon atom through which the substituent on nitrogen is bonded lies in the plane of the "aza-allylic" portion of the molecule. The origin of the *syn*-effect and the synthetic opportunities presented by the behaviour of lithiated imines have both served as foci for research efforts.

Enolate chemistry provides an example of how knowledge of solution structures can provide new perspectives on the understanding of patterns of reactivity. Seebach et al. and Dunitz et al. determined the crystal structure of a lithium enolate which afforded insight into reactivity patterns^{13,14}. Similarly, Jackman and Lange studied the effect of changing the coordinating ability of solvents on the ratio of carbon versus oxygen methylation of lithio *iso*-butyrophenone and concluded that aggregate structure was a determining factor in the regioselectivity of the reaction¹⁵.

Until recently the exact nature of the lithiated imine prior to alkylation has not been investigated; nor has the origin of the *syn*-effect been satisfactorily and conclusively established. In the research reported herein the solution structure of a lithiated N-alkyl aldimine will be explored, with an expectation that this may eventually serve as a foundation for further investigations into the origin of the *syn*-effect or for improvement of synthetic approaches.

1.2 Aggregation of Lithiated Organo-nitrogen Molecules.

Many organolithium compounds have been prepared and studied, including alkyllithiums¹⁵⁻²⁸, lithium enolates²⁹⁻³³,

lithium amides^{30,34-38}, lithium anilides^{39,40}, lithiated imines⁴¹⁻⁴³, lithiated aromatics⁴⁴⁻⁴⁸, lithiated sulfones²⁰ and others^{20,35,45,49-63}. It is the rule, rather than the exception, that organolithiums form aggregates. In all probability lithiated aldimines would be expected also to exhibit aggregation behaviour, since there is no reason to expect them to behave differently from the majority of other organolithium compounds.

Organolithiums are known to form a variety of oligomers in solution, ranging from dimers to nonamers, and often in solution exist as mixtures undergoing rapid exchange^{16-19,21,24,26,29,31,35-37,40,53,57,64,65}. It has been found that the position of the equilibrium among interconverting species can be dramatically influenced by variations in solvent^{16,17,27,33,53}, concentration^{24,53} and temperature^{17,24-26,53}. Several trends are evident. For a given organolithium, higher oligomers are favoured in non-polar, hydrocarbon solvents and lower aggregates tend to be favoured in media containing polar, donor solvents³¹ such as ethers^{16,17,27,31}, hexamethylphosphoramide (HMPA)⁴⁰ or amines^{16,21,27} and by decreased concentration^{16,19,66}. The degree of aggregation can also be affected by the steric bulk of the lithiated molecule and by internal chelation of the lithium^{47,20}.

An investigation of the solution structure of a lithiated N-alkyl acetalimine should begin with a review of the structures of other lithiated organo-nitrogen molecules, such as amido lithiums, imido lithiums, species formed upon lithiation of carbazoles, pyrazines and disilazanes, and of course, the solution structures of other lithiated imines and lithiated hydrazones.

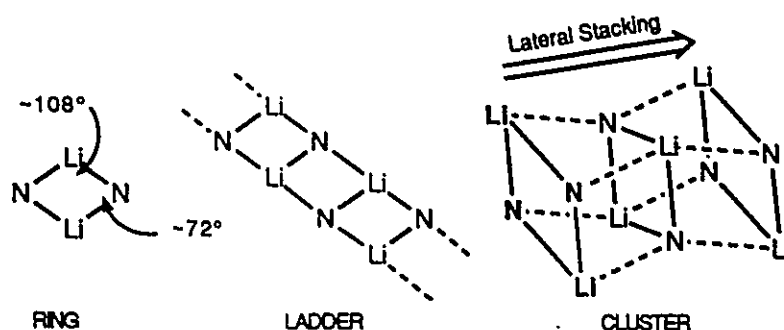
In many cases, NMR has proven to be one of the most valuable tools for investigation of solution structures, while X-ray crystallography has been the obvious choice for solids.

X-Ray crystal structures of lithiated organo-nitrogen molecules have been published on a regular basis by Snaith and co-workers in Scotland. They, and others, have found that a large variety of amido and imido lithiums crystallize as hexamers^{35,51}, tetramers^{35,59}, trimers^{34,35,67} and dimers^{35,36,52,56-58,60,61,68-70}. Only when crystallized as adducts with coordinating solvents such as diethyl ether^{35,56,70}, HMPA^{35,62}, N,N,N',N'-tetramethylethylenediamine (TMEDA)⁵⁸, N,N,N',N'',N''-penta-methyldiethylenetriamine (PMDETA)³⁴ or pyridine³⁵ were dimers or monomers found, but these solvents do not always cause low states of aggregation: diphenylimido lithium crystallizes as a tetrameric 1:1 adduct with pyridine⁵⁹ and as a hexamer with HMPA⁵¹ and pyrrolidino-lithium crystallizes as a trimer in the presence of PMDETA⁶⁷. The groups of Lappert, Seebach, Boche and Schleyer have also reported crystal structures of an lithium amidosilazane⁵², a lithio pyrazine⁵⁷, a lithium imide⁵⁸, and a lithio carbazole⁷⁰, respectively, and found structures generally consistent with the trends found by Snaith and coworkers. (The nomenclature is inconsistent in the literature; for example, a lithio amide is the same as an amido lithium, but IUPAC nomenclature favours the latter format.)

Common to all of these lithiated organo-nitrogen crystal structures is a framework of alternating lithium and nitrogen atoms (Figure 2). In dimers there is always a planar Li-N-Li-N ring

structure^{35,52,57,58,61,69-71}, where usually the angle at lithium is in the range of $108\pm 4^\circ$ and the angle at nitrogen is closer to $72\pm 4^\circ$. Higher aggregates may have a lithium-nitrogen framework of a form best described as a "ladder"^{35,72,73}, composed of an extension of the dimeric-type planar rhomboid structures, or a framework like one of a variety of cluster-like structures usually consisting of stacked Li-N rhomboids^{35,72,73}.

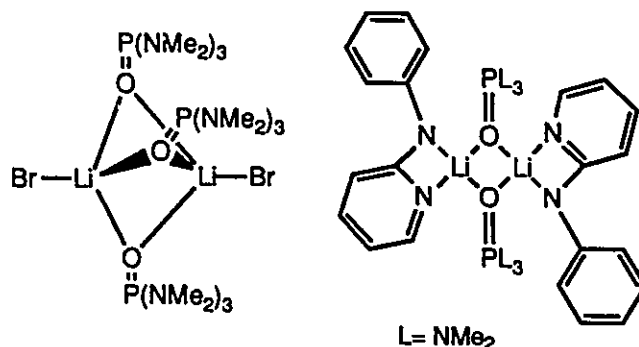
Figure 2: Typical structural types for Li-N aggregates



In solution chemistry, HMPA has traditionally been viewed as a solvent which breaks up aggregates^{74,75} by strongly coordinating (via the oxygen atom) to lithium and solvating lithium better than it can be solvated internally by the organic anion. This conventional interpretation is generally substantiated by the crystal structures of lithiated organo-nitrogen compounds, in that the HMPA adducts are often lower order oligomers, such as dimers, in which HMPA is coordinated to lithium. Interestingly, the HMPA adduct with lithio diphenylimide⁵¹ serves as an example of this model, while also

illustrating some of the dangers of reliance on "conventional wisdom". This adduct has been found to have the formula $[\text{Li}\cdot 4\text{HMPA}]^+ [(\text{N}=\text{CPh}_2)_6\text{Li}_5\cdot 3\text{HMPA}]^-$, in which HMPA has succeeded in strongly solvating and stripping away a single lithium atom, and yet the species remains a hexamer. Thus the model in which HMPA is able to strongly coordinate to lithium is supported, but the expected conversion into lower order aggregates was not observed. Two crystal structures have also been reported in which HMPA serves as a bridging ligand through oxygen, where four-membered Li-O-Li-O rings are formed within a dimeric species^{62,76} (Figure 3).

Figure 3: HMPA as a bridging ligand



Snaith and coworkers have suggested that the N-Li bonds are ionic in character and that the tendency to aggregate is dominated by the need of the lithium ion to be strongly solvated and that aggregation into polymers is prevented, only by the steric requirements of the organic moieties attached to nitrogen^{72,73,76-78}. Indeed, one of the few monomeric organolithium molecules yet discovered is the highly hindered lithio 2,4,6,tri-*tert*-butylbenzene⁴⁷ crystallized as a diamine solvate,

although the equally hindered lithium tri-*tert*-butyl-aniline crystallized as a dimeric etherate⁷⁸.

Only when chelating ligands are used have monomeric lithiated organo-nitrogen species been identified in the solid. Among the chelating ligands reported to favour monomeric species are TMEDA³⁴, a bidentate ligand, and its tridentate homologue, PMDETA³⁴ and also N,N,N',N'-tetramethyl-1,3-propanediamine⁴⁷. As with HMPA, the deaggregating effect is not universal, in that dimeric and tetrameric TMEDA adducts have been reported⁵⁸. The success, relative to HMPA, of these ligands in forming monomers may lie in their multidentate character, and their comparatively small steric bulk, since lithium may be reluctant to coordinate with more than one ligand as large as HMPA⁷⁵. Theoretical calculations have shown that amide coordination to the metal cation results in a strong thermodynamic stabilization of the ion pair (Li-N bonding is ionic in character) due to an electrostatic field effect⁷⁹.

Although comparisons between crystal and solution structures must always be made with caution, the crystal structures described above serve to illustrate the variety of structural types possible for lithiated organo-nitrogen molecules, and to illustrate the ubiquitous planar Li-N-Li-N ring in dimeric aggregates.

The crystal and solution structures of a variety of lithiated hydrazones, amides, anilides and imines have also been studied. These studies have a greater relevance to the study of the lithiated imine reported herein than the crystal structures discussed above, since in most cases they involve solutions of lithiated organo-nitrogen compounds, and because, like lithiated N-alkyl-

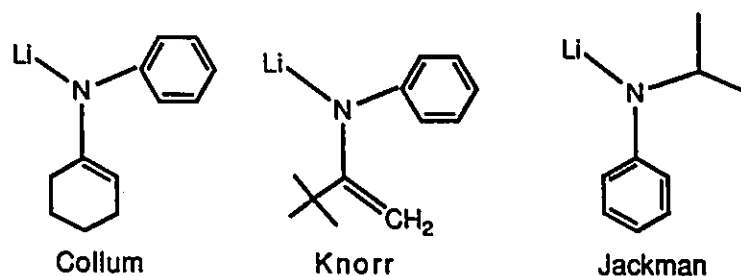
acetaldimines, they all have two substituents on nitrogen. In this regard, because of the potential for internal chelation, perhaps lithiated hydrazones should be considered separately, except for their similarity to lithiated imines as enolate equivalents.

The studies of lithiated organo-nitrogen molecules in solution by Collum are perhaps the most comprehensive. Using NMR and cryoscopy for solution studies and comparing these results to X-ray crystal structures, Collum and co-workers have elucidated the solution structures of some lithium amides, lithiated imines and lithiated hydrazones. In THF, three lithium amides (cyclohexyl-*iso*-propyl³⁶, diphenyl³⁷ and di-*iso*-propyl³⁸) and lithiated cyclohexanone phenylimine⁴² were found to exist primarily as dimers possessing the Li-N-Li-N four-membered ring, with small amounts of a monomer which increased with increasing THF concentration. Similar results were reported by Seebach and Bauer, who found that dilute THF solutions of lithium di-*iso*-propylamide consisted of 5:1 mixture of monomer and dimer¹⁹, and by Jackman et al., who found that lithium N-*iso*-propylanilide existed as a dimer in diethylether solutions and that monomer and a triple ion were formed upon addition of HMPA⁴⁰. Lithiated hydrazones were also found to be aggregated, as tetramers in which lithium was also internally solvated by the β -nitrogen atom^{48,71}.

To date all of the lithiated imines whose structures have been elucidated have had a phenyl group bonded directly to the nitrogen. Specifically these molecules have been lithiated cyclohexanone N-phenylimine (Collum and Kallman)⁴², the lithiated N-phenylimine of methyl-*tert*-butylketone (pinacolone) [N-(2,2-dimethyl-1-methylene-

propyl)-N-lithio-benzen-amine] (Knorr et al.)⁴³, and lithium N-*iso*-propylanilide (Jackman et al.)⁴⁰, whose structure is very similar to that of a lithiated imine (Figure 4). All have been found to be predominantly dimers in ether solvents. Knorr found that his lithiated imine was a dimer in the solid, and that the lithium was η^3 coordinated by a lone pair on nitrogen and an adjacent 'double bond' from the benzene ring.

Figure 4: Literature examples of some lithiated imines



This raises the question as to whether the phenyl substituent is a determinant of solution aggregate structure in these lithiated imines. That question will be addressed in the work presented in this thesis, since the lithiated imine whose solution structure is the subject of this research possesses only aliphatic groups.

1.3 The *Syn* -Effect

The behaviour of some lithiated imines has been thoroughly studied, and some of the more important aspects are summarized here. By studying the deprotonation of N-alkyl imines of 3-pentanone labelled with ^{13}C at the *syn* methyl group, Bergbreiter, Newcomb and

coworkers have demonstrated that deprotonation of a symmetrical ketimine with lithium di-*iso*-propylamide (LDA) is not strongly regioselective with respect to the *syn* and *anti* positions but that selectivity for *anti* deprotonation increased with increasing bulk of the nitrogen substituent⁹. The thermally equilibrated anions were found to have *syn* geometry about the aza-allylic portion of the molecule (on the basis of the *syn* alkylation product). They also found that there was an isomerization about the C=N bond in the starting imines resulting from a reversible aldol-type attack of initially formed lithiated imine upon the neutral imines⁸. Bergbreiter, Newcomb et al.¹⁰, Jung and Shaw⁸⁰ and Fraser et al.⁸¹ also observed, independently, a lack of strong *syn/anti* regioselectivity in the initial site of deprotonation of unsymmetrically deuterium-labelled N,N-dialkylhydrazones with LDA. (Deprotonations with alkyllithiums instead of LDA may result in different regiochemistry in the deprotonation and subsequent alkylation of imines⁸².)

The strongest evidence for the *syn* stereochemistry of the lithiated imine comes from the stereochemistry of the alkylation products, in which the substituent on nitrogen is *syn* to the newly introduced group^{8,11,83}. It has been assumed on the basis of the *syn* stereochemistry of the product that the lithiated intermediate must have had *syn* geometry. This would seem to be a fairly reasonable assumption, since only the *syn* product is observed even though the *anti* product is thermodynamically more stable^{8,11,12,83}. In most of such cases the initially observed *syn* product isomerizes thermally to the *anti* isomer^{8,11,83}. (Various mechanisms for isomerizations

about C=N bonds have been proposed⁸⁴⁻⁸⁷, but a summary of them is beyond the scope of this discussion).

In fact, the evidence of predominantly *syn* geometry in the lithiated molecule provided by the *syn* stereochemistry of the product is not in itself compelling, since there are at least two other explanations for the formation of the less stable *syn* alkylation product. The first alternative explanation is that the lithiated molecules possess a geometry that is neither *syn* nor *anti*, but that the initially formed alkylation product has a lower energy pathway to the *syn* geometry than to the *anti*⁴³. Knorr's crystal structure of the lithiated N-phenyl imine of pinacolone⁴³ has shown that in at least that example the configuration about the aza-allylic moiety is neither *syn* nor *anti*, but in Knorr's report it was a solid structure and the lithiated imine was atypical, since it possessed a bulky *tert*-butyl group at the formyl carbon and a phenyl substituent on nitrogen, all of which could introduce an unusual bias to the stereochemistry. The second alternative explanation is that the anions possess genuine *syn* and *anti* geometries in rapid equilibrium but that there is a lower energy pathway to *syn* alkylation products.

Surprisingly, in most cases where alkylation of a lithiated imine or related molecule results in a product having a *syn* orientation of the newly introduced alkyl group with respect to the substituent on nitrogen, the *syn* geometry of the lithiated precursor has not been directly established. The most direct indication of *syn* geometry in the lithiated imine is based on the ¹³C NMR chemical shift difference upon lithiation of imines, where *syn* carbon atoms α to nitrogen were observed to have an upfield shift upon lithiation^{7,88}.

The magnitude of the thermodynamic preference for the *syn* geometry in lithiated imines is difficult to estimate since none of the *anti* isomer is observed in most cases. The only cases where the *anti* geometry is observed occurs in lithiated endocyclic ketimines^{8,9} where excessive ring strain would be introduced upon adoption of the *syn* geometry and is suspected in lithiated aldimines where the nitrogen bears a bulky *tert*-butyl substituent⁷. An attempt has been made to estimate the magnitude of the thermodynamic preference for the *syn* stereochemistry in lithiated imines¹¹. In typical cases where alkylation of a lithiated aldimine yields >96% of the *syn* product, as determined by NMR at -20°C, the *anti* isomer of the lithiated imine must be at least 1.2 kcal mole⁻¹ less stable. Assuming that the same steric factors are important in both the neutral and the lithiated imines, it appears that this relative instability occurs in spite of the 3.0 kcal mol⁻¹ preference for the *anti isomer* of the neutral imine. (NMR at 25°C reveals less than 0.5% *syn* isomer of the neutral imine). The sum of these two values leads to the conclusion that the *anti* isomer of the lithiated imine would be at least 4.2 kcal mole⁻¹ less stable than the *syn* isomer at 25°C.

There is one example of a lithiated imine in which the *syn* and *anti* isomers are reported to exist in equilibrium. According to Bergbreiter, Newcomb and coworkers, upon lithiation of N-cyclohexyl propionaldimines in the presence of HMPA up to 20% of the *anti* isomer was observed⁹⁰. The proportion of the *anti* isomer was dependent upon the concentration of HMPA and in the absence of HMPA only the *syn* isomer was observed. They suggested that the two isomers observed represented one species with an **E** configuration at

the partial carbon-carbon double bond and the more stable *syn* stereochemistry of the substituent on nitrogen and another species with a more stable *Z* configuration at the partial carbon-carbon double bond and the less stable *anti* stereochemistry of the nitrogen substituent. It may be suggested that the competing steric requirements of the N-cyclohexyl group and the methyl of the propyl chain in the *Z* isomer were responsible for destabilizing the *syn* isomer relative to the *anti* isomer. The role of HMPA was suggested to be one of catalyzing the isomerization, but a more reasonable explanation may be that HMPA affects the distribution of the two isomers at equilibrium. The role of HMPA remains unsatisfactorily explained and the *syn* and *anti* geometry of the lithiated imine is only inferred.

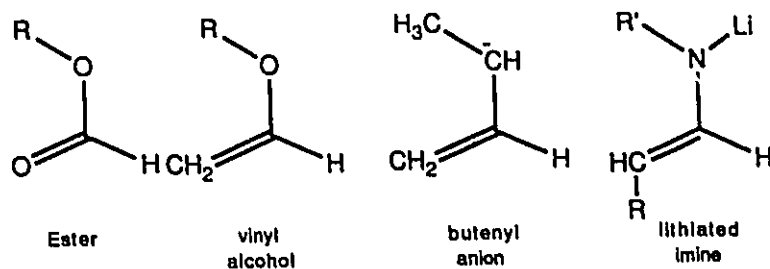
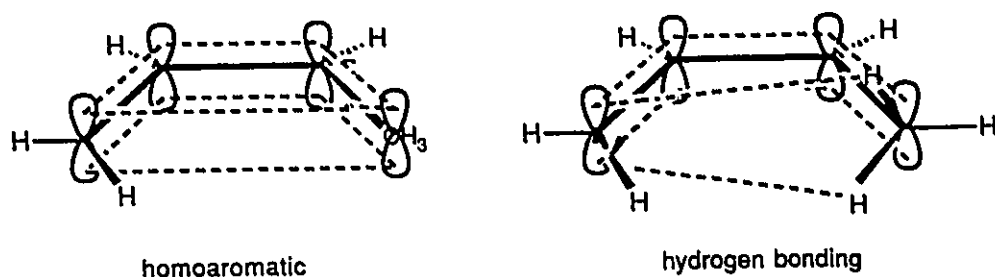
The origin of the *syn*-effect remains ambiguous, in part because of the experimental limitations imposed by the failure in most cases to observe the *syn* and *anti* isomers simultaneously, which would allow an examination of the factors affecting their equilibrium. This makes lithiated N-alkyl propionaldimines a potentially valuable tool for exploring the causes of the *syn*-effect. In the work reported here, the role of HMPA in the context of its effect on the aggregation and the *syn-anti* equilibrium of lithiated N-*iso*-propyl propionaldimine will be examined.

1.4 The Origin of the *Syn*-Effect.

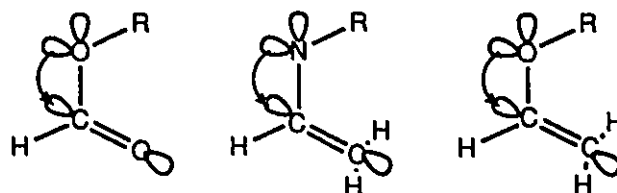
The origin of the *syn*-effect has been investigated extensively using theoretical and computational methods rather than chemical

experimentation. Analogous *syn* geometry has also been reported as preferred in vinyl ethers⁹¹, methyl formate esters⁹², and butenyl (allylic) anions⁹³, all of which are isoelectronic with lithiated imines (Figure 5). (Various nomenclature has been used to describe this geometry: *syn*, *endo*, *cis* and *Z*.) Each of these types of molecule has been the focus of molecular orbital calculations to determine the origin of this geometry. It is tempting to ascribe a common origin for all of these systems, but there is not even a consensus for any single system. These explanations serve as simple models to illustrate the various theories which have been used to explain lithiated imine stereochemistry.

For the allylic anion alone there have been three explanations for the observed 2 kcal mole⁻¹ preference for the *endo* (*Z*) configuration. Schleyer et al. have suggested that homoaromatic stabilization across the termini of the 4-atom system using a pseudo π -orbital at the methyl group is responsible for the effect⁹⁴ (Figure 6). They argue that in the anionic allylic system there are six ($4n+2$) π -electrons occupying the system, making it homoaromatic in the *endo* configuration. In the cation, however, there are only 4 π -electrons, making the *endo* configuration anti-aromatic, and therefore less stable than the *exo* configuration, in agreement with experimental observations. Schlosser and Hartman have suggested that hydrogen bonding between the protons of the methyl group (C-4) and the excess electron density at C-1 stabilizes the *endo* configuration⁹³ (Figure 6).

Figure 5: Structures isoelectronic to lithiated imines**Figure 6:** Homoaromatic and hydrogen-bonding explanations of the *syn*-effect

Bank et al. suggested that unfavourable interactions between the dipole moment of the methyl group and the negative charge of the allylic portion of the molecule in the *exo* configuration of the anion are removed by adopting an *endo* configuration⁹⁵. The stability of the *cis* conformation of formate esters has been studied computationally by Epiotis et al., who concluded that the source of stability of this geometry is an $n \rightarrow \sigma^*$ hyperconjugative interaction between the lone pair electrons on oxygen and the σ^* orbital of the C=O double bond⁹⁶ (Figure 7). The stability of the *cis* geometry in vinyl ethers may result from the same type of interaction⁹⁷.

Figure 7: $n \rightarrow \sigma^*$ interactions

Each of the above explanations may be applied to the aza-allylic anion formed upon deprotonation of enolate equivalents. In lithiated oximes, oxime ethers and N,N-dialkyl hydrazones chelation arguments have been invoked to explain the *syn*-effect⁹⁸. In these molecules interactions are also possible between the aza-allylic moiety and lone pairs on the hetero atom bonded to nitrogen in the molecules listed above, making the homoaromatic argument attractive. The chelation argument suggests that the metal ion (Li^+) is chelated between the aza-allylic portion and the heteroatom bonded to nitrogen^{48,55,61,71}. In lithiated imines, however, chelation is clearly impossible due to the lack of a suitable heteroatom adjacent to nitrogen.

Theoretical calculations by Houk, Fraser et al. led to the conclusion that origin of the *syn*-effect in lithiated imines may be the result of a dipolar interaction⁹⁹. These calculations suggested that the magnitude of the *syn*-effect in lithiated imines was too large to be the result of homoaromaticity involving a pseudo π -orbital at the N-alkyl group or from hydrogen bonding. It was also argued that in lithiated ketimines, $n \rightarrow \sigma^*$ interactions would require that the $\sigma^*_{\text{C-C}}$ orbital of the double bond be of significantly lower energy than the $\sigma^*_{\text{C-C}}$ orbital of the single bond, which according to others may be an

unreasonable assumption¹⁰⁰. Houk, Fraser et al. concluded that the *syn*- effect in lithiated imines was the result of a dipolar interaction in which the repulsion between the partial negative charge at the terminal carbon of the allylic system and the nitrogen lone pair is minimized in the *syn* configuration. Streitwieser et al. have recently reported that ab initio molecular orbital calculations reveal that the origin of the *syn* effect in oxime carbanions is electrostatic and that 1,4 -through-space conjugative interactions are insignificant¹⁰¹.

Another proposal can be made: that the *syn*-effect may be simply the result of steric interactions between a highly solvated lithium atom bonded to nitrogen and the substituents on C-3 which makes the *syn* configuration the less hindered one. The role of steric hindrance in the origin of the *syn*-effect can be evaluated only when the solution structures of lithiated imines are well characterized.

The above proposals are not mutually exclusive, and the *syn*-effect may be the result of several factors acting in concert.

1.5 Purpose.

In 1981 Fraser et al. reported that the low temperature ¹³C and ¹H NMR spectra of lithiated N-*iso*-propylacetaldimine exhibited two signals for each of the imine nuclei¹⁰², and that the barrier for interconversion of these two species was 12.5±.5 kcal mole⁻¹. Sound reasons were provided in support of an explanation of this exchange phenomenon as slow rotation of the *iso*-propyl group with respect to

the aza-allylic portion of the molecule. Since 1981 several reports have appeared in the literature in which similar low temperature NMR behaviour for other lithiated organo-nitrogen molecules has been observed and established to be the result of exchange among various aggregate structures^{16,17,20,23,24,26,36,37,40-43,53,64,103}. At the time of Fraser's 1981 paper no example was known of inter-aggregate exchange in organolithiums having a barrier as large as 12.5 kcal mole⁻¹^{26,28,31}. The research reported herein represents a re-investigation of the NMR behaviour and solution structure of lithiated *N-iso*-propylacetaldimine within the context of aggregation.

A further purpose of the research reported in this thesis is to elucidate the solution structure of lithiated *N-iso*-propylacetaldimine, to examine the effect, if any, of dominant solution structures on alkylation stereochemistry, and to examine the effect of additives on the aggregation behaviour and the alkylation stereochemistry of lithiated *N-iso*-propylpropionaldimine.

1.6 Selected NMR Methods.

A number of NMR techniques have been used in the study of the solution structures of lithiated aldimines, and the reader must have an elementary understanding of these techniques in order to fully appreciate the work presented in this thesis.

The study of lithiated *N-iso*-propylacetaldimine has as its starting point an observation of an unusual duplicity of signals for the lithiated imine carbon and hydrogen atoms in low-temperature

^{13}C and ^1H NMR spectra¹⁰². These two species were found to be interconverting via a two-site chemical exchange process, the origin of which will be elucidated in this thesis. The activation energy for this process was determined at the coalescence temperature.

The coalescence temperature, T_C , is the temperature at which the two signals observable at lower temperatures can be no longer resolved as discrete signals¹⁰⁴⁻¹⁰⁷. For coalescences of ^{13}C signals especially, the broadening of the signals near the coalescence temperature is often so extreme that the signal-to-noise ratio is so low that no signal can be seen at T_C unless a very large number of transients is acquired.

The barrier for interconversion between two equally populated sites can be calculated using this equation^{102,107,108}:

$$\Delta G^\ddagger = 4.57 \text{ cal mol K}^{-1} T_C \left[10.32 + \log_{10} \left[\frac{T_C}{2.22 \text{ Ks } \Delta\nu} \right] \right]$$

where T_C is the coalescence temperature ($^\circ\text{K}$), and $\Delta\nu$ is the frequency separating the two resonances at the coalescence temperature. Obviously, at the coalescence temperature one cannot determine the frequency difference between the two signals, so this difference must be estimated from the frequency differences at temperatures well below coalescence where the signals are well resolved.

For exchange between unequally populated sites the barrier calculated from the coalescence temperature represents a composite of the barriers for the forward and reverse reactions, which can be empirically calculated to be a weighted average of the barriers for the forward and reverse reactions¹⁰⁹. It should be noted that the

coalescence temperature provides a measure of the activation barrier only at that temperature.

Under appropriate conditions, T_1 relaxation times may provide information about molecular size^{29,31,107,110,111}, and thus it was proposed that the measurement of ^{13}C relaxation times for lithiated imine and solvent resonances would be a useful tool for the investigation of aggregates and solvation.

A measured T_1 is a composite of dipole-dipole relaxation and relaxation processes resulting from other influences, such as spin rotation, chemical shift anisotropy and scalar coupling. In the case of ^{13}C , relaxation is usually dominated by the dipole-dipole mechanism^{105,107,110}, although cases of contributions to the relaxation by spin rotation are common^{105,111}.

The lifetime of a species undergoing two-site chemical exchange with another species is $(1/k_{\text{exchange}})$ and the relaxation of each of the signals is characterized by its own T_1 . If the lifetime of the magnetic excited state is equal or greater than the time during which a species resides in a certain chemical state, or in other words, if the rate of chemical exchange is faster than the individual rates of dipole-dipole relaxation the observed relaxation rate will be averaged among all the exchanging species by the chemical exchange.

It has been established that, except for very small molecules, the nuclei of ^{13}C atoms bearing protons relax by dipole-dipole interactions, where the rate of relaxation, $1/T_1^{\text{DD}}$, is characterized by the equation^{31,110}:

$$\frac{1}{T_1^{\text{DD}}} = n \hbar^2 \gamma_H^2 \gamma_C^2 r^{-6} \tau_c$$

All terms except τ_c are constant: n = number of attached protons, γ =

gyromagnetic ratio, and r = C-H internuclear separation. The term τ_c is the correlation time for rotational reorientation, which is in turn characterized by equation (M):

$$\tau_c = \frac{V \eta}{kT}$$

V is the molecular volume and η is the viscosity of the medium. Thus it follows that T_1^{DD} is inversely proportional to viscosity, and more importantly, to molecular volume. This derivation uses the assumption that the molecule is spherical and much larger than the solvent. In more quantitative studies these relationships have been used to determine actual molecular volumes^{29,31}. In the work presented here relative volumes will be considered only qualitatively:

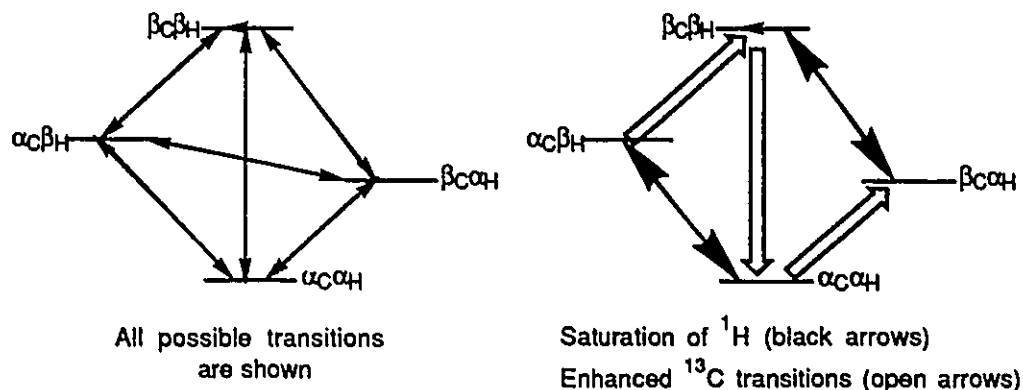
$$\frac{1}{T_1^{DD}} \propto V \eta$$

That the relaxation is dominated by dipole-dipole interactions, and therefore that T_1 is related to volume, can be established by measuring the nuclear Overhauser effect (NOE) of saturation of proton resonances on the carbon nuclei of interest: a full NOE proves that relaxation is in the extreme narrowing regime^{106,112}.

The nuclear Overhauser effect is a term describing the enhancement of signal intensities for one type of nucleus (ie. ^{13}C) induced through decoupling of another magnetically active nucleus (ie. ^1H) by means of radio-frequency saturation^{106,108,112}. For carbon atoms possessing directly bonded protons the most common means of relaxation of ^{13}C nuclei is via dipole-dipole interactions with its protons, to which the ^{13}C nuclei are coupled. For a simple case of a single ^{13}C nucleus bearing one proton there are four possible spin

states: $\alpha_C\alpha_H$, $\beta_C\alpha_H$, $\alpha_C\beta_H$ and $\beta_C\beta_H$, as illustrated schematically in Figure 8¹⁰⁶.

Figure 8: The nuclear Overhauser effect



In the scheme on the left in Figure 8 all possible transitions between states for absorption and release of energy are shown. Upon saturation with the proton frequency, populations of the levels are perturbed, causing greater population differences between the populations of the carbon spin states α_C and β_C , which results in enhanced absorptions for carbon and therefore more intense resonance signals. The magnitude of the enhancement is measured by comparing ^{13}C signal intensities between spectra acquired with proton decoupling (nuclear Overhauser enhanced) and with decoupling only during the F.I.D. acquisition (suppressed Overhauser).

Such enhancements due to the nuclear Overhauser effect for ^{13}C as the result of ^1H decoupling can have a maximum value of 2.988, meaning that the enhanced signal is 2.988 times more intense than the signal without an NOE. Throughout subsequent discussions the term NOE will refer the Nuclear Overhauser Effect, as defined

above.

A full NOE can be obtained only under conditions where the means of relaxation of the ^{13}C nuclei of interest is completely by dipole-dipole interactions with directly bound protons. The NOE measurement allows one to determine whether dipole-dipole relaxation dominates (extreme narrowing conditions), and therefore whether a correlation between T_1 and molecular volume is valid.

Proton-proton nuclear Overhauser effects can permit determination of close spatial relationships between ^1H atoms within a molecule^{113,114}. The method relies on the fact that, in dilute solutions, the relaxation of a ^1H nucleus is primarily via intra-molecular dipolar interactions¹⁰⁷. By perturbing the thermal equilibrium distribution of magnetic spin states at one proton (by saturation), neighbouring nuclei will have perturbations in their Boltzmann equilibrium distribution which result in an enhancement of the signal intensity for the second nucleus. In principle, the magnitude of these enhancements may be up to 50% and can permit quantitative determinations of internuclear distances, but in practice quantitative measurements are difficult and only qualitatively can internuclear spatial relationships be determined.

The NOE-difference experiment is the most common method of measuring a proton-proton nuclear Overhauser effect, for which two spectra are required. In one of the spectra, one set of protons of interest are saturated with a narrow, selective band of radio frequency irradiation during a pre-acquisition period prior to the radio frequency pulse in order to perturb the Boltzmann distributions. The

decoupler is turned off during the acquisition to allow for observation of coupling. The second spectrum is acquired with the decoupler set to a very distant frequency. The second spectrum is then subtracted from the first, resulting in a negative signal for the irradiated protons and a positive signal for any protons experiencing a nuclear Overhauser effect. Quantitative results are obtained from the integrals of these signals.

Chapter 2: Results and Discussion

2.1.1 Lithiated N-*iso*-propylacetaldimine: General Observations and Effect of Temperature.

A series of temperature dependent changes occurred in the ^{13}C NMR spectrum of lithiated N-*iso*-propylacetaldimine, **1**. A standard sample of **1**, [0.67 M in tetrahydrofuran/hexanes (1.8:1 by volume)], prepared by deprotonation of N-*iso*-propylacetaldimine, **1-H**, with LDA, was found to exhibit a sharp signal for each of the carbon atoms in its room temperature ^{13}C spectrum¹⁰². Except for the signal of the methyl carbons of the *iso*-propyl group, which was obscured by hexanes resonances, the signals of the anion were well resolved from other resonances. The anion NMR signals all had chemical shifts distinct from those of the initial imine, **1-H**, as listed in Table 1.

Table 1

^{13}C Chemical Shifts for **1-H** and **1**^a

<u>Carbon Atom</u>	<u>Parent Imine</u>	<u>Lithiated Imine</u>
<i>iso</i> -propyl methyl	25.5	obscured
<i>iso</i> -propyl methine	62.9	51.8
"Formyl"	157.5	154.1
Terminal methyl/ methylene	23.0	66.0

^a δ in ppm relative to THF (δ 69.0); 20°C

As the temperature was lowered each of the observable lithiated imine ^{13}C signals broadened, passed through a coalescence temperature and eventually became two signals¹⁰² (Figure 9). Excluding the aforementioned *iso*-propyl methyl carbon signals, all of the other carbon atoms gave two signals which could be readily observed, except for the downfield signal of the terminal methylene carbon, which, on the basis of its pattern of coalescence behaviour and its observation in solvents other than THF (*vide infra*), was determined to lie under the THF solvent peak at 69 ppm. The chemical shifts and coalescence temperatures are shown in Table 2.

Table 2
 ^{13}C NMR (75 MHz) Coalescence Behaviour of 1

<u>Carbon Atom</u>	<u>+20°C</u>	<u>-30°C</u>	<u>T_c</u>	<u>ΔHz</u>
formyl	154.1 ^a	158.0 152.0	$-7\pm 2^\circ\text{C}$	450 ± 5
methylene	66.0	69.8 ^b 63.0	— —	— —
methine	51.8	58.0 48.3	$10\pm 2^\circ\text{C}$ —	730 ± 5

^a δ ppm

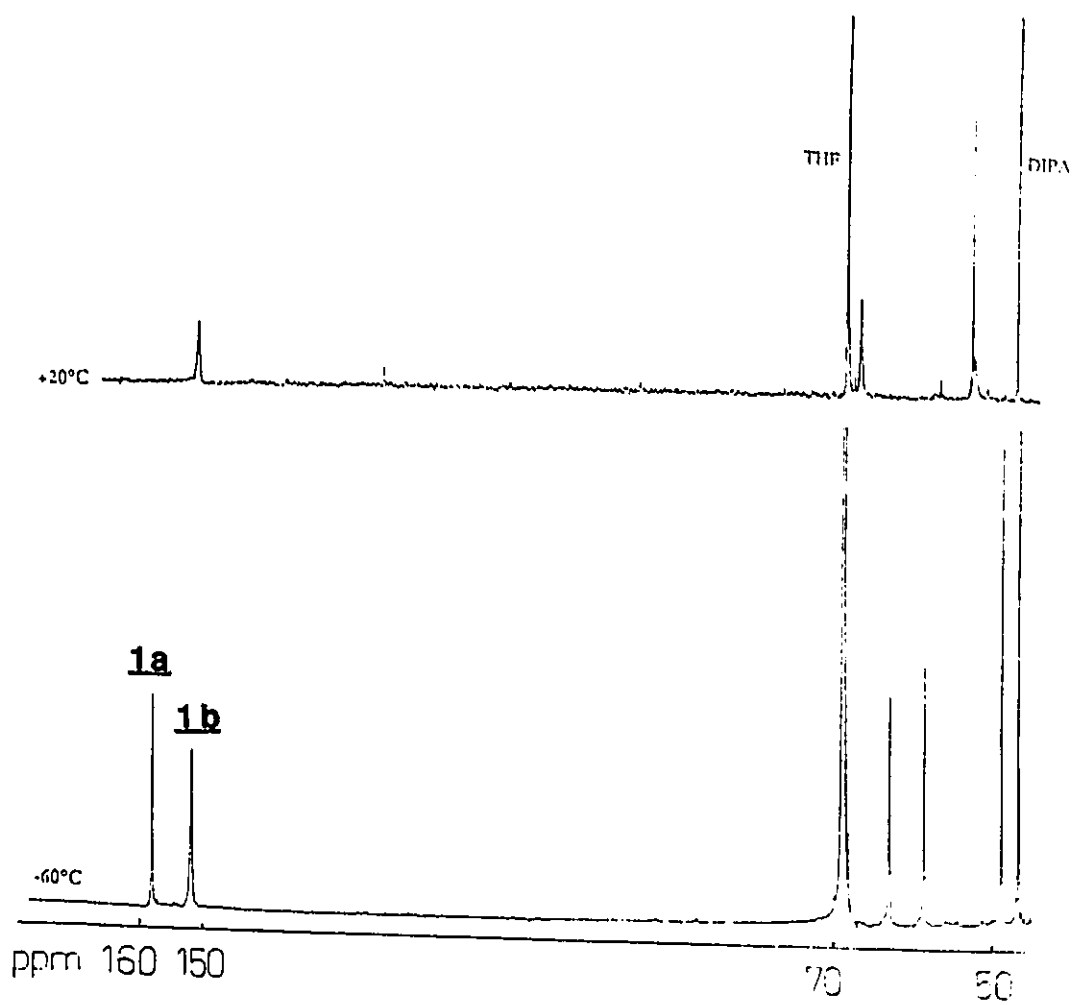
^b obscured by THF

The barrier to interconversion between 1a and 1b was determined from the coalescence temperature^{102,108} to be 12.5 ± 0.5 kcal mole⁻¹.

The resonances of the formyl carbon occupy an otherwise

Figure 9

^{13}C spectra of **1** at +20°C and -60°C (0.67 M in THF/hexanes).



vacant region of the spectrum (150-160 ppm), so subsequent attention and discussion will concentrate on the behaviour observed at the formyl carbon, although most behaviours were seen to be duplicated at the other carbon atoms.

At -30°C the ratio of the minor signal **1a** (formyl carbon: 158ppm) to the major signal **1b** (formyl carbon: 152 ppm) was 1:1.2 and the peaks remained broad. As the temperature was lowered further, to -60°C , the ratio of **1a** to **1b** changed to 1:1.5 and the signals sharpened further, although the upfield signal (**1b**) was broader than the downfield one (Table 3 and Figure 10).

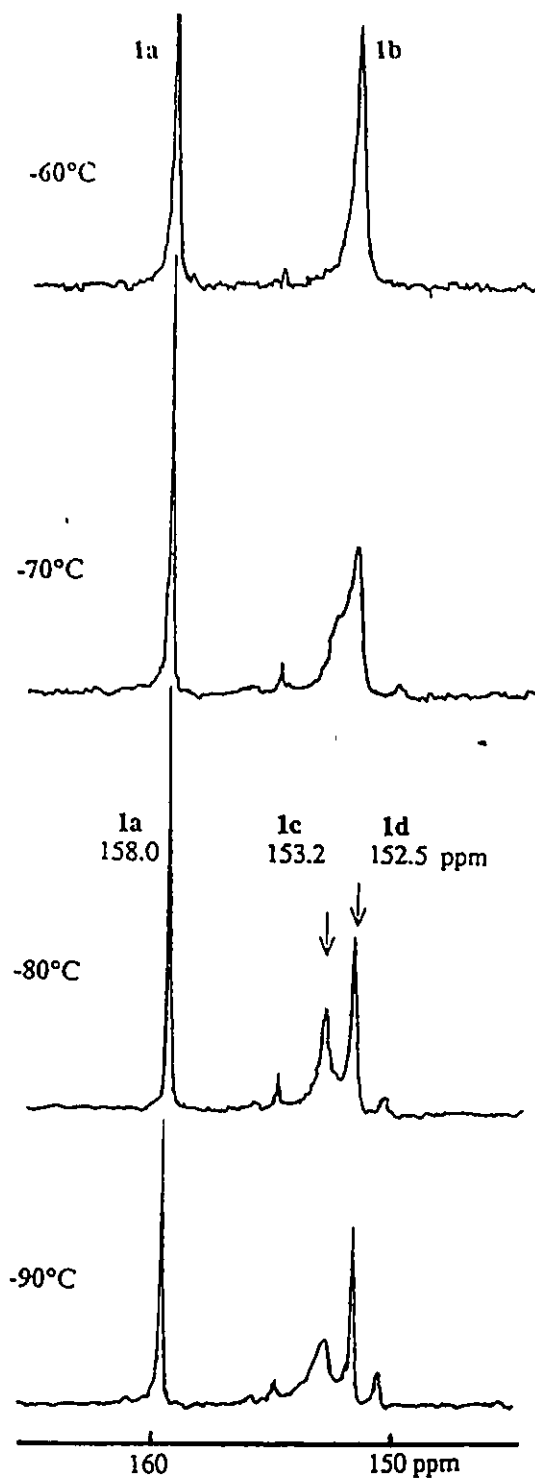
Table 3

Temperature dependence of 1		
<u>Temperature</u>		<u>1a:1b</u>
-20°C		1:1.1(\pm .1)
-30°C		1:1.2
-40°C		1:1.3
-50°C		1:1.4
-60°C		1:1.5
-70°C	(1b → 1c+1d)	1: (1.7)
-80°C	(1c+1d)	1: (1.8)

As the temperature was lowered further from -60°C another decoalescence was observed. The upfield signal (**1b**) separated into two signals at -80°C , while the downfield signal sharpened. The three signals at -80°C have chemical shifts of 158.0ppm (**1a**), 153.2 ppm (**1c**) and 152.5 ppm (**1d**) (Figure 10). (Smaller signals in the formyl region were not reproducible and may be impurities or minor species.)

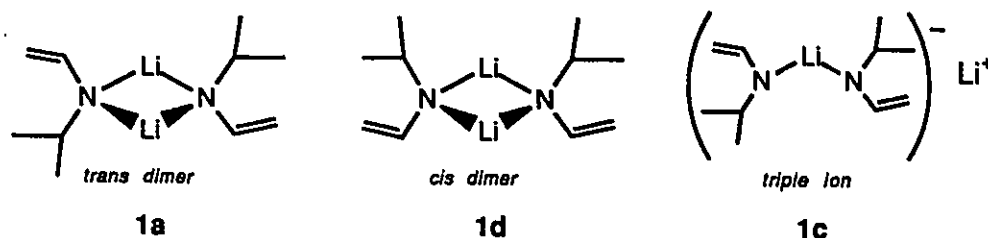
Figure 10

^{13}C spectra of 1 at -60°C to -90°C (formyl carbon).



Upon further cooling there was little further change except for a slight broadening of the signal **1c**. Since no further decoalescences were observed at accessible temperatures ($\geq -100^\circ\text{C}$) the working assumption was made that the three signals **1a**, **1c** and **1d** observed at -80°C represent three discrete species. For the benefit of the reader, at this point it will be revealed that the results of subsequent experiments will lead to the conclusion that **1a** and **1d** are a pair of stereoisomeric dimers and that **1c** is more highly solvated triple ion as illustrated in Figure 11. A large body of evidence leading to these conclusions will be presented first in order to build convincing support for this eventual conclusion (see section 2.1.10).

Figure 11: Structures assigned to species **1a**, **1c** and **1d**



The behaviour observed in the ^{13}C spectrum of **1** is mirrored in the ^1H spectrum (Figure 12). At 20°C the ^1H spectrum of the lithiated imine in THF(H_2O) solvent consisted of a doublet of doublets at $\delta 6.68$ ppm ($J_{\text{cis}}=7.8$ Hz, $J_{\text{trans}}=13.6$ Hz) for the formyl proton, a pair of doublets at $\delta 2.96$ ppm ($J_{\text{trans}}=13.6$ Hz) and $\delta 2.67$ ppm ($J_{\text{cis}}=7.8$ Hz) for the two methylene protons, and a multiplet at $\delta 3.1$ ppm and a doublet at $\delta 0.92$ ppm for the protons of the *iso*-propyl group. Superimposed on the lithiated imine spectrum is the solvent spectrum

and that of di-*iso*-propylamine. As the temperature was lowered all of the resonances of **1** broadened and passed through coalescence temperatures. The formyl proton had a coalescence temperature of $-23 \pm 3^\circ\text{C}$ and displayed two signals below this temperature, which both became resolved into doublets of doublets as the temperature was lowered to -40°C (Figure 13). The other protons either remained too broad below their coalescence temperatures to allow any meaningful description or interpretation or they lay under solvent or di-*iso*-propylamine peaks.

The coalescence temperature for the formyl proton was $-25 \pm 3^\circ\text{C}$, and the activation barrier for this exchange process was calculated to be $12.0 \pm 2 \text{ kcal mole}^{-1}$, the same value as reported previously by Fraser et al.¹⁰² and as measured in the ^{13}C and ^1H spectra.

The two signals observed for the formyl proton at low temperature have unequal integrals, and the ratio of the major (upfield) species to the minor is the same as that observed in the ^{13}C spectrum over the temperature range of -40°C to -60°C . The activation barrier was found to be the same, within the limits of uncertainty, for the exchange processes observed in the ^{13}C and ^1H NMR spectra. Furthermore, the signals for the major species in both the ^1H and ^{13}C spectra are much broader than the minor species. This correspondence of behaviour between the ^1H and ^{13}C spectra allows us to state that it is the same exchange phenomenon which can be observed in the NMR spectra of both nuclei. We can therefore assign the major and the minor species observed in the proton spectrum as **1b** and **1a** respectively.

Figure 12
 ^1H spectrum of 1.

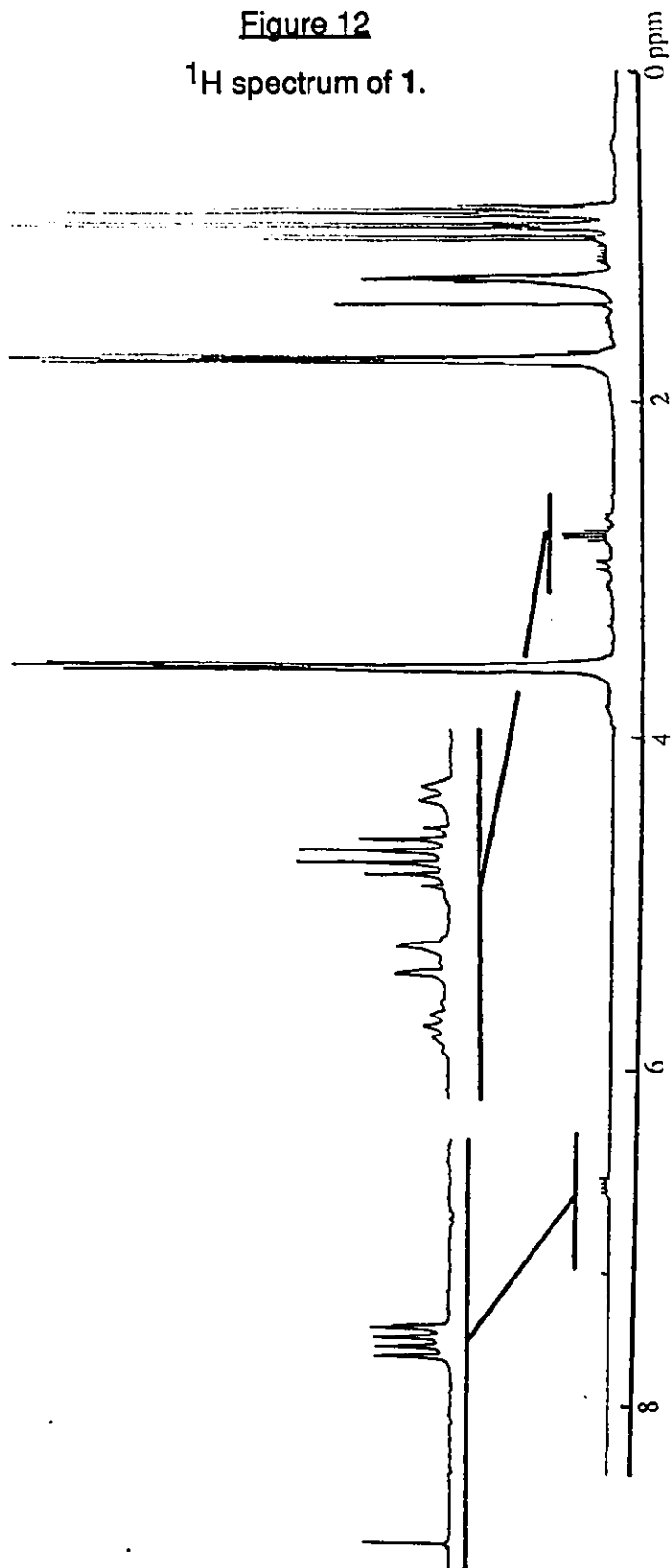
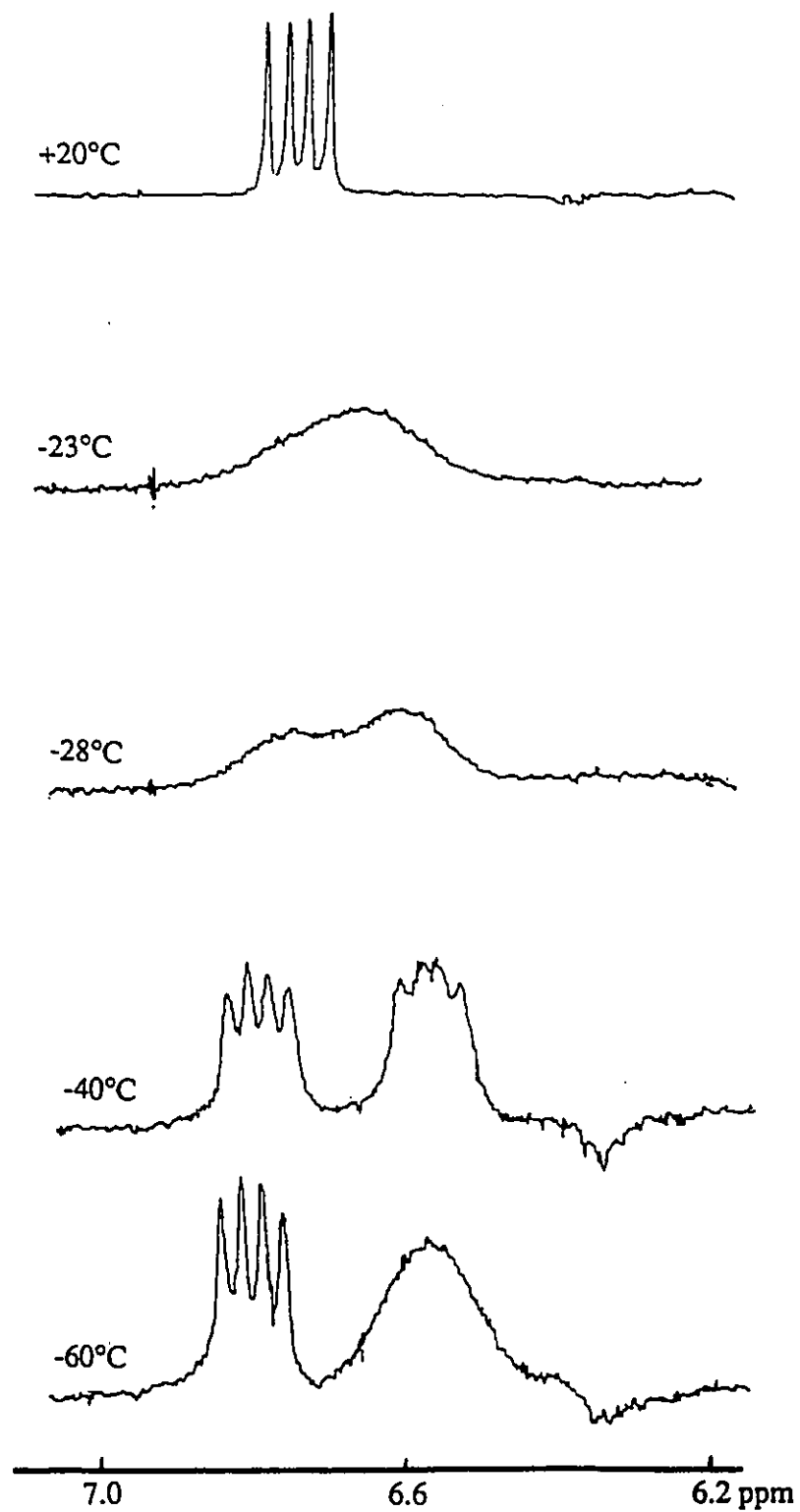


Figure 13

^1H spectra of 1- Coalescence of formyl proton.



Lithiated *N*-*iso*-propylacetaldimine was previously studied by Fraser et al. who used ^{13}C (20 MHz) and ^1H (100 MHz) NMR to study the temperature-dependent behaviour down to -60°C ¹⁰². The data reported above at temperatures $\geq -60^\circ\text{C}$ are a repeat and confirmation of the observations made by Fraser. The following experiments represent an attempt to unravel the origin of the low temperature NMR behaviour observed for **1**. Since greater detail is available from the ^{13}C spectrum than from the ^1H spectrum, most of the subsequent investigations were performed using ^{13}C NMR.

A temperature of -80°C was selected for most further experiments since at this temperature the ^{13}C NMR signals for species **1a**, **1c**, and **1c** are at their optimal resolution and because this is very close to the temperature of the dry-ice/acetone bath (-78°C) in which one usually performs alkylation reactions^{8,12,83,90,115}.

2.1.2 Exchange Phenomena

In the previous section the temperature dependent behaviour of lithiated *N*-*iso*-propylacetaldimine was described. In the ^{13}C NMR spectrum a coalescence of resonances for the formyl carbon was observed at -7°C (75MHz) and a second apparent coalescence was observed at $\sim -70^\circ\text{C}$.

For the higher temperature coalescence the barrier to interconversion between **1a** and **1b** was determined from the coalescence temperature to be 12.5 ± 0.5 kcal mole⁻¹. Since the ratio

of the two interconverting signals may not be 1:1 at the coalescence temperature (see Table 3), this activation barrier represents a weighted average of the barriers for the forward and reverse reactions¹⁰⁹.

The second apparent coalescence, between the two signals **1c** and **1d** and which occurs at -70°C , may result either from true chemical exchange or a fortuitous coincidence of temperature dependent chemical shifts at temperatures above -70°C . This concern arises due to the temperature dependence of the chemical shift of signal **1b** (152.0 ppm at -60°C), the unusual shape of the signal at the coalescence temperature (see Figure 11) and because the chemical shifts of **1c** (153.2 ppm) and **1d** (152.7 ppm) are not distributed on either side of 152.0 ppm as would be expected for a well-behaved coalescence behaviour. Should this behaviour be the result of chemical exchange, an activation barrier can be roughly calculated to be 10 ± 1 kcal mole⁻¹. This value is sufficiently close to the barrier calculated for the higher temperature coalescence to allow one to suggest that a similar chemical exchange process may be responsible for both the lower and higher temperature phenomena. The parallel temperature dependent behaviour observed in the ^{13}C and the ^1H NMR spectra may support the contention that it is a second exchange process which is responsible for the coalescence of signals for **1c** and **1d** in the ^{13}C spectrum. In both the ^{13}C and ^1H NMR spectra one exchange process is observed at a higher temperature and then a second seems to occur at lower temperatures, although in the ^1H spectrum it appears that the chemical shift difference between the two new species (**1c** and **1d**) is insufficient to be resolved at 300MHz.

There have been numerous reports in the literature of coalescence behaviour for lithiated organic molecules similar to the coalescence observed for **1**, and they have been variously interpreted as resulting from aggregation phenomena^{16,17,20,27,31,36,37,40,42,53,103}, rotamers^{102,103} and solvation states^{16,17,20,31,40,103}. When originally reported by Fraser in 1981, the higher temperature exchange process observed in NMR spectra of **1** was interpreted as slow rotation of the *iso*-propyl group¹⁰². This interpretation was based on studies of the effect of various substituents and on molecular orbital calculations. At that time there had been few reports^{26,28,31} of inter-aggregate exchange among various organolithium species which were slow enough to be observable by low-temperature NMR spectroscopy. Since 1981 there has been a steady flow of papers emanating from the laboratories of Seebach, Fraenkel, Jackman, Snaith, Collum, Thomas, and others, reporting observation by NMR of chemical exchange among organolithium aggregate structures^{16,17,24,25,27,29,31,35-37,40,42,47,53,64,103}.

The activation barriers reported for inter-aggregate exchange processes for alkyllithiums have ranged from 7 to 14 kcal mole⁻¹^{24,25,27,28,64}. The activation barriers reported here for the chemical exchange among species **1a**, **1c** and **1d** fall within this range, so it is entirely possible that the low-temperature NMR behaviour of lithiated *N-iso*-propylacetaldimine may also be due to inter-aggregate exchange. Researchers in the laboratories of Collum, Knorr and Jackman have independently obtained evidence for similar exchange phenomena for some other lithiated organo-nitrogen

compounds, and have all concluded these to be the result of interconversion of various aggregated structures but have never reported the magnitude of the barriers for interconversion^{36-41,43}. More specifically, Collum and Knorr and their colleagues, on the basis of their discoveries of interconverting dimeric lithiated organo-nitrogen molecules, have suggested that the observations reported by Fraser in 1981 should be reinvestigated in the context of aggregation^{41,43}. In the next section the involvement of aggregation of lithiated imine **1** as a factor in its low-temperature NMR behaviour will be examined.

2.1.3 Is this an Aggregation Phenomenon? Effect of Mixed Lithiated Imines.

The origin of the multiplicity of signals observed for the lithiated acetaldimine **1** may arise from a number of causes, among them hindered rotation about bonds^{102,103} or aggregation. It has been suggested by both Collum and Knorr that interconversion of various aggregated species may explain the exchange behaviour reported by Fraser for **1**^{41,43}.

In order to determine whether aggregation may play a role in the exchange process, an experiment was devised¹¹⁶ in which a mixture of two lithiated imines was prepared. The hypothesis was that if the ratio of the species **1a:1c:1d** was altered by the addition of another lithiated imine it could be said that intermolecular effects were responsible, most reasonably involving hetero-aggregation of the two different lithiated imines.

It was desirable to select as the second lithiated imine one which presented a simple ^{13}C spectrum, ideally a single peak at -80°C . Lithiated *N-tert*-butylacetaldimine, **2**, matched the ideal, since a single ^{13}C NMR signal was observed for the formyl carbon at -80°C and since this lone peak has a chemical shift (153.0 ppm) which is different from that of **1a**, **1c** or **1d**.

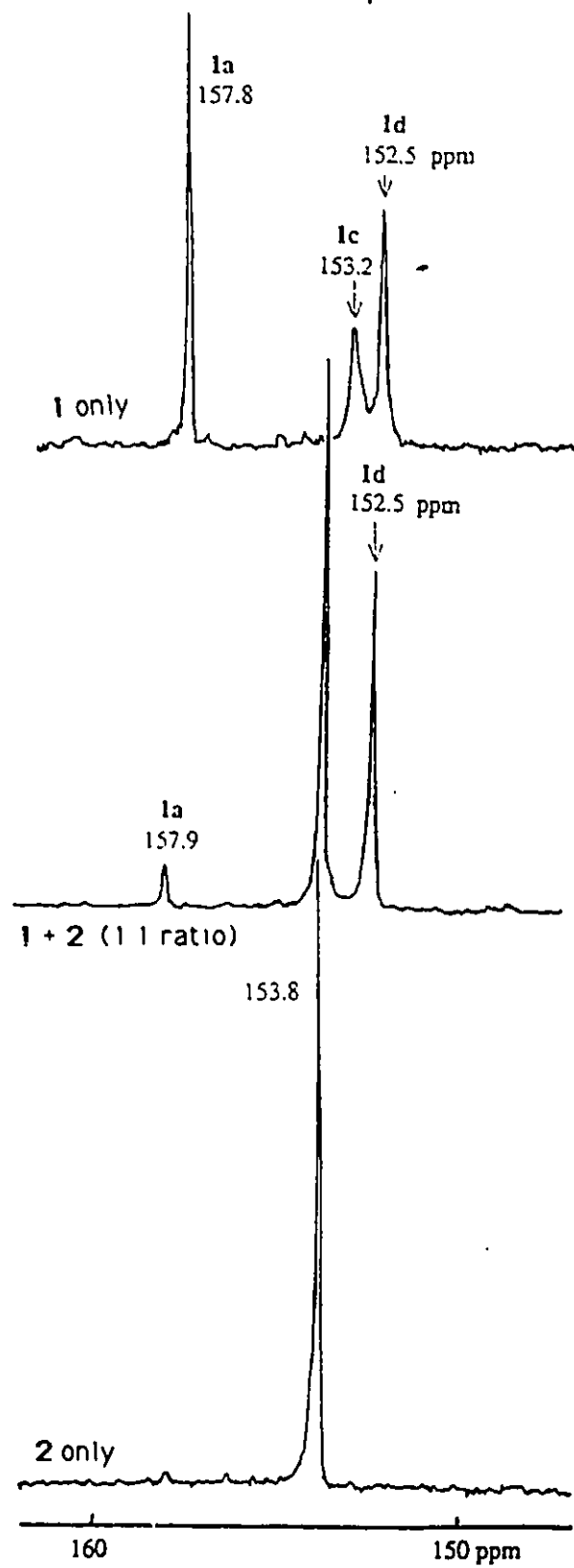
NMR samples of each of the pure lithiated imines **1** and **2** were prepared such that the two samples had equal volumes and concentration. The ^{13}C spectra of the individual imines were measured at -80°C and then the solution of **2** was transferred by cannulus to the NMR tube containing **1**. The ^{13}C NMR spectrum of this sample of mixed lithiated imines was then measured at -80°C . The initial spectra of **1** and **2** and the spectrum of the mixed lithiated imines are shown in Figure 14. The signal for **2** remained unchanged as a result of mixing, but the relative proportions of **1a**, **1c** and **1d** changed quite dramatically.

In the mixed lithiated imine sample the concentration of species **1c** was reduced below the limit of detection, and the ratio of **1a** to **1d** changed from 1:1 to 1:6.5. The ratio of **2** to the sum of all species **1** remained unchanged, so therefore the signal for **1c** is not hidden under the signal for **2**. The strong effect of **2** on the ratio of species observed for **1** can lead to at least three suggestions as to the nature of **1a**, **1c** and **1d**:

- 1) Species **1a**, **1c** and **1d** are all monomers possessing different degrees of solvation. If solvent coordinates much more strongly (or weakly) to **2** than to **1**, the more highly solvated (or poorly solvated) species arising from

Figure 14

Mixed lithiated imines experiment.



- 1 are strongly disfavoured.
- 2) Species **1a**, **1c** and **1d** are rotamers within a common or variable state of aggregation, and the formation of mixed aggregates with **2** disrupts the distribution of rotameric forms.
 - 3) Species **1a**, **1c** and **1d** have different states of aggregation, (but not necessarily different levels of aggregation: monomer, dimer, trimer etc.), whose relative proportion is disrupted by hetero-aggregation with **2**.

Hypothesis (1) can be discarded by an examination of the conditions of the experiment. The concentration of THF in the solution is ~10 times the total concentration of imines. Under such conditions of a large excess of coordinating solvent it is impossible that **2** could coordinate enough solvent to completely eliminate species **1c**, since lithiated species are constrained to 4 or less solvent molecules per lithium by the limited coordination sphere of lithium⁶³.

Both hypotheses (2) and (3) require that at least one of the species **1a**, **1c** and **1d** is an aggregated species and that some of the aggregates are a mixture of **1** and **2**. Therefore aggregation is at least partially responsible for the multiplicity of signals observed in low temperature NMR spectra of **1**. The involvement of rotamers as well as aggregation would be expected to lead to a more complex set of NMR signals than would aggregation alone.

Inherent in this interpretation is the assumption that the chemical shifts of these lithiated acetaldimines are sensitive to the type of aggregation, but not to the identity of their partner(s) in

aggregates. Since all of the signals observed in this mixed lithiated imine experiment are at chemical shifts identical to those observed for pure **1** and **2**, it can be safely assumed that they are the same types of species (ie. dimers, clusters, etc.) which are observed in both pure and mixed samples.

Upon addition of PMDETA, a ligand which is expected to break up aggregates^{34,66,72,73}, the ratio of species for lithiated imine **1** in the mixed lithiated imine sample returned to the ratio observed for pure **1** in the presence of PMDETA, demonstrating that **2** has no effect on **1** when aggregation is reduced. A more detailed examination of the effects of PMDETA on lithiated imine **1** follows in Sections 2.1.5 and 2.1.6.

2.1.4 Effect of Solvent and Concentration on **1**.

The chemical literature dealing with lithiated organic molecules demonstrates overwhelmingly that solvation of the lithium is a crucial factor in determining the solution and crystalline structure(s) of the lithiated molecules. THF is known to coordinate strongly to lithium through a lone pair of electrons on the oxygen atom. This coordination is stronger than is possible by acyclic ethers, such as diethylether, which is a less polar and poorer donor solvent than THF^{117,118} since the ring tends to pull back the α -methylene groups leaving the oxygen lone pairs more exposed in THF. Indeed, a passing observation was made that **1** appears to be less soluble in diethylether than in THF/hexanes.

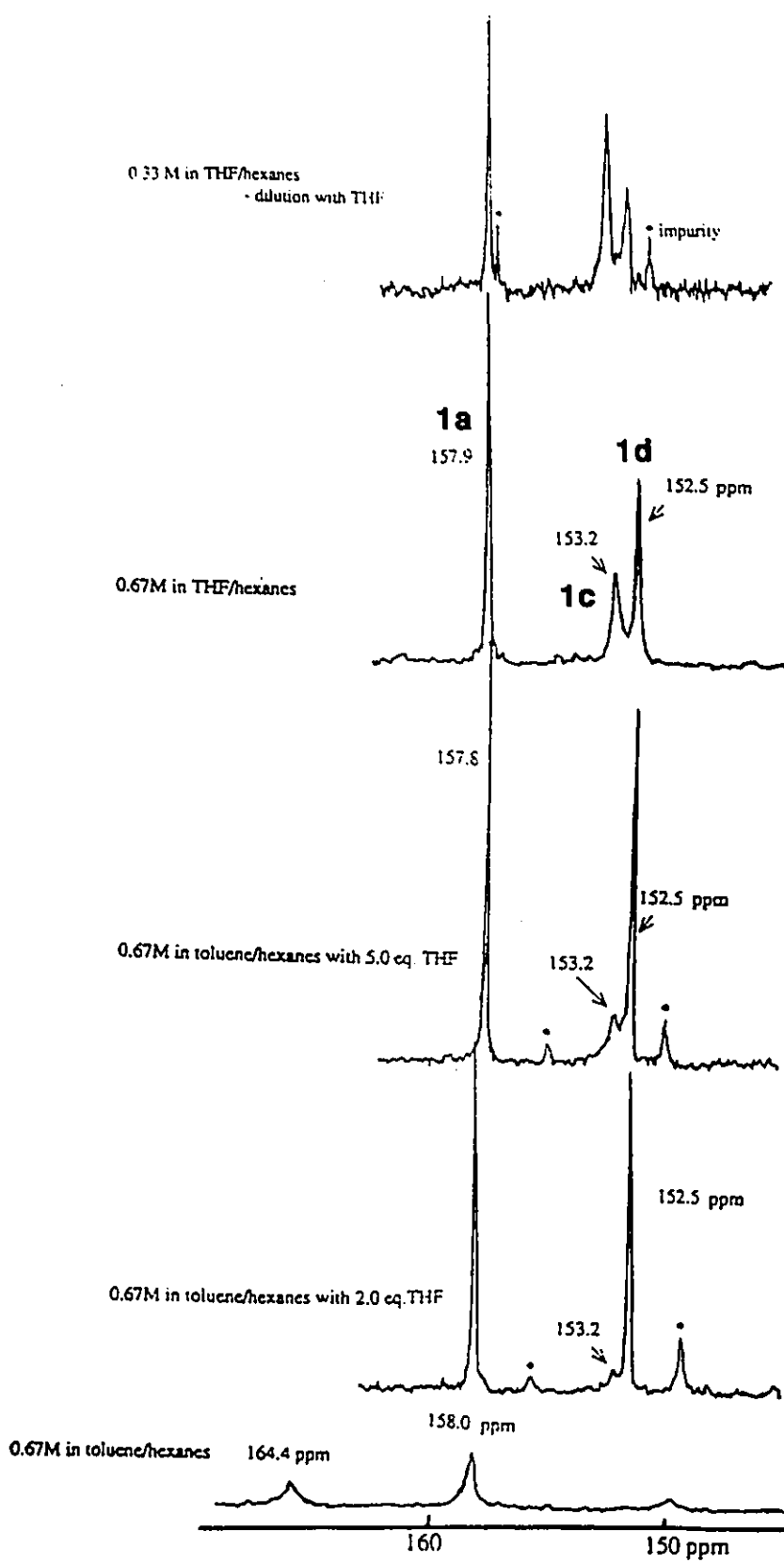
In the previous section it was demonstrated that the

behaviour observed in the low temperature ^{13}C NMR spectrum of lithiated imine **1** has at least some involvement of an aggregation phenomenon. In order to further investigate the aggregation of this lithiated imine an examination of the effect of changing the polarity and coordinating ability of the solvent towards lithium and of changing the concentration of the lithiated imine **1** was conducted.

In order to examine the role of THF in determining the solution structures of **1**, a 0.67 M solution of the lithiated imine was prepared in toluene/hexanes solvent (1.8:1 by volume). Toluene was selected because it is a non-polar, non-coordinating solvent in which lithiated imines are soluble, and because it is stable to strongly basic conditions and has a low freezing point (-95°C)¹¹⁹. To this solution were added aliquots of THF and the effect of adding THF was monitored by ^{13}C NMR at -80°C . One equivalent of THF adds approximately 5% to the volume of the solution: addition of 5 equivalents resulted in a net dilution to 0.5 M. Figure 15 shows the effect of increasing THF concentration on **1**.

A solution containing no THF exhibited two very broad signals (line-width ≥ 10 Hz) at 164.4 ppm and 158.0 ppm. When one equivalent of THF was added only species **1a** and **1d** were observed, in a 1:1 ratio. When 2 equivalents of THF were added all three of the species **1a**, **1c** and **1d** were observed, in the ratio of 45% : <5% : 50% ($\pm 5\%$). At 5 equivalents of THF the ratio of **1a** : **1c** : **1d** changed to 38% : 21% : 41% ($\pm 5\%$). In a standard solution of **1** in THF/hexanes the ratio of **1a** : **1c** : **1d** is 36% : 28% : 36% ($\pm 5\%$). (In toluene/hexanes solutions of **1** having only one or two equivalents of THF added a new signal was observed at 69.8 ppm, which is almost certainly one of the resonances

Figure 15
Effect of [THF] on 1.



due to the methylene carbon, but which is obscured by the intense THF signal at 69 ppm at higher THF concentrations.)

For the solution of **1** in toluene/hexanes to which 2 equivalents of THF were added (comprised of **1a** and **1d**) the coalescence temperature for the formyl carbon signals was found to be in the range of -10°C to 0°C. This indicates that the barrier for interconversion of these two species is not greatly affected by THF concentration.

When 0.67 M solutions of **1** in (a) toluene/hexanes diluted with 2 eq. THF, (b) toluene/hexanes diluted with 5 eq. THF or (c) THF/hexanes were further diluted by doubling their volumes by addition of toluene, which has the effect of both bulk dilution and decreasing the THF concentration, the proportion of **1c** generally decreased relative to **1a** and **1d**. In contrast, when a 0.67 M solution in THF/hexanes was diluted to 0.33 M by the addition of THF species **1c** increased relative to **1a** and **1d**. (Table 4).

In all cases the ratio of **1a** to **1d** was virtually insensitive to total concentration or to THF concentration, remaining at 1 : 1 within the limits of uncertainty in the determination of the relative areas of signals. **1a** and **1d** must have a common level of aggregation and solvation; otherwise their relative ratio would be dependent upon total concentration. The proportion of **1c** relative to **1a** and **1d** was moderately sensitive to THF concentration, increasing with increasing THF concentration. This increase was not the result of bulk dilution, since dilution with toluene had the opposite effect on the proportion of **1c** than did dilution with THF.

Table 4
Effect of [THF] on 1

<u>Conditions</u>	<u>[THF]</u>	<u>[1]</u>	<u>1a:1b:1c</u>
THF/hexanes	6.23	0.67	36:28:36
toluene/hex + 5 THF	2.61	0.52	38:21:41
toluene/hex + 2 THF	1.34	0.61	>45:<5:50
THF/hex: dilute w. THF	11.8	0.33	22:55:22
THF/hex: dilute w. toluene	3.12	0.33	39:21:40
toluene/hex + 5 THF	1.30	0.26	38:21:41

It can be concluded that species **1c** is more highly solvated by THF than either **1a** or **1d**, and that **1a** and **1d** share a similar degree of solvation. It is not possible to make any conclusions regarding the relative states of aggregation of **1c** compared to **1a** and **1d** on the basis of these experiments, only that **1a** and **1d** share a common level of aggregation.

By examining the nature of species in toluene/hexanes solutions containing only very small amounts of THF (≤ 2 equivalents) it may be possible to estimate the number of solvent molecules coordinated to **1a** and **1d**. (**1a** and **1d** are the predominant species with 2 equivalents of THF present). When 1 equivalent (per lithium present in the solution) of THF is present the spectrum was identical to that observed when 2 equivalents were present, except that none of **1c** was observed. Since **1a** and **1d** had sharp signals only when 1 or more equivalents of THF are present, and they appeared unchanged as more THF or toluene was added, it is reasonable to surmise that **1a** and **1d** are solvated by one THF molecule per lithium. Various

solvation models will be examined in Section 2.1.12.

2.1.5 The Effect of Strongly Coordinating Ligands on 1: Displacement of THF

Hexamethylphosphoramide (HMPA) and pentamethyldiethylenetriamine (PMDETA) are ligands which are known to bind strongly to lithium in lithiated organic^{34,35,50,61,62,67,69,72,73,76} and inorganic compounds⁶⁸. The usual effect of these ligands is to displace coordinated solvents, such as ethers, from the metal. Often the binding of these ligands to lithium is strong enough to overcome and replace intra-aggregate bonds, resulting in disruption of the aggregation and the formation of lower states of aggregation^{72,73,77}, such as monomers.

HMPA coordinates lithium through the oxygen atom, and is a stronger Lewis base than most ether solvents^{74,75}. PMDETA coordinates through the electron lone pairs on each of the three nitrogen atoms. In principal PMDETA can coordinate via one, two or all three of its nitrogen atoms: coordination by two^{35,72,73} and three nitrogens^{34,103} has been reported. Undoubtedly the "chelate effect" provides a driving force for multidentate binding of lithium by PMDETA. Similar bidentate ligands are TMEDA^{30,44,46,52,58,60,72,73}, ethylenediamine⁴⁵ and N,N,N',N'-tetramethylpropanediamine⁴⁷, which have been shown to coordinate strongly to lithium.

The effect of these ligands on the coordination of THF to the lithium atoms of 1 was examined by monitoring the T_1 of the THF

carbon nuclei as a function of added ligand. In theory, the T_1 relaxation time is inversely proportional to molecular volume.

The T_1 of the α -carbon (C_1) of free THF solvent should be long, reflecting the slow relaxation of the free solvent, which is a small and highly mobile molecule, and should be similar to that measured for THF in a 1.8:1 mixture of THF and hexanes (~ 10 s). The T_1 of THF bound to lithiated imine aggregates should be much shorter, reflecting the fast relaxation in large molecules, since the THF will be part of large species with low mobility. In a solution of **1** in toluene/hexanes containing only 1 equivalent of THF, where all of the THF are likely to be bound to lithium, the T_1 of C_1 was found to be $0.5 \pm .05$ s at -60°C . This value will be taken as the T_1 of bound solvent.

In standard 0.67 M THF/hexanes solutions of the lithiated imine there is an excess of THF, so the measured relaxation rate (T_1^{-1}) of the single observed NMR signal of the THF C_1 carbon atom will represent a weighted average of the relaxation rates of free and bound THF, as expressed in this equation:

$$\frac{1}{T_1} = \frac{1}{T_{1\text{free}}} X_{\text{free}} + \frac{1}{T_{1\text{bound}}} X_{\text{bound}} \quad X = \text{mole fraction}$$

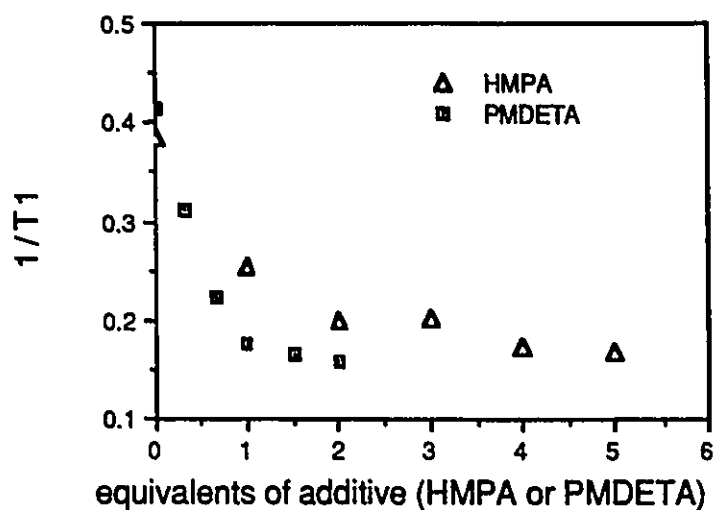
To a standard 0.67 M solution of **1** in THF/hexanes were added portions of the ligand (PMDETA or HMPA). After the addition of each aliquot the T_1 relaxation times of C_1 and C_2 of THF were measured. A plot of the inverse of the THF carbon relaxation times versus the number of equivalents of PMDETA and HMPA is shown in Figure 16.

NOE measurements on the THF carbon nuclei showed an NOE in the range of 2.6 to 3.0 over a range of additive concentrations. This

confirms that the relaxation of these nuclei falls in the extreme narrowing domain, and therefore that dipole-dipole relaxation dominates. Under these conditions a correlation exists between T_1 and molecular volume. (For simplicity, only the T_1 of C_1 will be discussed, although the behaviour at C_2 parallels that at C_1 .)

Figure 16

Plot of T_1 of THF(C_α) vs [HMPA] and [PMDETA]



As PMDETA was added at -60°C the relaxation rate of THF decreased, which can be interpreted as an increasing contribution of free THF (which relaxes more slowly) to the averaged relaxation rate which was being measured. In other words, the THF was being displaced by PMDETA from coordination to lithium. A control experiment was performed in which PMDETA was added in portions to a solution of THF and hexanes (1.8:1). The relaxation rate of THF increased (from 0.1s^{-1} to 0.13s^{-1}) with 4 equivalents of added

PMDETA, as might be expected for what appeared to be an increasingly viscous solution. This shows that the decrease in the relaxation rate of THF upon addition of PMDETA to a solution of 1 was not the result of dilution or change in medium.

These results show that PMDETA effectively displaces THF from coordination to the lithiated imine. As will be discussed later, during the addition of PMDETA the types of lithiated imine species changes due to the addition of PMDETA, and it cannot be determined from this single experiment whether PMDETA behaves as a mono-, bi- or tri-dentate ligand, nor can the number of THF molecules displaced from any one species be determined.

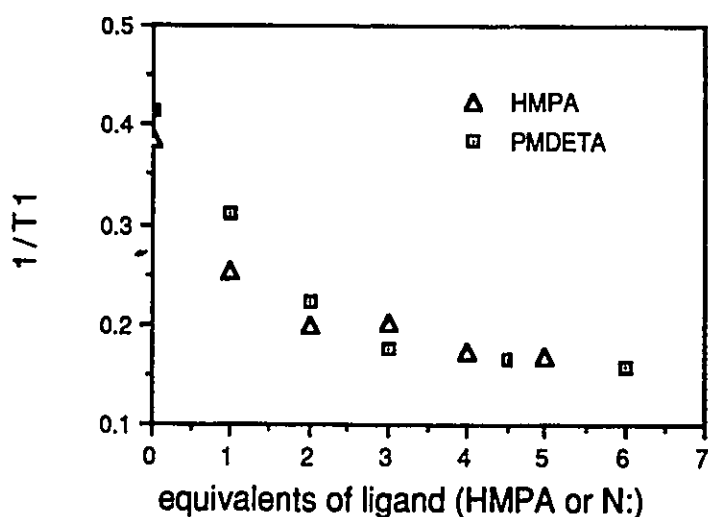
As with PMDETA, the addition of HMPA to a THF/hexanes solution of 1 at -60°C also resulted in a decrease in the rate of relaxation of the ^{13}C resonances of THF. A control experiment in which the T_1 of THF was measured as HMPA was added to a 1.8:1 mixture of THF and hexanes revealed a slight increase in T_1 (decrease in relaxation rate) with added HMPA and the solution became noticeably more viscous. This increased viscosity may account for the change in the THF T_1 in the control sample.

The shape of the plots of T_1^{-1} vs [PMDETA] and T_1^{-1} vs [HMPA] suggest that PMDETA binds more strongly to lithium than does HMPA, since with addition of PMDETA there is a more rapid decrease in the relaxation rate than upon addition of HMPA, where the decrease in ^{13}C relaxation rate is indicative of displacement of THF from the lithium ions. This apparently stronger binding of PMDETA to lithium may be simply the result of the fact that PMDETA is a tridentate ligand.

In order to make a valid qualitative comparison of the binding constants of HMPA and PMDETA one should consider PMDETA to be a tridentate ligand such that the concentration of binding sites (nitrogen atoms) is three times the concentration of PMDETA. (Although there is evidence from the literature of PMDETA behaving as both a bidentate and a tridentate ligand, in the absence in this work of any evidence favouring either case, PMDETA will be arbitrarily considered to be tridentate). When the relaxation rates of the THF carbon atoms are plotted against $3X[\text{PMDETA}]$ and $[\text{HMPA}]$ on the same graph (Figure 17) the effect of PMDETA appears to be essentially the same as the effect of HMPA. This demonstrates that PMDETA is not an inherently stronger binding ligand for lithium than HMPA.

Figure 17

Plot of T_1 of THF(C_α) vs $[\text{HMPA}]$ and $3X [\text{PMDETA}]$



Thus it can be concluded that both PMDETA and HMPA are able to displace THF from coordination to 1, and that PMDETA and HMPA

displace THF and therefore bind to lithium with similar strength.

2.1.6 Effect of PMDETA : New Species.

It was found that concurrent with the solvation of the lithiated imine by PMDETA and HMPA was a change in the proportions of **1a**, **1c** and **1d** and the introduction of new lithiated imine species. This is a further indication that solvation plays a role in determining the solution structures of **1**.

Addition of PMDETA caused a number of changes in the types of species observed in the ^{13}C spectrum of a 0.67 M solution of lithiated imine **1** in THF/hexanes at -80°C , as illustrated in Figure 18. When 0.33 equivalents of PMDETA were added the signal for **1a** became broad, and the signals for **1c** and **1d** appeared to coalesce. At 0.5 equivalents the broadening of all of the signals increased and then at 0.66 equivalents the signals began to sharpen again. When a total of 1.0 equivalent had been added the signals were again as sharp as those in the initial condition before addition of PMDETA but the chemical shifts were different than in the absence of PMDETA. The chemical shift of the signal arising from coalescence of the signals for **1c** and **1d** was the same as that of **1c** (153.2 ppm), while the signal arising from the coalescence observed at the signal for **1a** was shifted downfield to 159.0 ppm. The ratio of the integral of the peak at 153.2 ppm to that at 159 ppm was 3:1.

It appears that the addition of small amounts of PMDETA causes an increased rate of exchange among the species **1a**, **1c** and

Figure 18
Effect of PMDETA on 1.



1d, resulting in the coalescence, while at the same time causing species **1c** to predominate. During the coalescence process it appears that the signal which arose at 159 ppm was indeed a new species (**1e**) rather than species **1a** shifted to lower field, since in the spectra of solutions containing 0.5 and 0.66 equivalents of PMDETA two peaks were apparent in the region of 158-160 ppm. The small signal further downfield from that of **1e** may be an impurity or yet another minor species of **1**. It is not possible to interpret the changes observed in the lowfield region: the most simple observation is that the major species in the presence of 1 equivalent of PMDETA is **1c**. On the basis of the effect of changing the polarity of the solvent the species **1c** has been previously established (Section 2.1.4) to be the most highly solvated of **1a**, **1c** and **1d**. When PMDETA was added to toluene/hexanes solutions of **1** which contained 2 equivalents of THF, very similar observations were made, except that two signals were observed to arise from the coalescence at 158-160 ppm; one at 159 ppm and another at 157 ppm.

Given the chelating ability of PMDETA, it is not surprising that it favours the most highly solvated species **1c**, as established in the previous section. At concentrations of PMDETA below 1 equivalent, where PMDETA has not fully displaced THF from the lithium atoms of **1**, rapid exchange between species partially and fully solvated by THF and/or PMDETA is a likely explanation for the coalescence observed.

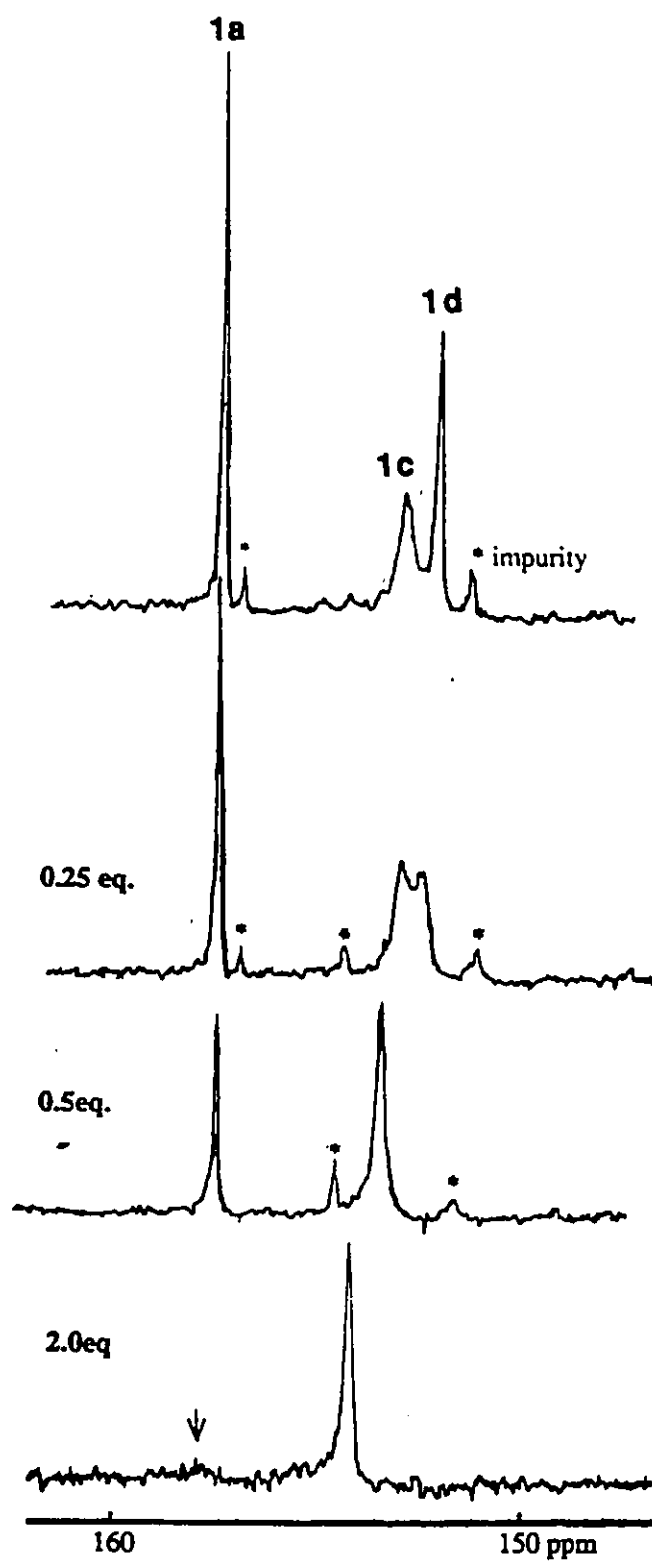
It was found that the ^{13}C signals of the PMDETA ligand itself were exceptionally broad, in the range of 18 to 35 Hz at half

height, even when one equivalent of PMDETA was present. PMDETA, in absence of **1**, has ^{13}C linewidths in the order of 3 to 5 Hz, suggesting that the large linewidths observed in the presence of **1** were the result of some type of exchange process. It was found that the linewidths were independent of concentration, demonstrating that the exchange process is intramolecular. One explanation may be that only two of the three nitrogen atoms of PMDETA can coordinate to **1** at any given moment and that there is moderately fast interchange among the three possible combinations of coordinating nitrogen atoms. Another possible explanation is that there are various conformations of the PMDETA chelate (with three nitrogens coordinated to lithium) and of the lithiated imine relative to PMDETA which are interconverting, akin to the various conformers of PMDETA-chelated *neo*-pentyllithium reported by Fraenkel et al.¹⁰³

2.1.7 Effect of HMPA : New Species.

HMPA was found also to affect the proportions of **1a**, **1c** and **1d** in a 0.67 M solution of **1** in THF/hexanes at -80°C (Figure 19). Addition of 0.25 equivalents of HMPA resulted in a broadening of the signals for **1c** and **1d**, and appeared to favour the conversion of **1d** into **1c** while simultaneously the proportion of **1a** decreased. As more HMPA was added the proportion of **1c** increased at the expense of **1a** and **1d**, and the signal for **1c** shifted downfield. The signal for **1c** initially had a chemical shift of 153.2 ppm but as more HMPA was

Figure 19
Effect of HMPA on 1.



added it moved downfield, eventually to 154.5 ppm when 2 equivalents of HMPA were added. Upon addition of 2 more equivalents of HMPA **1c** was the dominant species, the concentration of **1d** was reduced to zero, and **1a** was reduced to ~10% of the total.

It appears that the addition of HMPA favours species **1c** at the expense of **1a** and **1d**. That a highly polar solvent such as HMPA should favour the formation of **1c** is consistent with the previous interpretation that **1c** is a highly solvated species. The gradual downfield shift of the signal attributed to **1c** may result from a sensitivity of the chemical shift of species **1c** to the nature of the solvent which is coordinated to it (either THF or HMPA) or to bulk solvent polarity.

Solutions of **1** in toluene/hexanes show a similar behaviour upon addition of HMPA: **1c** is favoured at the expense of **1a** and **1d** and the resonance for **1c** gradually shifts downfield.

An attempt was made to study the binding of HMPA to lithium via ^{31}P NMR. Unfortunately, the ^{31}P chemical shifts of free HMPA and of what was presumed to be lithium-coordinated HMPA were found to be the same, and no lithium-phosphorus coupling¹²⁰ was observed even at temperatures as low as -125°C , thus precluding a simple NMR investigation. Further ^{31}P NMR studies were not attempted.

In summary, HMPA has been shown to displace THF from coordination to the lithiated imine **1**, and to favour the formation of the most highly solvated species, **1c**.

2.1.8 Is Di-*iso*-propylamine Coordinated to 1?

Collum⁴¹ et al. and Tamm et al.³³ have shown that di-*iso*-propylamine, the conjugate acid of the LDA used in the lithiation, can coordinate to lithiated species. In order to fully characterize the solution structure of the lithiated imine **1** it must be determined whether di-*isopropylamine* (DIPA) is coordinated to **1**. Three experiments were used to approach this question.

In the first experiment the supernatant was removed from a sample of lithiated imine **1** which had been precipitated from THF/hexanes solution by allowing it to stand at -78°C for 24 hours. The ¹³C NMR spectrum of **1** redissolved in fresh THF showed a 50% reduction in the intensity of the signal for the methine carbons of DIPA (46.0 ppm), as calibrated against the signals of **1**. This suggests that DIPA is not strongly coordinated to crystalline **1**.

The second and third experiments investigating possible coordination of DIPA to **1** used the measurement of T_1 as a probe of the molecular volume of DIPA. In one experiment **1** was prepared as a THF/cyclohexane solution by deprotonation of **1-H** using *sec*-butyllithium instead of LDA. DIPA was then titrated into the solution of **1** and the T_1 of the methine carbon of DIPA was measured at -60°C at various concentrations of DIPA over the range of 0.33 to 3.0 equivalents. Over this range the T_1 of DIPA remained constant at 2.9 ± 0.3 s, indicating that the molecular volume of DIPA remained constant over the range of DIPA concentration for which T_1 was measured. If DIPA was coordinating to the lithiated imine its T_1 should be very much lower when coordinated than when unbound.

Therefore DIPA did not coordinate to the lithiated imine, and thereby become part of a much larger, less mobile species. A secondary observation was that the sample of **1** prepared with *sec*-butyllithium, and thus free of DIPA, had the same ratio of species and the same temperature dependent behaviour as a sample prepared using LDA as the base and that the ratio of species was unaffected by added DIPA.

In the third experiment a standard sample of **1** was prepared using LDA as the base and PMDETA was titrated into the solution. The T_1 of DIPA was measured at -60°C over a range of PMDETA concentrations from 0 to 1.5 equivalents and was found to be constant, indicating constant molecular volume for DIPA. Assuming that PMDETA, because it is a tridentate ligand, would bind to lithium much more strongly than DIPA, PMDETA should displace any DIPA from **1** and therefore cause an increase in the T_1 of DIPA. The lack of a measurable effect of PMDETA on the T_1 of DIPA demonstrates that PMDETA does not displace DIPA from **1**. Thus we can conclude that DIPA is not coordinated to **1**.

The three experiments above demonstrate that DIPA does not coordinate to **1** in either the solid or in THF solutions.

2.1.9 T_1 Measurements on **1a**, **1c** and **1d**; Relative Sizes of these Species

The T_1 relaxation times of species **1a**, **1c** and **1d** were measured in an endeavour to determine qualitatively the relative molecular volumes of the aggregates whose structures are

represented by the ^{13}C signals **1a**, **1c** and **1d**.

The T_1 's of the ^{13}C signals of the formyl carbons of **1a**, **1c** and **1d** were measured at -80°C in a standard 0.67 M solution in THF/hexanes using the inversion-recovery (180- τ -90) method. Nuclear Overhauser enhancement (NOE) measurements of the three signals were made in order to determine whether these nuclei were undergoing relaxation in the extreme narrowing region, where it is possible to make a correlation between molecular volume and T_1 . The results of the T_1 and NOE measurements are reported in Table 5 (theoretical maximum = 2.988).

Table 5
 T_1 and NOE data at -80°C

<u>Species</u>	<u>T_1</u>	<u>NOE</u>
1a	0.21 \pm .03s	2.3 \pm .2
1c	0.18 \pm .03s	2.3 \pm .2
1d	0.19 \pm .03s	2.3 \pm .2

The $^1\text{H}/^{13}\text{C}$ heteronuclear NOE measurements are the best values determined in a series of experiments in which variations were made in the pre-acquisition period during which the NOE is allowed to equilibrate. It was found that the NOE was sensitive to the length of this delay, possibly due to the counteracting effects of the physical desirability of as long a pre-acquisition period as possible and the technical consideration in which undesirable heating of the sample may occur during the period in which the decoupler is

on.

The NOE measurements show that dipole-dipole relaxation is not the sole mechanism of relaxation of the carbon nuclei. It is possible that the low temperature may have caused an increase in τ_c such that the relaxation was no longer in the extreme-narrowing regime, but such a thermal effect should be accompanied by a lengthening of the T_1 relative to that measured at a higher temperature. T_1 Relaxation times of the formyl carbons of **1a** and **1b** were measured at -60°C and were found to be longer ($\sim 0.3\text{s}$) than at -80°C . More likely, another relaxation mechanism, such as that caused by paramagnetic impurities such as oxygen may account for the failure to observe a full NOE at -80°C .

It is possible to roughly estimate the lifetime for chemical exchange among **1a**, **1c** and **1d** at -80°C based on the rate of exchange measured at the coalescence temperature for **1a** and **1b**. If, for simplicity, one considers the exchange process to be between two sites, the residence time for each species undergoing chemical exchange (τ_{ex}) at -7°C can be calculated to be 0.001s . The entropies of activation for some interaggregate exchange processes in alkyllithiums have been reported, and have varied from $20\text{ cal mole}^{-1}\text{ K}^{-1}$ for exchange via a dissociative mechanism to $-30\text{ cal mole}^{-1}\text{ K}^{-1}$ for an associative mechanism²⁴. Using these values as a range for an estimated entropy of activation for the exchange among species for **1**, then τ_{ex} at -80°C can be estimated to be in the range of 300 to 0.02s ¹²¹. This means that the lifetime for chemical exchange at -80°C may be shorter than the T_1 relaxation time. This result should be taken as an indication that the relaxation rates for each of the

species have be averaged by chemical exchange if the exchange is fast. It should be noted, however that the identical T_1 and NOE values measured for each of the three species suggest that they have very similar structures: this is certainly true, since all are variants of lithiated imine **1**.

At -60°C a full NOE (2.8 to 3.0) was measured for **1a** and **1b** and the T_1 relaxation times of the two signals were the same (0.33 ± 0.03 s). The NOE results demonstrate that dipole-dipole relaxation is dominant at -60°C , but do not provide any indication of whether the relaxation times are averaged by chemical exchange, which should be faster at -60°C than at -80°C . Since, at -60°C , a full NOE was measured for the two signals it can be inferred that the three species **1a**, **1c** and **1d**, which are represented at -60°C by the two signals **1a** and **1b**, should have full NOE enhancements at -80°C and that the relaxation at -80°C is by the dipole-dipole mechanism.

Thus it may be said that although a full NOE was not measured for **1a**, **1c** and **1d** at -80°C that the relaxation must be by the dipole-dipole mechanism, and therefore that it is valid to apply the relationship between T_1 and volume. Thus it can be concluded that the three species **1a**, **1c** and **1d** have similar molecular volumes therefore a common or similar level of aggregation, whether that be monomeric, dimeric, trimeric, etc., provided that chemical exchange is slow relative to the relaxation rates. It has already been established in the experiment involving a mixture of lithiated imines that at least some of the three species **1a**, **1c** and **1d** are aggregated. In conjunction with the T_1 result it can be concluded that all of the three species have similar degrees of aggregation. If all species have

a similar level of aggregation and at least one is known to be aggregated, it can also be concluded that none is a monomer.

2.1.10 ^{15}N and ^6Li Doubly Labelled Samples: Lithium-Nitrogen Connectivities in 1

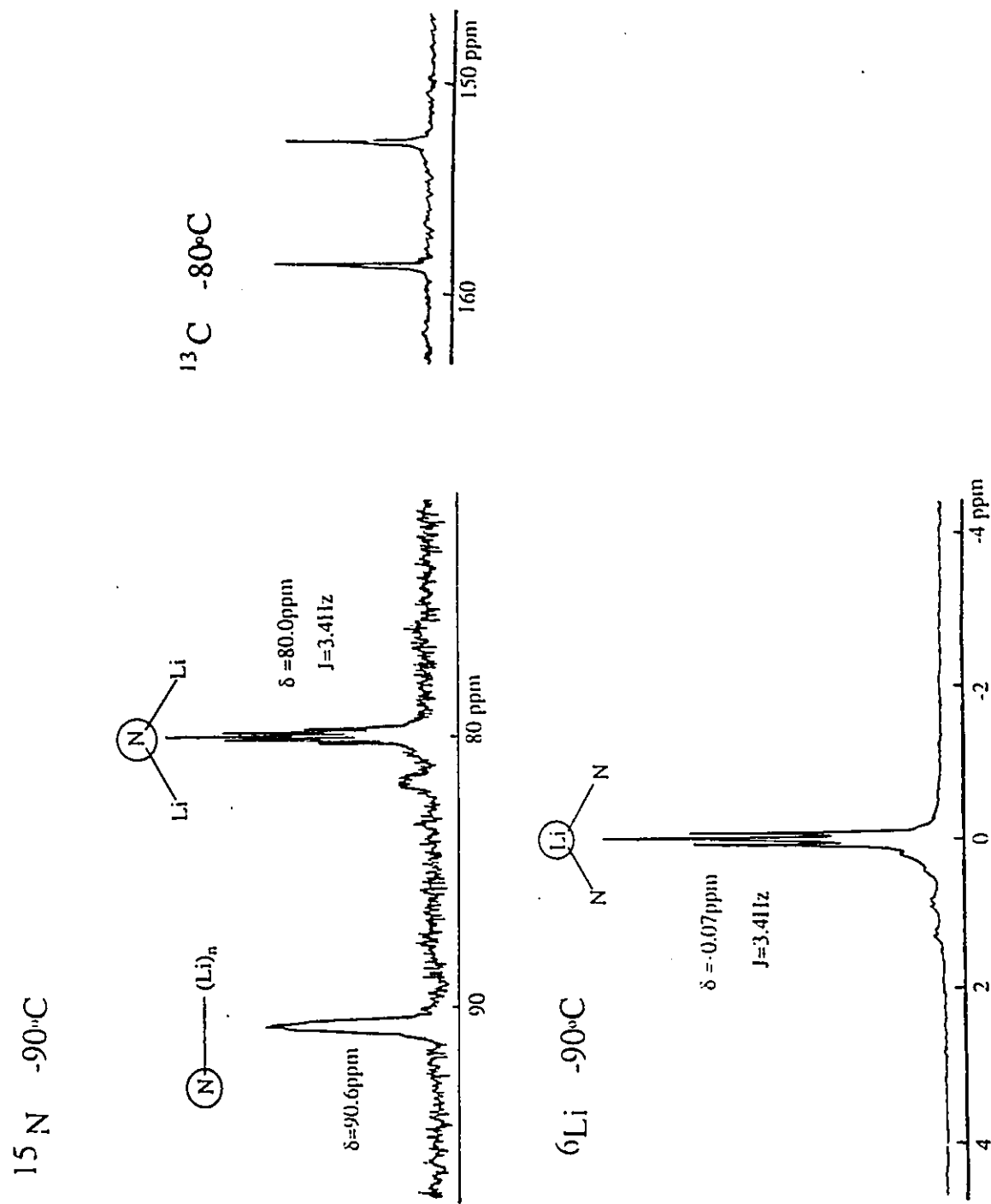
It has been demonstrated by Jackman and coworkers, and later by Collum and coworkers, that heteronuclear coupling between ^{15}N and ^6Li in doubly labelled samples (>95% labelled at both nuclei) can be a powerful tool for the determination of lithium-nitrogen connectivities in N-lithiated molecules such as lithium amides and lithiated imines^{16,36-40,42}. Here are described the results of $^{15}\text{N}/^6\text{Li}$ double labelling NMR experiments as applied to the problem of the solution structures of lithiated N-*iso*-propylacetaldimine.

Doubly labelled $^{15}\text{N}/^6\text{Li}$ samples of lithiated imine 1 ($^{15}\text{N}/^6\text{Li}$ -1) were prepared in a variety of solvents, and their ^{15}N , ^6Li and ^{13}C NMR spectra were measured. Preliminary experiments were conducted in order to select conditions which provided relatively simple ^{13}C and natural abundance ^6Li spectra and these same conditions were then repeated for the double labelling experiment. The ^6Li spectra were measured at -90°C because preliminary experiments showed a coalescence of ^6Li signals beginning, in most samples, at temperatures higher than -90°C . The ^{15}N spectra were measured also at -90°C for comparison to the ^6Li spectra. As discussed in a previous section, there is little difference between the ^{13}C spectra at -80°C and -90°C .

A sample of $^{15}\text{N}/^6\text{Li}$ -1 was prepared as a 0.67 M solution in toluene/pentane to which two equivalents of THF were added (see Figure 20). The ^{13}C spectrum at -80°C revealed this sample to contain 1a and 1d in roughly equal proportion and a small amount of 1c. The $^{15}\text{N}\{^1\text{H}\}$ spectrum of this sample had three signals: a broad peak at 90.6 ppm, a quintet (1:2:3:2:1, $J_{\text{N-Li}} = 3.4$ Hz) at 80.0 ppm and a minor, broad peak at 82 ppm. The ratio of the two major signals was 1:1. The quintet indicates that the ^{15}N nucleus resonating at 80.0 ppm is coupled, and therefore bound, to two identical ^6Li nuclei (the spin of ^6Li is $1^{1/2}$). It was not possible to resolve the broad downfield signal (90.6 ppm) by either raising or lowering the temperature by 10°C , but it was noted that the upfield quintet broadened slightly at -100°C . The minor species observed in the ^{15}N spectrum was not resolved, but its envelope appears to be flat on top, suggestive of a 1:1:1 triplet rather than a singlet or other 'sharp' signal type. It has been reported that the fluxionality of similar aggregate systems causes broadening of the lines resulting in a failure to resolve the ^{15}N - ^6Li couplings, thus making the double labelling NMR experiment ineffective^{37,42}. Such fluxionality may be the cause of the poor resolution observed for the ^{15}N signal at 90.6 ppm.

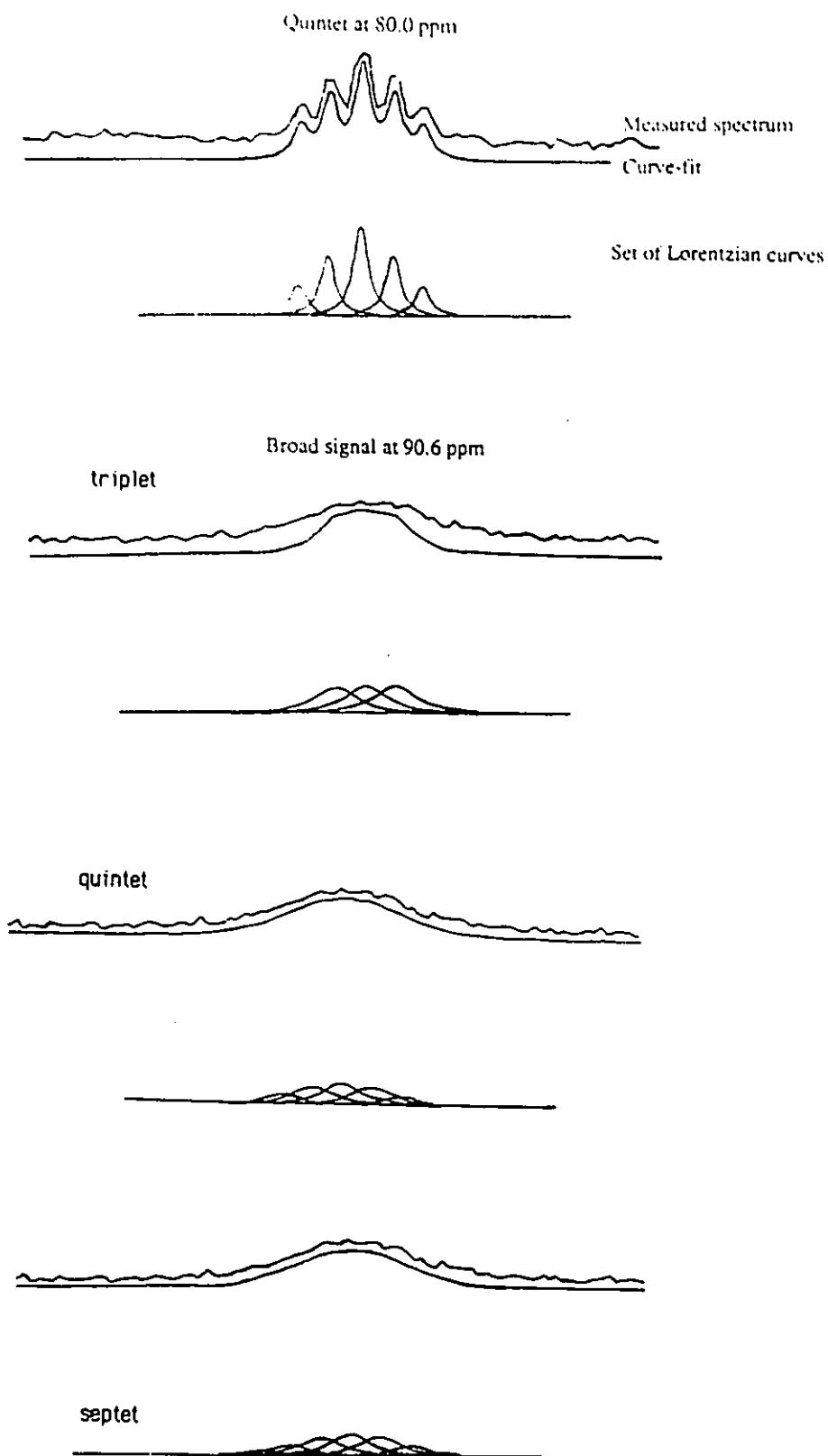
The linewidth and shape of the broad signal at 90.6 ppm are suggestive of an envelope of a quintet of coupling to ^6Li similar to that of the upfield quintet, especially since the alternative coupling pattern of a 1:1:1 triplet (bound to one ^6Li) would have a very differently shaped envelope. A more quantitative approach was used

Figure 20

 ^{15}N - ^6Li -1 in toluene/pentane with 2 eq. THF.

to test the hypothesis that the broad downfield signal is essentially identical to the well resolved quintet at 80.0 ppm except for a large difference in linewidths. Using a curve-fitting program available in the XL-300 software¹²³, a set of five Lorentzian curves were generated to fit the 1:2:3:2:1 quintet at 80.0 ppm (Figure 21). This set of five curves was then shifted downfield such that they were centered at the mid-point of the broad signal at 90.6 ppm. The ¹³C spectrum showed that the two major species were present in a 1:1 ratio, so the intensities of the generated signals were kept constant while the linewidth of each of the five generated signals was increased equally. It was possible to create a reasonably close fit of the quintet to the observed spectrum using this method, while a poor match of peak shapes was obtained when attempting to fit a 1:1:1 triplet to the signal at 90.6 ppm. (The splitting of all of the multiplets was kept constant at 3.4 Hz, since that was the coupling observed at lithium.) A 1:3:6:7:6:3:1 coupling pattern (N bound to three ⁶Li) would also fit the observed envelope very well, suggesting a ladder-type structure. A ladder structure is unlikely, however, since it would also require that some of the lithium nuclei be bound to three nitrogens, resulting in a quartet in the ⁶Li spectrum. Also, the ratio of the two species in question, **1a** : **1d**, was found to be insensitive to concentration or to THF concentration: that these species should be unequally solvated or unequally aggregated, as would be required should one species possess a ladder-type structure, is inconsistent with the experimental observations. It can be concluded that the two major signals in the ¹⁵N NMR spectrum are both quintets representing species in which the nitrogen atoms are

Figure 21
Curve-fitting for ^{15}N spectrum.

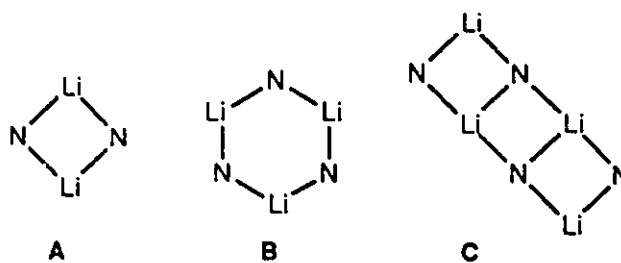


each bound to two lithium atoms.

In the ${}^6\text{Li}$ spectrum only one signal was observed, which was split by the ${}^{15}\text{N}$ nuclei (the spin of ${}^{15}\text{N}$ is $-1/2$ 122) into a 1:2:1 triplet with $J_{\text{N-Li}} = 3.4$ Hz, indicating that all lithium atoms have a similar environment and that they all are bound to two nitrogen atoms. The fact that only one ${}^6\text{Li}$ signal was observed, having well resolved coupling, tends to support the assertion that the broad ${}^{15}\text{N}$ signal at 90.6 ppm has a coupling constant to ${}^6\text{Li}$ similar or identical to that of the well resolved quintet at 80.0 ppm. A small broad signal downfield and partially overlapping the triplet in the ${}^6\text{Li}$ spectrum may correspond to the minor species (1c) observed in the ${}^{13}\text{C}$ and ${}^{15}\text{N}$ spectra. Thus it can be concluded that the majority of lithium nuclei have a common magnetic and chemical environment, and that most of the lithium atoms are bound to two nitrogen atoms. Collum reported similar results for *cis* and *trans* dimers in solutions of lithium *iso*-propylcyclohexyl amide, for which two ${}^{15}\text{N}$ signals but only one ${}^6\text{Li}$ signal were observed³⁶.

Based on the patterns of the ${}^{15}\text{N}$ - ${}^6\text{Li}$ couplings, it can be deduced that in the two major species, 1a and 1d, all of the nitrogen is bonded to two lithiums and that all of the lithium is bonded to two nitrogens. 1a and 1d must contain rings of alternating lithium and nitrogen atoms as shown in Figure 22.

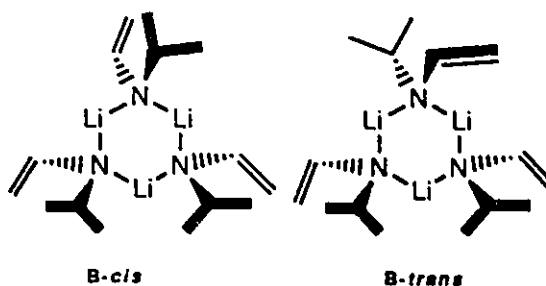
Figure 22: Possible lithium-nitrogen connectivities



In structure C, a ladder type structure, the central lithium and nitrogen atoms must be bonded to three other nuclei while the terminal lithium and nitrogen atoms would have two directly bonded nuclei: this clearly does not fit with the observed coupling pattern. Therefore **1a** and **1d** must possess a structural element such as structure A or structure B (or possibly a higher cyclic aggregate).

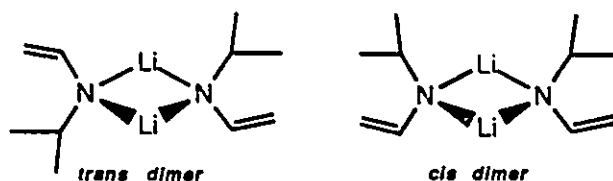
T_1 Measurements and the insensitivity of the ratio of **1a** to **1d** indicate that species **1a** and **1d** have the same level of aggregation. The lithium spectrum of a mixture of **1a** and **1d** has a single signal, suggesting that the two species have similar structures with respect to the lithium nuclei. These observations lead to the reasonable conclusion that the two species **1a** and **1d** are probably stereoisomeric forms of a single type of aggregate, such as a cyclic dimer or trimer of a structure consistent with the ${}^6\text{Li}$ - ${}^{15}\text{N}$ coupling patterns. Following the arguments put forth by Collum^{36,37} for lithium dialkylamides, it is possible to differentiate between cyclic dimers and trimers. A cyclic trimer would have two possible structures: all *cis* (structure B-*cis*) or *cis-cis-trans* (structure B-*trans*) (Figure 23).

Figure 23: Possible isomeric trimers



Structure *B-cis* would have only one signal in the ^{13}C and ^{15}N NMR spectra, while structure *B-trans* would be expected to have a set of two signals in the ^{13}C and ^{15}N NMR spectra, in a ratio of 2:1. This is clearly at odds with the observed spectra. Structure A, however, can exist in only a *cis* or a *trans* geometry, and each form would have only one signal in the ^{13}C and ^{15}N NMR spectra.

Figure 24: *Trans* and *cis* dimers of 1



Thus it can be concluded that 1a and 1d are a 1:1 mixture of isomeric closed dimers whose structures are shown in Figure 24. These dimers each possess a four membered ring of alternating lithium and nitrogen atoms forming the framework for the aggregate.

This conclusion has some support from the chemical literature, since for the structurally related lithium amides there have been only three examples^{34,36,46,124-127} of cyclic trimers, and in all cases there

was no coordinating solvent present. Snaith has concluded that higher oligomers are possible only for ligand-free lithium amides^{35,72,73}.

Another doubly labelled sample of lithiated imine 1 was prepared in toluene/pentane and 4 equivalents of HMPA were added. This sample should demonstrate the effect solely of HMPA since the HMPA does not compete with THF for coordination sites on lithium nor is it assisted by THF in solvating the lithium. At -80°C the ^{13}C spectrum of this sample had two signals for the formyl carbon, at 154.5 and 154.0 ppm, in a 4:1 ratio. (see Figure 25) The ^{15}N NMR spectrum at -90°C also exhibited two signals in a 4:1 ratio, at 108.0 ppm and 104.7 ppm. The downfield (major) ^{15}N signal was split into a 1:1:1 triplet ($J_{\text{N-Li}} = 6.6$ Hz) and the upfield signal was split also into a triplet ($J_{\text{N-Li}} = 7.3$ Hz). The lithium spectrum had a triplet ($J_{\text{N-Li}} = 6.4$ Hz) at 1.4 ppm, a doublet ($J_{\text{N-Li}} = 7.5$ Hz) at 0.6 ppm, a sharp singlet at -0.7 ppm and a broad 'lump' ranging from 0.0 to 1.5 ppm. A curve-fitting program was used to estimate the integrals of each of the signals, and the ratio of the triplet:doublet:singlet was determined to be 2:1:2 (Figure 26). The broad lump was discounted as an impurity peculiar to this sample, since it was not observed in the ^6Li spectrum of a similar natural abundance sample (see Figure 25), but its estimated area was considered during the curve-fitting procedure.

The ^{15}N and ^6Li spectra bear a striking resemblance to those recorded by Jackman for a lithiated aniline under similar conditions, including the addition of 4 equivalents of HMPA⁴⁰. Jackman's interpretation may be a reasonable explanation for the results

Figure 25

^{15}N - ^6Li -1 in toluene/pentane with 4 eq. HMPA.

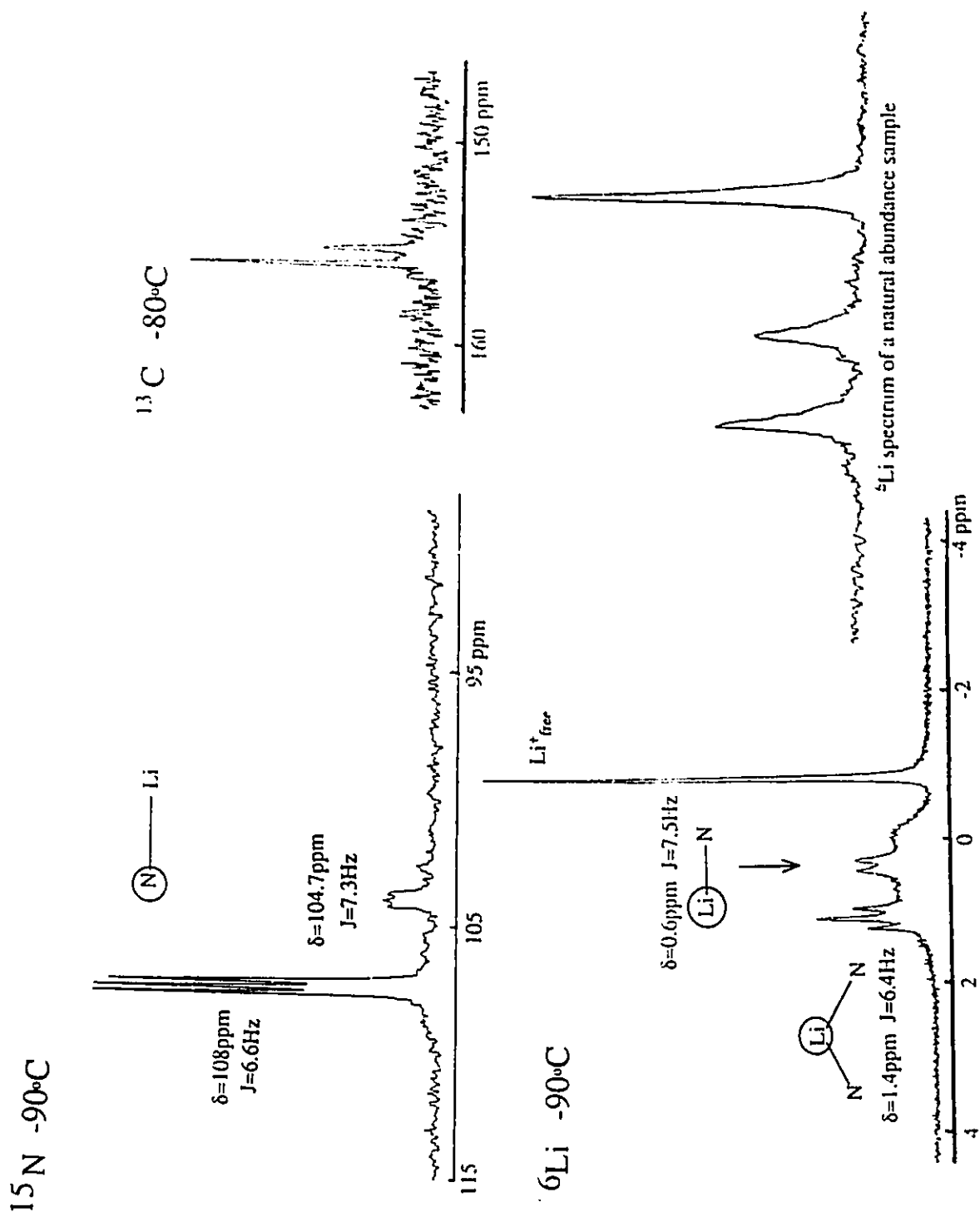
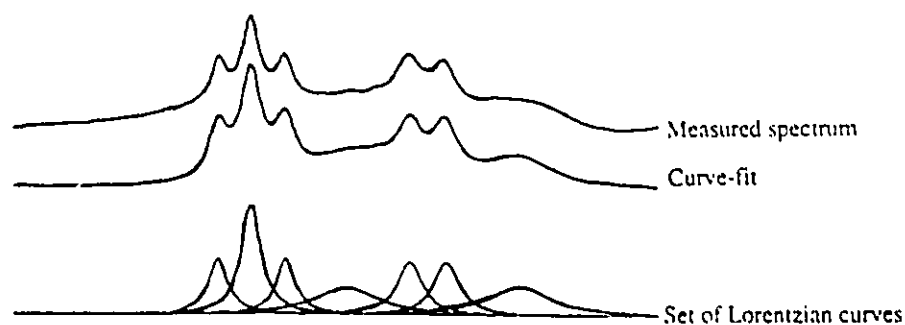


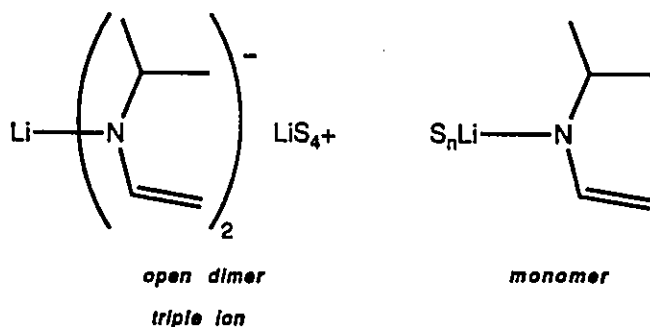
Figure 26: Curve-fit for ${}^6\text{Li}$ spectrum (triplet and doublet only).



reported here: that the lithiated imine exists as a mixture (4:1) of two species, one of which has two different kinds of lithium.

The major species in the ${}^6\text{Li}$ spectrum has one lithium atom bonded to two nitrogen atoms, giving rise to the triplet in the ${}^6\text{Li}$ spectrum, and another lithium not bound to nitrogen, giving the singlet. In this species all of the nitrogens are bound to one lithium atom, resulting in the 1:1:1 triplet in the ${}^{15}\text{N}$ spectrum. This species can be described as an "open dimer" or a "triple ion"^{27,40,55}. Its structure is shown in Figure 27.

Figure 27: Triple ion and monomer of 1



The minor species is one in which each lithium is bound to one

nitrogen and *vice versa*, resulting in a doublet and a triplet in the ^6Li and ^{15}N spectra, respectively, and can be only a monomer.

It is likely that the triple ion structure is favoured under these conditions as a result of the strongly coordinating nature of HMPA, which is able to partially strip lithium from nitrogen to produce "free lithium", which is probably highly solvated by HMPA. Similarly the lithium of the monomeric species is likely to be highly solvated by HMPA. Even under these forcing conditions HMPA alone is unable to solvate the lithium well enough to reduce it to predominantly monomeric structure. Previously (Section 2.1.7) it was shown that HMPA does not strongly displace THF from coordination to the lithiated imine.

It has been previously determined that the addition of HMPA to THF/hexanes solutions of **1** favours **1c**, and T_1 measurements have suggested that **1c** is of similar size to the closed dimers **1a** and **1d**. We can therefore conclude that the signal at 153.2 ppm in THF/hexanes solutions of **1**, which has been described as the single species **1c**, is a triple ion. It should be noted that at temperatures below -80°C the signal at 153.2 ppm in THF/hexanes solutions of **1** broadens further. Thus the possibility remains that this signal does not represent a single species but results from two species, the triple ion and another one, likely a monomer.

The effect of PMDETA was also investigated using the $^6\text{Li}/^{15}\text{N}$ double labelling technique. To a 0.67 M solution of $^{15}\text{N}/^6\text{Li}$ -**1** in toluene/pentane was added 2 equivalents of THF and 1 equivalent of PMDETA (see Figure 28). The investigation was

complicated by the observation in the ^{13}C spectrum of new species introduced in the region of 157 to 160 ppm by the addition of PMDETA, as previously observed in similar natural abundance samples.

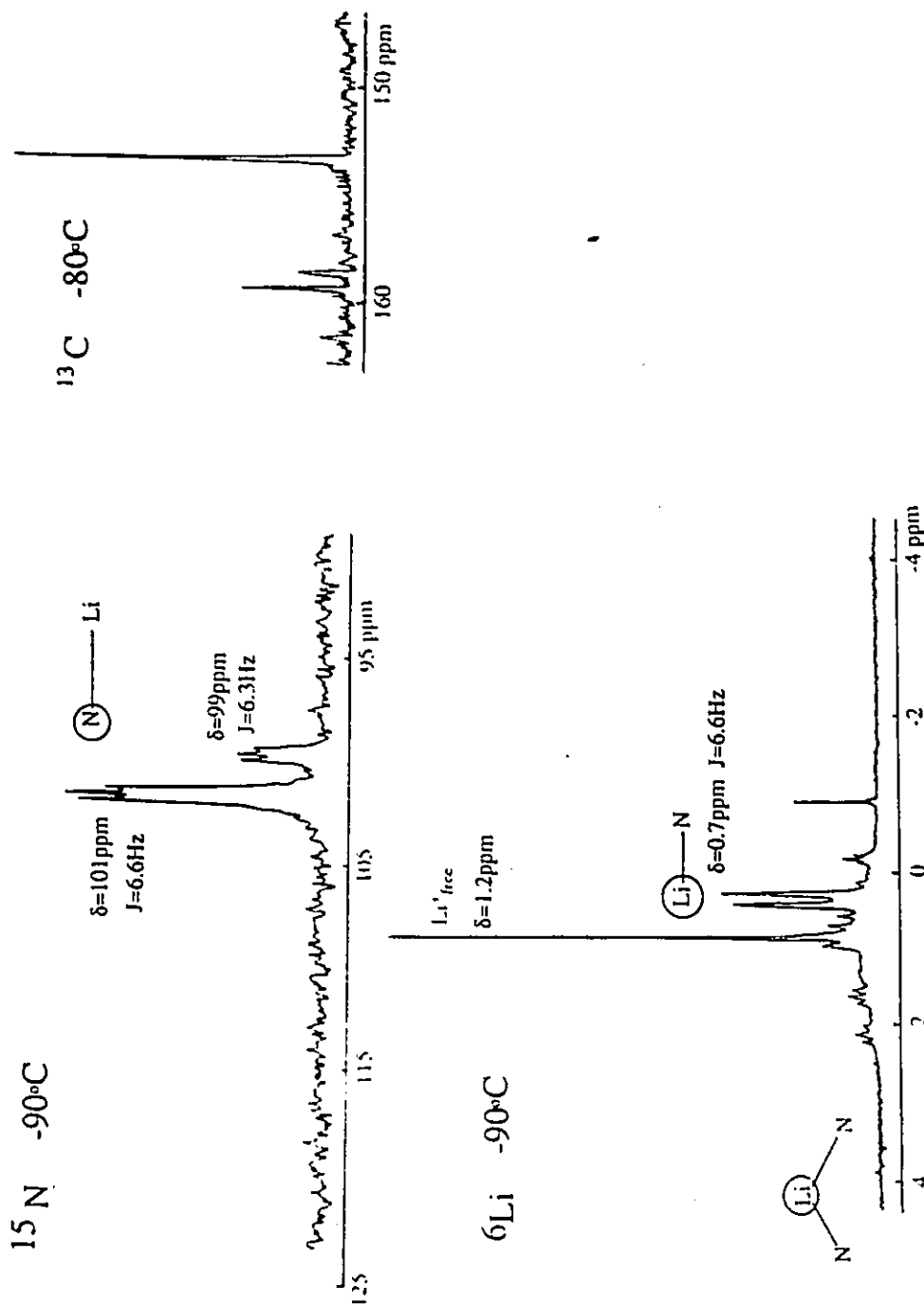
The ^{15}N spectrum exhibited two triplets, one at 101 ppm ($J_{\text{N-Li}} = 6.6$ Hz) and the other at 99 ppm ($J_{\text{N-Li}} = 6.3$ Hz), in a ratio of approximately 3:1. The ^6Li spectrum consists of a sharp singlet, indicating lithium not bound to nitrogen, a doublet ($J_{\text{N-Li}} = 6.6$ Hz), indicating lithium bound to one nitrogen, and a series of three or more 1:2:1 triplets, indicating lithium bound to two nitrogen atoms.

The ^{15}N spectrum of the lithiated imine sample containing PMDETA shows that all of the nitrogen atoms in both species are bound to only one lithium atom. The species present must be either triple ions or monomers: there cannot be any closed dimers. The coupling patterns in the ^6Li spectrum suggests that there is a mixture of triple ions and monomers formed by the addition of PMDETA. The doublet in the ^6Li spectrum must be a monomer, and the triplets and the sharp singlet are characteristic of triple ions. That there is a variety of triple ion structures may be explained by analogy to the solution structure of *neo*-pentyllithium in the presence of PMDETA reported by Fraenkel¹⁰³, in which rotamers about the lithium- CH_2 bond and various conformers of the PMDETA ligand were observed in low temperature ^{13}C NMR spectra. Similar slow rotations may be responsible for the behaviour observed in the low temperature NMR spectra of 1.

In the chemical literature there are examples of correlations

Figure 28

^{15}N - ^6Li -1 in toluene/pentane with 2 eq. THF and 1 eq. PMDETA



between chemical shifts and aggregate structure. For example, in many organolithium compounds the ^{13}C resonance of the carbon closest to lithium in the more highly aggregated species is downfield from the less highly aggregated species^{17,26,32,37,42,53,103,128,129}, but there are enough exceptions from this trend^{15,31} that ^{13}C shifts should be considered a poor indicator of aggregate structure. Collum has claimed a correlation between ^{15}N - ^6Li coupling constants and aggregate structure in which dimers have couplings in the range of 3-4 Hz and monomers have couplings in the range of 6-7 Hz³⁷. Since the range of coupling constants is small and the set of data limited to a few examples such correlations should at this stage be viewed with extreme caution. (Recently Collum reported that dimeric di-*iso*-propylamine had $J_{\text{N-Li}}=5.0$ Hz³⁸.) Nevertheless, the ^{15}N - ^6Li coupling constants measured for lithiated imine 1 are consistent with the trends described by Collum: the dimer has $J_{\text{N-Li}}=3.4$ Hz while the triple ion has $J_{\text{N-Li}}\sim 6.5$ Hz and the monomer has $J_{\text{N-Li}}\sim 7.4$ Hz. In the three examples^{39,40,42} in which lithiated organo-nitrogen compounds have been investigated by ^{15}N - ^6Li double-labelling NMR experiments and in which both dimers and monomers have been observed, no trend was observed in the ^{15}N NMR shifts of monomers relative to the ^{15}N NMR shifts of the more highly aggregated species. Therefore, ^{15}N shifts do not afford information regarding aggregate structure. Similarly, no trend exists in ^6Li NMR shifts with respect to aggregation states.

2.1.11 Molecular Mechanics Calculations

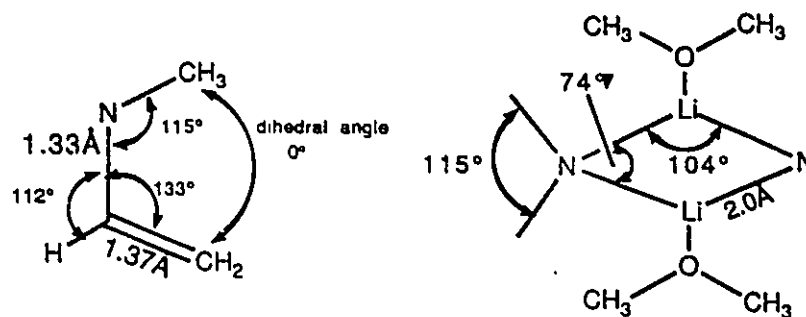
Molecular mechanics calculations have been found to be a useful method for predicting energies of many molecules and transition state structures¹³⁰. In molecular mechanics calculations the total energy of a molecule is calculated as the sum of all the energies associated with bonds, bond angles, torsion angles and non-bonded (van der Waals) interactions¹³¹. Each of these factors is expressed as a force constant (or a van der Waals repulsive potentials) whose magnitudes are determined empirically. Starting from a prescribed geometry, the geometry of the molecule whose energy is to be determined is modified such that a minimum is found on the potential energy surface. The key to success in molecular mechanics calculations is to use a good set of force-field parameters for the system under study.

Molecular mechanics calculations were applied to the structures of the lithiated imine **1** in an effort to determine if the relative energies could be calculated for the *cis* and *trans* dimeric structures assigned for species **1a** and **1d**.

MM2 molecular mechanics calculations were used to estimate the relative stabilities of the *cis* and *trans* dimers of lithiated *N-iso*-propylacetaldimine. The program used for the calculations did not have force-field parameters suitable to the Li-N-Li-N ring and parameters were not readily available, so the geometry of the ring was held rigid using bond lengths and bond angles typical of those reported from X-ray crystallographic studies of lithiated organo-nitrogen molecules (Figure 29).

The angle at nitrogen was set at 74° , the angle at lithium at 104° , the Li-N bond length was set at 2.0\AA , and the ring was restricted to a plane, as is experimentally typical of lithium-nitrogen rings^{34,35,50,56-58,60,62,67,72,73,76,78}. The organic portion of the molecule was treated as an ene-amine, whose force constants were easily parameterized using data included in the program, except that the optimal lengths and angles through the aza-allylic portion of the molecule were set at the angles calculated by Fraser and Houk for lithiated imines using 4-31G molecular orbital calculations⁹⁹.

Figure 29: Optimal geometries for MM2 calculations



Each of the lithium atoms was solvated by a molecule of dimethyl ether, which was intended to approximate solvation by THF. The solvent was placed in the plane of the N-Li-N-Li ring, with the lithium having a trigonal-planar geometry.

The *cis* and *trans* dimeric structures were optimized starting from *syn* geometry at the aza-allylic portion, and local minima were determined. No effort was made to determine minimized energies for dimers containing *anti* lithiated imines. It was found that the energies of the *cis* and *trans* dimers differed by only 0.154 kcal

mole⁻¹, which means that the ratio of the two closed dimers should be approximately 60:40 (*cis:trans*) at -80°C.

As described above, in the calculations the lithium-nitrogen ring structural element was kept rigid. This rigidity would be expected to increase the amount of strain in the molecule, since it might be expected that twisting or other motions of the ring would serve to reduce unfavourable steric interaction. Thus, should some flexibility of the ring be allowed one might expect the energies of the optimized structures to be lowered and the energy difference between the *cis* and *trans* dimeric structures to be less.

The small calculated energy difference between the two dimers is in agreement with the experimental observation that **1a** and **1d** are in equal proportion at -80°C, and is therefore supportive of the conclusion that those two species are isomeric forms of closed dimers.

2.1.12 Models for Inter-Aggregate Exchange.

Having established that species **1a** and **1d** are a pair of cyclic dimers, and that species **1c** in THF/hexanes solutions is most likely an open dimer, attention can now be focussed on the degree of solvation of the three species.

It was found previously that the proportion of **1c** relative to **1a** and **1d** was sensitive to THF concentration and to bulk concentration, but that the ratio of **1a** to **1d** was insensitive to these changes in the medium. These observations indicate that the two species **1a** and **1d** are equally solvated while species **1c** is more

highly solvated than the other two species. Using these observations in conjunction with the structural information provided by the double-labelling experiment it was possible to develop several models for the equilibrium among species **1a**, **1c** and **1d**. Model equilibrium equations were proposed in which species **1c** was an open dimer, consistent with the double-labelling results, and also a monomer.

In all of the models species **1a** and **1d** were considered as identical dimers in order to simplify the calculations. The sum of **[1a]** + **[1d]** will be referred to as **[D]**, and the concentration of triple ions will be termed **[T]**. The term S_{free} refers to solvent which is not coordinated to lithium, **S** to solvent coordinated to the lithium, and **M** to monomer.

Model 1: Triple Ion \leftrightarrow Dimer



$$K = \frac{[D.nS] [S_{\text{free}}]^{(m-n)}}{[T.mS]}$$

$$m=3,4,5; \quad n=2,3,4 \\ m > n$$

$$[S_{\text{free}}] = [S_{\text{total}}] - m[T.mS] - n[D.nS]$$

Model 2: Monomer \leftrightarrow Dimer



$$K = \frac{[\text{D.nS}] [\text{S}_{\text{free}}]^{(m-n)}}{[\text{M.mS}]^2}$$

$$m=3; n=2,3,4$$

$$[\text{S}_{\text{free}}] = [\text{S}_{\text{total}}] - 2m[\text{M.mS}] - n[\text{D.nS}]$$

For each of the models the equilibrium constant K was determined for "standard" conditions, having 0.67M of 1 in THF/hexanes solution. Under these conditions the total THF concentration was 6.23M, and the ratio of 1a:1c:1d was 36:28:36. For a triple ion/dimer equilibrium the concentrations of the species would be $[\text{D}] = (0.36 \times 0.67 \text{ moles l}^{-1})$ and $[\text{T}] = (0.28/2 \times 0.67 \text{ moles l}^{-1})$, while for a monomer/dimer equilibrium the concentrations would be $[\text{D}] = (0.36 \times 0.67 \text{ moles l}^{-1})$ and $[\text{M}] = (0.28 \times 0.67 \text{ moles l}^{-1})$.

Once the equilibrium constant was determined for standard conditions the ratio of species was predicted from the model for other conditions of lithiated imine concentration and THF concentration. Each of the models was tested by accurately recalculating the ratio of species under the standard conditions used for deriving the equilibrium constant. The three cases to which each of the models was applied were (1) 0.33 M 1 in a mixture of THF, hexanes and toluene, having 3.12 M THF, (2) 0.33 M 1 in THF/hexanes, having 11.8 M THF, and (3) 0.52 M 1 in toluene/hexanes with 2.61 M THF added. The results are tabulated in Table 6.

Table 6

Models for aggregation and solvation.

<u>MODEL</u>	<u>m</u>	<u>n</u>	<u>predicted ratio 1a:1c:1d</u>		
			<i>conditions</i> →	(1)	(2)
<i>observed</i>	-	-	39:21:40	22:55:22	38:21:41
<i>triple ion/</i>					
dimer	3	2	42:16:42	28:42:28	47:6:47
"	4	2	45:10:45	17:66:17	49:2:49
"	4	3	42:16:42	27:46:27	48:4:48
"	5	2	47:6:47	17:66:17	-----
"	5	3	45:10:45	17:66:17	48:4:48
"	5	4	42:16:42	27:46:27	47:6:47
<i>monomer/</i>					
dimer	3	2	50:~0:50	6:88:6	-----
"	3	3	45:10:45	15:70:15	-----
"	3	4	42:16:42	28:44:28	-----

The results of the calculations of various equilibria show that models in which there is a lesser degree of [THF] dependence fit the observed concentration and THF dependence of the proportions of 1a, 1c and 1d better than do models having a greater dependence on THF concentration. Although none of these simplified models fits the observed data under all combinations of total concentration and THF concentration, triple ion/dimer equilibria appear to be more appropriate. This is consistent with the previous assignment of the

solution structures of **1a**, **1c** and **1d** based on $^{15}\text{N}/^6\text{Li}$ couplings. The equilibrium models also allow some insight into the degree of solvation of the triple ion and the dimers. Models in which the triple ion ($[\text{Li}(\text{NR}_2)_2]^- \cdot \text{Li}^+$) is solvated by only one more THF molecule than the dimer appear to predict ratios of species better than models in which the triple ion is solvated by two THF molecules more than the dimer: the ratio appears to be only moderately sensitive to THF concentration. The failure to fit exactly any of the experimental results may be due to the simplicity of the models, which do not account either for the coexistence of dimeric species possessing different degrees of solvation or for the coexistence of both monomers and triple ions.

It can be tentatively concluded that the dimer is solvated by either 2,3 or 4 THF molecules and that the triple ion is solvated by one more THF molecule than is the dimer.

2.1.13 Alkylation Products of 1.

To this point it has been assumed that the lithiated imine **1** possesses *syn* geometry. Although studies by Fraser have shown that changes in ^{13}C chemical shifts upon lithiation of imines can be indicative of stereochemistry^{7,88}, the stereochemistry of the alkylation products is the most compelling evidence for the stereochemistry of the anion. In order to confirm the *syn/anti* stereochemistry of **1**, methylation reactions were performed using conditions which were reported to result in a high proportion (>95%)

of *syn* alkylation products. Other alkylation reactions were conducted in solvent mixtures in which the structures of the dominant species were known in order to determine if differences in solution structures (ie. dimers *versus* triple ions and monomers) influence the proportion of *syn* and *anti* alkylation products.

Samples of lithiated imine **1** in a variety of solvent conditions were alkylated by dropwise addition of methyl iodide with vigorous stirring at -78°C , following as closely as possible the method which is reported to give >95% *syn* alkylation^{11,12,132,133}. The ^{13}C NMR spectra of the samples were measured immediately after addition of the methyl iodide. The total elapsed time for sample manipulation prior to acquisition of the spectrum was less than 3 minutes. In the alkylated samples there was often a precipitate (presumably lithium iodide) which reduced the resolution of the spectra and may also have had an effect on chemical shifts.

A 0.12 M sample of **1** in THF/hexanes (20:1) was methylated as described above. These solvent conditions were selected in order to reproduce conditions known to result in exclusively *syn* methylation. It was found that there were two initially formed products, in a ratio of 90:10 (see Table 7). The major product exhibited ^{13}C NMR signals at 165.8 and 51.9 ppm, for the formyl and α -carbons of *N*-*iso*-propylpropionaldimine, while the minor product had shifts of 162.8 and 63.8 ppm. Upon warming the major initial product converted to the minor one, with a half-life at 0°C of less than 5 minutes. On the basis of known alkylation behaviour of lithiated imines^{9,11,12} and the observed chemical shift differences⁸⁸, it can be concluded that the dominant species formed

initially upon alkylation was the *syn* alkylation product, which isomerized to the *anti* upon warming. The chemical shifts of the formyl and α -carbon atoms of the *anti* isomer of the expected alkylation product, N-*iso*-propylpropionaldimine, independently synthesized, were found to be 161.7 and 63.2 ppm in THF solvent (relative to THF δ 69.0ppm). In most samples a side product was formed due to the alkylation of LDA, yielding methyl di-*iso*-propylamine. This compound has a ^{13}C NMR signal at 52.0 ppm, close to the *iso*-propyl resonance of the *syn* imine product.

A 0.67 M sample of **1** alkylated in toluene/hexane solvent to which 2 equivalents of THF and 4 equivalents of HMPA were added (composed predominantly of triple ion species **1c** and monomer) initially gave mostly the *syn* product, at 163.8 and 52.1 ppm, and a mixture of 5% of unreacted **1** and two other unidentified products (about 5-10% each), having shifts of 167.5, 165.6 ppm. After warming to +20°C for 1 hour and then again measuring the NMR spectrum at -80°C the dominant species was one having resonances at 161.7 and 63.0 ppm, which was assigned as the *anti* isomer. A sample of **1** in THF/hexanes (a mixture of **1a**, **1c** and **1d**) gave as the initially formed products two species with NMR resonances at 164.2 and 51.7 ppm and 162.0 and 63.6 ppm, respectively, in a 83:17(\pm 5) ratio. These were assigned as the *syn* and *anti* products. After warming the dominant species was the *anti* isomer, with a resonance at 162.0 ppm. A sample alkylated in toluene/hexanes to which 2 equivalents of THF were added (species **1a** and **1d**) gave as the alkylation product predominantly a species with a ^{13}C resonance at 170.1 ppm and a minor product (~16%) at 169.0 ppm. The chemical

shifts of these species suggest that the major product was the *syn* imine and after warming there was a single broad peak observed at 168.4 ppm, indicating isomerization to the *anti* product.

Table 7

Alkylation product *syn/anti* ratios for 1.

<u>Alkylation Conditions</u>	<u>%<i>syn</i></u>	<u>%<i>anti</i></u>
0.12 M in THF	90±5	10±5
0.67 M in THF/hexanes	83±5	17±5
0.67 M in toluene/hexanes	84±5	16±5
+ 2 eq. THF		
0.67 M in toluene/hexanes	90±5	10±5
+ 4 eq. HMPA		

In each of the samples the major initial product was the *syn* isomer, having a downfield chemical shift for the formyl carbon atom and an upfield chemical shift for the α -carbon, while the thermodynamically more stable product in each case was the *anti* isomer, exhibiting chemical shifts for the formyl carbon upfield and the α -carbon atom downfield from the kinetically favoured *syn* alkylation product. The variation of chemical shifts among the samples may be the result of solvent effects on the chemical shifts of the products, or the result of the effect of the lithium iodide precipitate.

The dilute THF sample gave mostly (90%) *syn* product, while

the more concentrated THF/hexanes solution of **1** gave a 83:17 mixture of *syn* and *anti* products. This difference may result from heating of the more concentrated sample during the alkylation.

The ratio of *syn* to *anti* products represents a minimum value since isomerization may have occurred prior to or during the NMR measurement, so the sample at the moment of alkylation may have had a higher proportion of *syn* products. Although it was found that at -78°C there was no isomerization of the product in 90 minutes, suggesting that the *syn/anti* ratios measured represent true product distributions at the moment of alkylation, the sample (or localized regions within the sample) may have briefly warmed during the alkylation such thermal isomerization was possible for a short period of time immediately following alkylation. The rate of isomerization may also be solvent dependent, which may account for the different ratios of initial alkylation products observed for each of the three samples discussed above.

It can be concluded that by changing the solvent in which alkylations of lithiated *N*-*iso*-propylacetaldimine are performed that no significant changes in alkylation geometry result. Thus, in this case at least, solvent, and therefore, by inference, the differences between the structures of the closed dimeric species **1a** and **1d** and the open dimer **1c**, appear not to have an effect on the preference for *syn* alkylation of this aldimine. Collum and colleagues have found evidence that triple ions were not the reactive species in the methylation of a lithiated hydrazone⁵⁵.

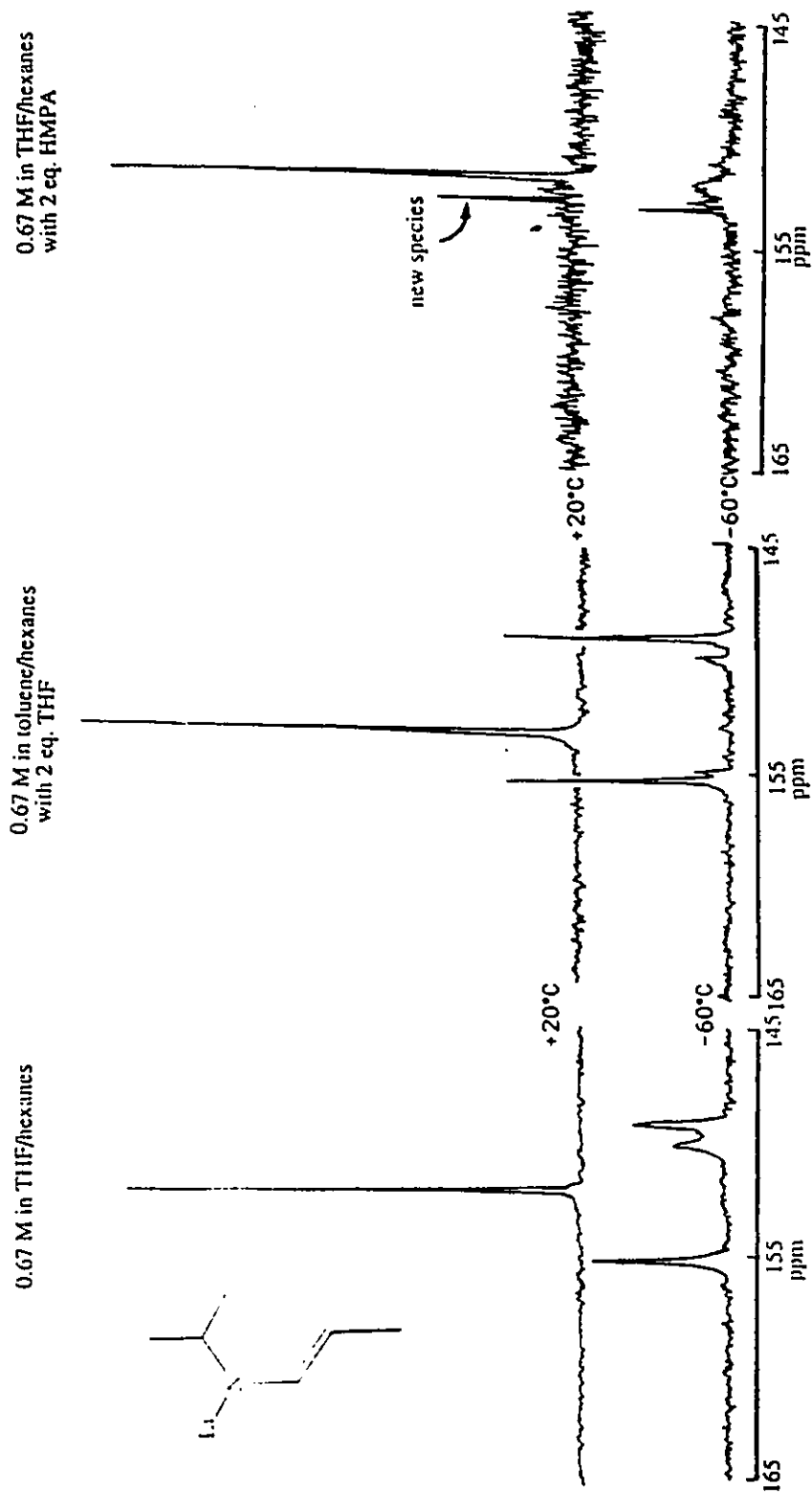
2.2.1 Lithiated N-*iso*-propylpropionaldimine (3): General Observations and Effect of Temperature.

Lithiated N-*iso*-propylpropionaldimine, (3), was prepared by deprotonation of the parent imine using LDA. At +20°C the ^{13}C resonance of the formyl carbon of the imine shifted upon lithiation from 161.7 ppm (relative to THF= δ 69ppm) to 152.1 ppm and broadened in a 0.67M solution in THF/hexanes. As the temperature of the sample was lowered the formyl carbon displayed a series of decoalescences. A coalescence occurred between -15°C and -30°C, below which two signals of roughly equal proportion were observed for the formyl carbon, at 155.3 and 150.0 ppm. Below -35°C there was little further change in the spectrum until temperatures approached -60°C, when the signal at 150.0 ppm became resolved as two signals, at 150.1 and 149.2 ppm. These patterns were generally repeated at the other ^{13}C signals of the lithiated imine. The anion precipitated from THF/hexanes (1.8:1) solution at lower temperatures.

A sample of lithiated imine 3 prepared in toluene/hexanes solution to which 2 equivalents of THF were added exhibited one signal at 152.4 ppm which underwent a decoalescence near -30°C, resolving into two signals of equal integral having shifts of 155.3 and 149.0 ppm, and a minor species at 150.2 ppm (see Figure 30). It may be proposed that the minor species is the same species as observed at 150.1 ppm in the THF/hexanes solution, but that it is a more highly solvated species, and therefore disfavoured under conditions of low THF concentration. Similarly the two major species at 155.3 and

Figure 30

^{13}C spectra of **3** at +20°C and -60°C (formyl carbon).



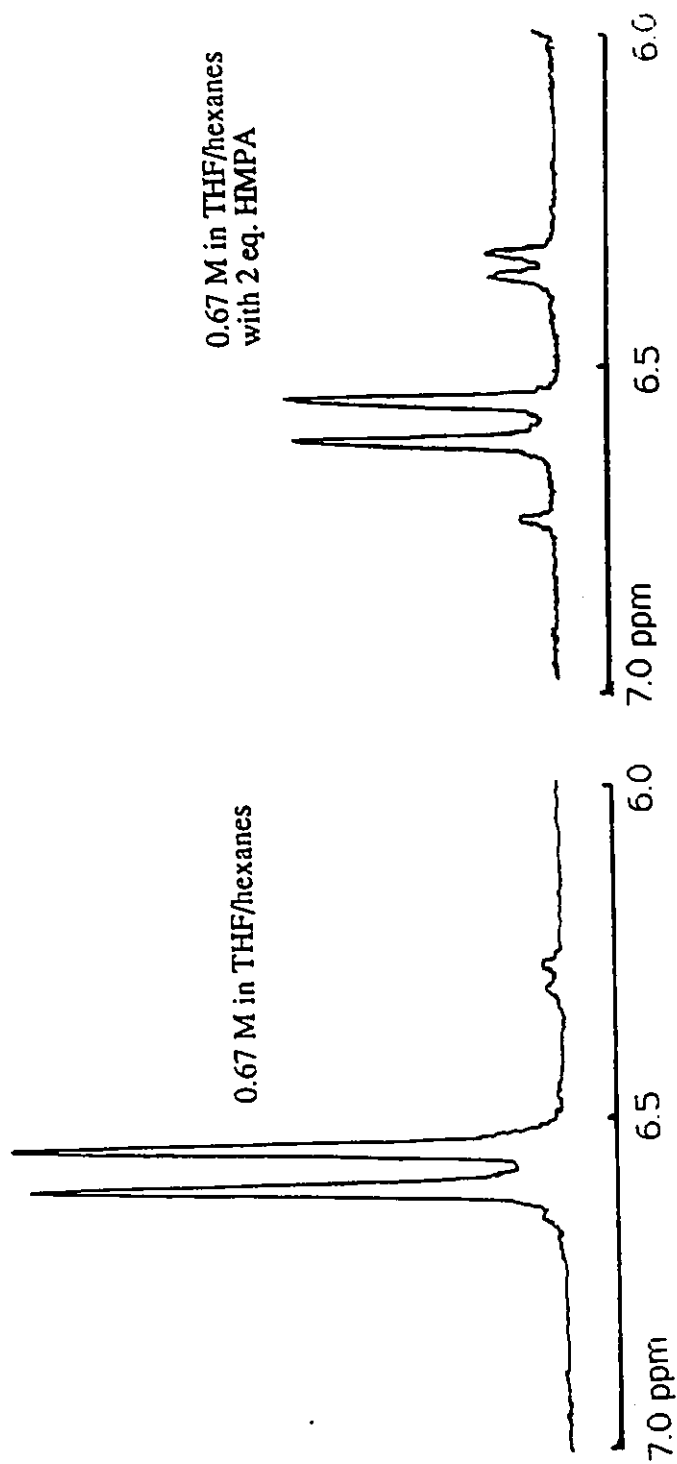
149.0 ppm may be the same two species which have similar chemical shifts in the THF/hexanes solution.

There is a very strong similarity between the temperature dependent behaviours of lithiated imines **1** and **3**, in that both exhibit three signals at low temperature in THF/hexanes solutions (see Figure 30), but that under conditions of low THF concentration only two of these signals predominated. In light of the parallel behaviours of lithiated imines **1** and **3** as a function of temperature and solvent, as observed in their NMR spectra, one may make conjectures about the solution structures of **3** based on the structures determined for **1**. Although it is always with caution that one makes inferences about one structure based on evidence from another molecule, the almost exact duplication of behaviour between **1** and **3** and the fact that they differ by only one methyl group justifies such an extrapolation. Thus it will be proposed that lithiated imine **3** exists in THF/hexanes solution as a mixture of dimers (155.3 ppm and 149.0 ppm) and a triple ion (150.1 ppm).

2.2.2 Lithiated N-/iso-propylpropionaldimine (3): Effect of HMPA.

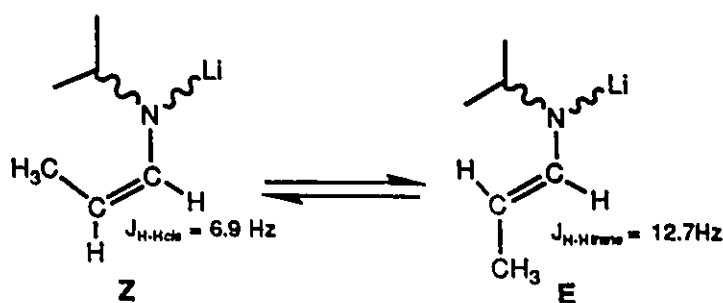
In only one respect did the behaviour of **1** and **3** differ substantially. In THF/hexanes or toluene/hexanes solutions of **3** to which 2 equivalents of HMPA have been added two signals were observed for the formyl carbon in the ^{13}C spectrum at +20°C. These two signals had chemical shifts of 153.2 and 152.1 ppm and were in a ratio of 1:4 in THF/hexanes (see Figure 30). In toluene/hexanes

Figure 31

 ^1H spectra of 3: effect of HMPA

solutions the two signals, at 153.5 and 152.6 ppm, were in a ratio of 1: 2.3 at +20°C. The behaviour in the proton spectrum mirrors that in the ^{13}C spectrum. At +20°C in the proton spectrum of a THF/hexanes solution of **3** to which 2 equivalents of HMPA were added (Figure 31) the formyl proton exhibited two doublets, in a 1:4 ratio. The major species, at 6.66 ppm, was a doublet with $J=12.7$ Hz, typical of coupling to a *trans* vicinal proton across a double bond, indicating that there is an *E* configuration at the partial C-C double bond (Figure 32).

Figure 32: ^1H - ^1H Couplings for **3**: Effect of HMPA



The minor species, at 6.27 ppm, had coupling indicative of a *Z* configuration ($J=6.9$ Hz). Similarly, in toluene/hexanes solutions of **3** containing 4 equivalents of HMPA the ^1H NMR spectrum exhibited two resonances for the formyl proton, having coupling similar to the THF/hexanes sample, and in a similar ratio as measured for the two signals in the ^{13}C spectrum. In toluene/hexanes solutions to which no HMPA was added only the major species ($J=12.7$ Hz) was evident, but the region of the spectrum was close to the resonances of the toluene and was partially overlapped by signals which were apparently spinning sidebands.

In the proton NMR spectrum of a 0.67 M THF/hexanes solution

of **3** a small amount, about 3%, of the minor species ($J=6.9$ Hz) was also observed (Figure 31) .

At +20°C in THF/hexanes the ratio of the minor species, **3-Z**, to the major species (**3a**, **3b** and **3c** are in rapid exchange at +20°C and exhibit a single signal: **3-E**) was dependent upon HMPA up to 4 equivalents, (see Table 8), beyond which no further change was observed. The addition of PMDETA or TMEDA did not cause an increase in the proportion of **3-Z** above 3%.

Table 8

Effect of HMPA on the ratio of **3-E** : **3-Z**

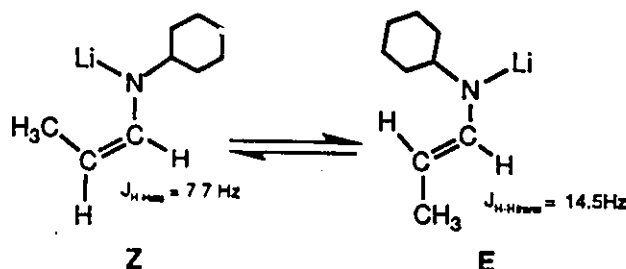
<u>Eq. HMPA</u>	<u>3-E:3-Z</u>
0	97:3
1	90:10
2	80:20
4	70:30
5	70:30

In a solution of the **3** in toluene/hexanes the ratio of **3-E** to **3-Z** was found to be only 75:25 even when 4 equivalents of HMPA were added, suggesting that perhaps the magnitude of the effect of HMPA on the stereochemistry of the lithiated imine is enhanced by the presence of THF, or in other words, that HMPA and THF work cooperatively. It was found that the addition of PMDETA to a THF solution of **3** did not produce a measureable amount of a species having a ^{13}C resonance in the region of 153-153.5 ppm, where the

signal for **3-Z** would be expected.

The behaviour observed for **3** is the same as reported by Newcomb and Bergbreiter and coworkers regarding the ^1H spectrum of lithiated N-cyclohexylpropionaldimine in THF solutions to which HMPA had been added⁹⁰. They had also observed (at +20°C) a single species in the ^1H NMR spectrum of THF solutions of the lithiated imine, but two species upon addition of 2 equivalents of HMPA. The coupling patterns of the two species indicated also an **E** configuration in the major species and a **Z** configuration in the minor species. Their interpretation was, as shown in Figure 33, that the **E** isomer had the usual *syn* configuration of the aza-allylic portion of the molecule, but that the **Z** isomer has an *anti* configuration of the aza-allylic moiety (likely due to the unfavourable steric interactions of the allylic methyl group and the N-cyclohexyl group).

Figure 33: Lithiated N-cyclohexylpropionaldehyde: **Z-anti** and **E-syn** isomers



The evidence offered by Newcomb and Bergbreiter concerning the *syn-anti* stereochemistry of their lithiated propionaldimine relies solely on inferences based on the stereochemistry about the partial C-C double bond. Proof of the possible *anti* configuration of the

aza-allylic portion in the **Z** isomer would require either direct evidence from NMR or evidence of initially formed *anti* alkylation products in a proportion similar to the proportion of the **Z** isomer.

One may speculate about the origin of the **E/Z** isomerism in **3** based on structural features established for lithiated **1** and extrapolated to **3**. In the absence of HMPA it has been proposed that the lithiated imine exists as a mixture of dimers and a triple ion. Upon addition of HMPA triple ions and monomers should be favoured. Since the **Z** isomer is observed only under such conditions, it may be suggested that the **Z** isomer is the preferred conformation of monomeric lithiated imine **3**. The new observation that small amounts of **3-Z** are present even in THF/hexanes alone shows that HMPA is not necessarily the only factor affecting the **E-Z** stereochemistry, although other ligands, such as PMDETA and TMEDA did not increase the proportion of **3-Z**. One possible explanation for this behaviour is that in the monomer there is η^3 -coordination of the aza-allylic moiety which stabilizes the *anti* isomer^{43,60}.

2.2.3 Alkylation Products of **3**.

Samples of lithiated imine **3** in a variety of solvent conditions were alkylated by either one of two methods: addition of methyl iodide with vigorous stirring at -78°C to a 0.67 M solution of **3** in a flask, followed by transfer via cannula to an NMR tube, or addition of methyl iodide directly to a dilute (0.12 M) solution of **3** in an NMR tube, and the ¹³C NMR spectrum of the samples were measured immediately after addition of the methyl iodide. The total elapsed

time for sample manipulation prior to acquisition of spectra was less than 3 minutes, during which time the mixture was kept at -78°C . The product of methylation of 0.12 M samples of **3** in THF/hexanes (20:1) was comprised of a mixture containing 93(\pm 5) % (Table 9) of a product characterized by ^{13}C resonances at 168.6 and 51.6 ppm and a remaining portion of a product having ^{13}C resonances at 166.3 and 63.4 ppm. Warming of the solution resulted in isomerization of the the major species to the minor, with a half-life of 125 minutes at -20°C . The initial major species was assigned as the *syn* isomer of the expected product, *N-iso-propyl-iso-butyraldimine*, while the minor product was assigned as the *anti* isomer. Alkylation of 0.67 M THF/hexanes (1.8:1) resulted in an initial product mixture which was 78 \pm 5% *syn*. This lower yield of *syn* products may be the result of isomerization due to heating of these more concentrated samples during the alkylation reaction. This heating may also account for the failure to obtain greater than 94% *syn* products from methylation of the 0.12 M samples of **3**. In most samples a side product was formed due to the alkylation of LDA, yielding methyldi-*iso*-propylamine. This compound has a ^{13}C NMR signal at 52 ppm, close to the *iso*-propyl resonance of the *syn* imine product.

A sample of the lithiated imine **3** was prepared as a 0.12 M solution in THF/hexanes (20:1) to which 2 equivalents of HMPA were added. A ^{13}C spectrum of this sample revealed that the ratio of **3-E** to **3-Z** was 80:20 (\pm 5) at both $+35^{\circ}\text{C}$ and at -80°C . When this sample, and another identical sample were alkylated, the ratio of *syn* to *anti* products was found to be 80:20 (\pm 5). It may be concluded that, within experimental error, the ratio of *syn* to *anti* alkylation

Table 9Alkylation product *syn/anti* ratio for **3**

<u>Alkylation Conditions</u>	<u>%<i>syn</i></u>	<u>%<i>anti</i></u>
0.12 M in THF (NMR tube)	93±5	7±5
0.12 M in THF/hexanes	80±5	20±5
+ 2 eq. HMPA		
0.67 M in THF/hexanes	78±5	22±5
0.67 M in THF/hexanes	33±10	66±10
+ 2 eq. HMPA		

products was the same as the ratio of the lithiated imine species **3-E** to **3-Z**. Therefore it can be concluded that the species **3-Z** has *anti* stereochemistry.

Upon methylation of a 0.67 M THF/hexanes solution to which 2 equivalents of HMPA had been added the major product formed initially was a product having resonances for the α -carbon atom at 62.7 ppm and for the formyl proton at 166.3 ppm, indicative of an *anti* stereochemistry. The minor species had a signal at 51.2 ppm, indicative of *anti* stereochemistry, and a weak signal at 165.3 ppm. Since the signal-to-noise ratio for the formyl carbon was poorer than at the α -carbon and the shift differences for the formyl carbon are typically much smaller than those at the α -carbon, the *syn/anti* ratio measured at the α -carbon was considered to be a better indication of the proportions of the species under consideration. The ratio of species measured at the α -carbon was 2:1, indicating a *syn/anti* ratio of 33:66 (± 10)%. A repeat of this alkylation experiment produced >60% *anti* alkylation product. A solution of the same

concentration, but with no HMPA, alkylated by the same method gave >75% *syn* products. These results tend to confirm that the addition of HMPA causes the formation of an *anti* anion which alkylates to give *anti* products. Again, local heating during the methylation reaction may account for the higher proportion of *anti* products than would be expected based on the ratio of 3-E to 3-Z (80:20 ±5).

2.3.1 Determination of *Syn/Anti* Stereochemistry.

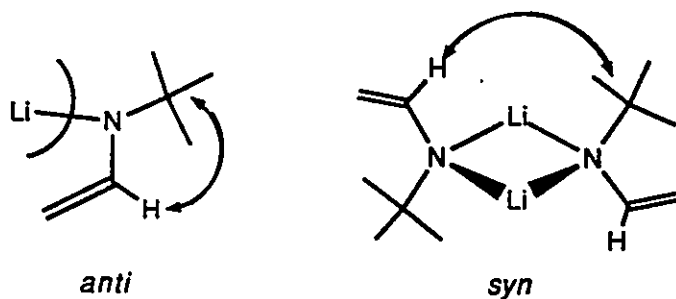
An effort was made to determine *syn/anti* stereochemistry using the NOE-difference NMR experiment to determine spatially close sets of nuclei^{113,114}. It was hypothesized that in *anti* lithiated aldimines protons on the nitrogen substituent should be close to the formyl proton, and that in *syn* lithiated imines the substituent should be close to the vinyl protons and that these close interactions should result in measurable NOE differences upon irradiation of the protons of the nitrogen substituent.

NOE-Difference spectra were measured at room temperature for N-*tert*-butyl-acetaldimine (2-H) and N-*iso*-propylacetaldimine (1-H) and their lithiated derivatives (2 and 1). All prior evidence suggests that both of the parent imines have *anti* stereochemistry at the C=N double bond and there has been some indication that the lithiated *tert*-butyl imine has *anti* stereochemistry about the aza-allylic portion^{7,11}. It remained to determine whether the *anti* stereochemistry would cause an NOE effect on the formyl proton upon irradiation of the protons on the nitrogen substituent, and to then

measure the NOE on the lithiated acetaldimines.

Irradiation of the *tert*-butyl group of imine **2-H** resulted in a $13\pm 5\%$ NOE at the formyl proton. The same experiment conducted on the lithiated imine **2** resulted in a 10% NOE at the formyl proton. When this result is considered in conjunction with the other published evidence (alkylation and ^{13}C shifts) it can be concluded that lithiated *tert*-butylacetaldimine **2** has *anti* stereochemistry. One caveat must be mentioned: the MM2 calculations indicated that the distance between the *tert*-butyl group and the formyl proton of the opposite lithiated imine, if both have *syn* geometry in a *trans* dimer, would be ~ 2.4 Å, which is approximately equal to the expected distance in an *anti* lithiated imine between the *tert*-butyl group and its own formyl proton (~ 2.3 Å) (see Figure 34).

Figure 34: Possible origins of ^1H - ^1H NOE in **2**



NOE difference measurements on *N*-*iso*-propylacetaldimine result in a 6% NOE at the formyl proton upon irradiation of the *iso*-propyl methyl protons. Irradiation of the methyl protons of the lithiated *iso*-propyl imine resulted in no NOE at the formyl proton and a detectable, but not quantifiable, NOE at the methine proton. The NOE at the *iso*-propyl methine proton serves to confirm that the experiment was conducted under conditions in which NOE effects can

be detected. The lack of a positive NOE at the formyl proton might be indicative of *syn* geometry about the aza-allylic portion of the molecule, but the absence of evidence can never be considered a proof. Only had an NOE been measured at the *endo* methylene proton could *syn* geometry be proven, but the *endo* methylene proton is likely to experience NOE effects only from its geminal (*exo*) partner, making it unlikely that irradiation of the *iso*-propyl methyl protons would result in NOE effects at the *endo* methylene proton.

2.4.1 Effect of a Chelating Bis-Phosphine Oxide on Lithiated Imines.

HMPA was found to have an effect on the types of aggregates predominating in solutions of lithiated imine **1**, causing dimeric structures to be converted into triple ions and monomers. It was proposed that a stronger effect may result from coordination of the lithium by a stronger ligand, in particular by a bidentate ligand of structure similar to HMPA. The ligand selected was nonamethylimidodiphosphoramidate (NIPA), having the structure $[\{(NMe_2)_2P(O)\}_2NMe]$, which has been shown to chelate extremely strongly to transition metal ions and main group metal ions¹³⁴⁻¹³⁸, including lithium ions¹³⁷. The most promising application is as a chelating ligand for the extraction of uranium from ores¹³⁸. To date there appears to have been only one report in the literature of the use of NIPA in organic chemistry, reporting the use of this ligand as a phase transfer catalyst¹³⁹.

Despite the promise of NIPA to be a strong ligand suitable to organolithium chemistry, it was found that NIPA was unstable to LDA,

presumably being deprotonated by this strong base, as evidenced by ^{13}C NMR spectra showing the formation of di-*iso*-propylamine and new resonances in the region typical of HMPA and NIPA (~38 ppm). Attempts to add NIPA to solutions of lithiated imine **1** resulted in an initial deposit of a colourless crystalline material which was followed shortly by apparent decomposition yielding a milky brown suspension. This behaviour may possibly be due to high acidity of the ligand, or to an increased reactivity of the lithiated imine when the lithium is chelated by NIPA. Further investigations were not conducted.

Chapter 3: Conclusions

3.1 General Conclusions

A multinuclear NMR approach has been used to elucidate the solution structure of a lithiated imine. From the preceding arguments, it has been concluded that lithiated *N-iso-propyl-acetaldimine* in THF/hexanes solution at -80°C exists as a mixture of two isomeric closed dimeric structures and a triple ion (or open dimer), whose proportions vary with concentration and especially with THF concentration. The closed dimers possess a four membered ring of alternating nitrogen and lithium atoms, and are solvated by two to four THF molecules per lithium, presumably by coordination to the lithium atoms. The results of molecular mechanics calculations are in agreement with the experimental observation that the two dimeric forms are present in equal proportion at -80°C . The triple ion structure possesses one lithium atom serving as a bridge between two nitrogen atoms, and another lithium atom which is not bonded to any nitrogen atoms. Since the triple ion is favoured by high THF concentration, and also by the addition of HMPA or PMDETA, it has been surmised that the "free" lithium of the triple ion is highly solvated. Only under conditions of high HMPA concentration or by the addition of PMDETA are substantial amounts of monomer formed. It

has been determined that di-*iso*-propylamine, the conjugate acid of LDA, does not play a role in the solvation of the lithiated imine.

The product of methylation of the lithiated imine **1** gave greater than 90% *syn* product, although under some conditions a lower ratio of *syn* to *anti* products was formed, presumably due to thermal isomerization resulting from the high exothermicity of the methylation reaction. The proportion of *syn* product appeared not to be affected by the choice of solvent or addition of HMPA, and it has therefore been concluded that ground state aggregate structures are not a determinant of alkylation geometries for this lithiated imine.

The temperature dependent ^{13}C NMR behaviour of lithiated *N*-*iso*-propylpropionaldimine, **3**, was found to be very similar to that of lithiated imine **1** and it was suggested that the solution structures of **3** were similar to those of **1**, except upon addition of HMPA. Upon addition of HMPA to solutions of **3**, a species which is a minor (3%) component in THF/hexanes solutions increased to 20% of the total. This species was found to have a **Z** configuration of the carbon-carbon partial double bond. Methylation of the lithiated imine **3** was found to give 93% *syn* product except in the presence of 2 equivalents of HMPA, in which case the *anti* methylation product was formed in a higher proportion reflecting the proportion of **Z** isomer of the anion. It has therefore been concluded that the species having a **Z** configuration about the carbon-carbon partial double bond has *anti* stereochemistry of the aza-allylic portion of the molecule.

3.2 Comparisons to Similar Molecules in the Literature

The structures of a number of lithiated amines and related lithiated organo-nitrogen molecules which bear structural similarities to lithiated imine **1** have been reported in the literature. These molecules have been found usually to exist as monomers, dimers or occasionally as trimers, or as a mixture of these, where the aggregates possess alternating lithium-nitrogen rings of types similar to those determined for the dimeric structure of **1**.

It is informative that there is a striking similarity between the NMR spectra, and types of species observed, for lithiated *N*-*iso*-propylacetaldimine and lithium *N*-*iso*-propylanilide (reported by Jackman⁴⁰). Both molecules exist as a mixture of a monomer and a triple ion in the presence of 4 equivalents of HMPA. There was also a strong similarity between the solution structures of **1** and lithiated *N*-phenylimine of cyclohexanone⁴², reported by Collum, in that in THF/hydrocarbon solutions the dominant aggregate forms were closed dimers.

Many of the lithiated molecules, including all of the lithiated imines, for which solution or crystal structures have been previously determined possessed a phenyl substituent on nitrogen. It had been shown by Knorr that it is possible for lithium to be bound to nitrogen but also to be π -coordinated to an adjacent partial double bond of the aromatic substituent⁴³. It thus follows that participation of the phenyl substituent may be a factor in determining the nature of the

major species in solution. The similarity now demonstrated among the solution structures of a lithiated N-alkyl acetaldimine, a lithiated N-phenyl ketimine⁴², a lithium N-alkyl anilide⁴² and a variety of lithium amides^{36,37} suggests that the involvement of the phenyl substituent is not a major determinant of solution structures in these lithiated nitrogen compounds.

That strong ${}^6\text{Li}$ - ${}^{15}\text{N}$ coupling was observed in the NMR spectra of both molecules, yet no ${}^{13}\text{C}$ - ${}^6\text{Li}$ coupling was observed in any of the ${}^{13}\text{C}$ or ${}^6\text{Li}$ NMR spectra, demonstrates that the lithium is coordinated only to nitrogen in both lithiated molecules. In *neo*-pentyllithium the ${}^{13}\text{C}$ - ${}^6\text{Li}$ coupling is 8.9 or 14.7 Hz, depending on aggregate structure¹⁶, and in *tert*-butyllithium it ranges from 4.0 to 5.4 Hz²⁵, so similar coupling would be expected if lithium were bound to carbon in the lithiated molecules, except that couplings of this magnitude may not be observable since the ${}^{13}\text{C}$ linewidths of lithiated imine resonances were in the range of 3-6 Hz. Thus it can be suggested that the lithium binds primarily to nitrogen in these cases, and that a description of lithiated imines as N-lithiated enamine-amines may be more appropriate. In other words the resonance structure in which the negative charge of the aza-allylic group lies on nitrogen appears to predominate on the basis of the observed coupling, although the chemical shift of the terminal methylene (66 ppm) is considerably upfield from the expected shift of a terminal methylene of an enamine (~105 ppm)¹⁴⁰.

3.3 Solution Structures vis a vis the Syn- Effect.

One of the reasons for study of the solution structures of lithiated imines is that information may be gained which may help to answer the question of the origin of the *syn*-effect.

NOE difference measurements on lithiated *N*-*iso*-propyl acetalimine have suggested that the *iso*-propyl group may occupy a position *syn* to the terminal methylene in the dominant conformation. The dominant species in 0.67 M solutions of 1 in THF/hexanes solutions are a pair of closed dimers.

The *syn*-effect manifests itself most clearly, and usefully, in the stereochemistry of the first-formed alkylation products. The stereochemistry of the actual reactive species must therefore be that which determines the product stereochemistry. It is beyond the scope of the work presented in this thesis to formulate any conclusions about the nature of the reactive species in alkylation reactions. It may be that the reactive species is not one which is observed under our conditions. Collum has demonstrated that the most reactive species in alkylations of lithiated amines is a mixed adduct or mixed dimer between the lithiated molecule and lithium bromide formed during the course of alkylation with a bromo-alkane⁶⁵. Alternatively, it has been suggested that HMPA generally increases the rate of alkylation reactions^{74,141}; perhaps the more reactive species in the present system is the triple ion, which is favoured by HMPA. Clearly, thorough kinetic measurements are required to investigate this problem.

In all previous discussions in the literature the *syn*-effect

has been regarded as unusual since it appears to possess a sterically unfavourable geometry. This sterically unfavourable geometry is most "apparent" when lithiated aldimines are drawn using conventional organic chemistry formalisms showing the aza-allylic backbone of the anion and either an unsolvated lithium atom bound to nitrogen or a free lithium ion. The results of the work presented in this thesis demonstrate that aggregation and solvation of the lithium are important structural features which have been generally neglected in previous treatments. When one considers the volume of the solvated lithium or of the other half of an aggregate compared to the bulk of the organic substituent on nitrogen in lithiated aldimines, the *syn* orientation of the organic substituent relative to the aza-allylic portion of the molecule becomes less surprising. In the case of most lithiated aldimines the *syn*-effect is observed, but one of the few cases in which *anti* stereochemistry predominates is in lithiated imines with the bulky *tert*-butyl substituent on nitrogen. For aldimines it is tempting to suggest that the *syn*-effect may be the result simply of competing steric influences which place the smaller group, typically the alkyl substituent on nitrogen, in the *syn* position, but in ketimines the *syn* and *anti* positions are approximately equally hindered. Thus evidence has been presented supporting an explanation of the origin *syn*-effect in lithiated aldimines resulting from the larger bulk of the solvated lithium or aggregated lithium compared to the bulk of the substituent on nitrogen, but any explanation of the *syn*-effect must be compatible with the behaviour of lithiated ketimines.

3.4 Suggestions for Further Research.

The most pressing problem presented is the determination of the nature of the reactive species in alkylation reactions of lithiated imines, which would require a study of the kinetics of the reaction. In the case of alkylation of lithiated *N*-iso-propylacetaldimine with methyl iodide the reaction appears to be instantaneous at -78°C , precluding investigation by NMR. Either the study of a slower reaction by NMR, possibly using a different leaving group on the electrophile or a less reactive electrophile, the use of fast-injection NMR techniques¹⁴², or the incorporation of a chromophore on the imine which is sensitive to alkylation to allow photometric study, would facilitate kinetic measurements. Infrared spectroscopy has also been introduced in recent years as a probe of aggregation of lithiated molecules¹⁴³, and may eventually find wider applications in organolithium chemistry.

Chapter 4: Experimental

4.1. General Procedures and Materials.

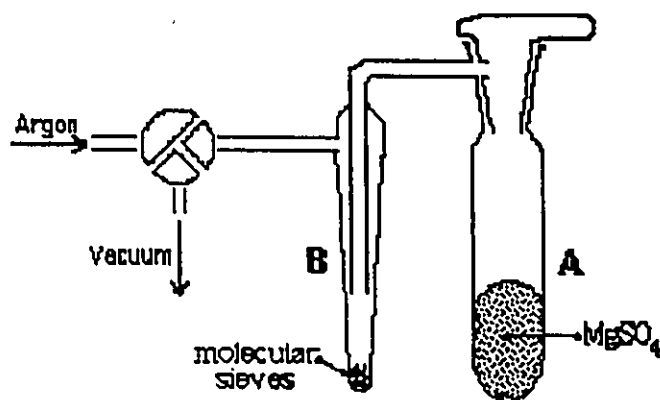
All chemicals were purchased from Aldrich, unless otherwise specified. Except where specified otherwise, all solvents were dried prior to use by distillation from sodium/benzophenone under an atmosphere of dry nitrogen¹¹⁸, and all reactions and manipulations were conducted under a positive pressure of argon. All glassware was flame-dried under vacuum, except for NMR tubes, which were dried for 24 h at 100°C then filled with argon while hot, and syringes, which were dried for 24 h at 100°C then cooled in a desiccator lined with dry silica (Drierite[®]).

4.2 Imine Synthesis

Aldimines were synthesised by stoichiometric reaction of the aldehyde and the primary amine⁸⁸. Acetaldehyde, propionaldehyde and *iso*-butyraldehyde were used without purification and the amines (*iso*-propylamine, *tert*-butylamine) were dried and purified by distillation from KOH in an inert atmosphere. The apparatus used for the reaction is shown in Figure 35. The vessel was flame dried at 0.1 mm Hg prior to use. The amine (0.06 moles) and then the aldehyde (0.06 moles) were added to 5g of MgSO₄ at -78°C in bulb A, which was accessible by removal of the tap stopper at the top of bulb A,

while passing a stream of argon through the vessel shown in Figure 35. After 10 minutes the reaction mixture was allowed to warm to room temperature and was then distilled to bulb B where it was trapped over 4 Å molecular sieves at liquid N₂ temperature.

Figure 35: Apparatus for aldimine preparation



The yields were typically 50% to 70% of imine which was >95% pure by ¹H NMR, the impurities being unreacted aldehyde or amine arising from inexact mixing of the reactants. The imines were stored at -10 °C under argon, and were used within 24 h of preparation. NMR data for the aldimines are shown in Table 10.

Table 10:
 ^1H and ^{13}C NMR Data for Imines

<u>Imine</u>	<u>Proton Shifts^a (δ ppm)</u> <u>and Couplings</u>	<u>Carbon Shifts^b (δ ppm)</u>
<i>N-iso-propyl-</i> <i>acetaldimine</i>	7.62 ppm (q) J= 4 Hz (1H)	157.5, 62.9, 25.5, 23.0
	3.25 ppm (m) J= 6 Hz (1H)	
	1.74 ppm (d) J= 4 Hz (3H)	
	1.07 ppm (d) J= 6 Hz (6H)	
<i>N-tert-butyl-</i> <i>acetaldimine</i>	7.8 ppm (q) J= 5 Hz (1H)	154.8, 57.8, 30.7, 23.6
	2.0 ppm (d) J= 5 Hz (3H)	
	1.2 ppm (s) (9H)	
<i>N-iso-propyl-</i> <i>propionaldimine</i>	7.52ppm (t) J=5.4 Hz (1H)	162.4, 63.2, 30.6, 25.8, 11.5
	3.22 ppm (m) J= 6.5 Hz (1H)	
	2.20 ppm (m) (2H)	
	1.25 ppm (t) J= 6.8 Hz (3H)	
	1.05ppm (d) J= 6.5 Hz (6H)	
<i>N-iso-propyl-iso-</i> <i>-butyraldimine</i>	7.45 ppm (d) J= 5.6 Hz (1H)	166.9, 62.8, 35.2, 25.4, 20.3
	3.20 ppm (m) J= 6.3 Hz (1H)	
	2.38 ppm (m) (1H)	
	1.20 ppm (d) J= 5.4 Hz (6H)	
	1.03 ppm (d) J= 6.8 Hz (6H)	

^a CDCl_3 solvent ^b THF solvent

4.3 Preparation of Lithiated Imine NMR Samples

The lithiated imines were prepared under argon at -78°C by deprotonation of the imine by LDA, using a 5% to 10% excess of LDA. All solvents [THF (BDH), toluene (Fisher), hexanes (Fisher), diethyl ether (Fisher)] were freshly distilled from sodium/benzophenone prior to use. Di-*iso*-propylamine was used without further purification except that it was stored under an inert atmosphere over 4Å molecular sieves. LDA was prepared by deprotonation of a solution of di-*isopropylamine* with 2.5 M n-butyllithium in hexanes (Aldrich), which was titrated against 2,5-dimethoxybenzyl alcohol¹⁴⁴ prior to use.

The lithiated imine samples were prepared in 10mm NMR tubes fitted to accept a screw cap. Typically, the tube was dried at 100°C and then filled with argon and capped with a septum. The tube was then placed under a positive pressure of argon via a needle to a gas line and cooled to -78°C . Solvents and di-*iso*-propylamine were added via syringe. To the cold NMR tube was then added an amount of 2.5 M n-butyllithium equimolar to the di-*iso*-propylamine and the tube was agitated to mix the reagents. After 10 minutes the imine was added, and the tube was again agitated, warmed briefly to room temperature and then re-cooled. Any additives such as hexamethylphosphoramide (HMPA), pentamethyldiethylenetriamine (PMDETA (K&K Laboratories)) or tetramethylethylenediamine (TMEDA)

were added via syringe at this time. The sample was then sealed by wrapping the septum top generously with Parafilm[®]. The sample was stored at -78°C until NMR measurements were conducted.

Resultant volumes in a standard lithiated imine sample prepared by the method described above are as follows: 2.2 ml THF, 0.43 ml di-*iso*-propylamine, 1.2 ml butyllithium in hexanes and 0.32 ml of N-*iso*-propylacetaldimine. This resulted in a total volume of 4.15 ml of a 0.67 M solution. Addition of HMPA or PMDETA resulted in dilution of the sample. One equivalent of HMPA had a volume of 0.5 ml and one equivalent of PMDETA had a volume of 0.61 ml.

Samples prepared by direct deprotonation of the imine with *sec*-butyllithium were prepared similarly, except that the *sec*-butyllithium (1.7M in ether) was added to a solution of the imine in THF.

4.4 Preparation of Doubly Labelled NMR Samples

¹⁵N and ⁶Li doubly labelled samples were prepared in a manner similar to natural abundance samples except that they were prepared on 1/4 scale in a small flask, then transferred via cannulae to argon filled 5mm NMR tubes which were fitted with a tap to allow either an argon flow or evacuation of the tube. The doubly labelled samples were then frozen at liquid nitrogen temperature, evacuated to 0.1 mm Hg and flame sealed.

¹⁵N-*iso*-propylacetaldimine was prepared by the method used for natural abundance acetaldimines, using ¹⁵N-*iso*-propylamine (MSD Isotopes-custom synthesis).

⁶Li-Butyllithium was prepared by reaction of BuCl with Li metal¹⁴⁵. 0.5g Lithium-6 metal (98% isotopic purity, Cambridge Isotope Laboratories) was washed with pentane and then pounded, in the ambient atmosphere, with a steel hammer and anvil into a thin foil (~1mm thick) in the presence of 10 mg sodium metal. The steel implements were polished prior to use in order to reduce the risk of introducing rust into the lithium, which would be a paramagnetic impurity in NMR samples. The foil was cut to ~60mm² flakes and placed in an argon-filled flask containing 50ml dry ethyl ether, and cooled to -78°C. To the lithium was added 0.6 mole equivalents of 1-chlorobutane (BDH) dropwise. The reaction was stirred magnetically for 24 h, during which time the reaction was allowed to warm to room temperature. The ether was then removed under vacuum, and the sample pumped at 0.1 mmHg for 1 h to remove ether and remaining 1-chlorobutane. The butyllithium was dissolved in 10ml of dry pentane and filtered through a fritted glass filter, using standard Schlenk-type methods. The filtrate was reduced in volume to ~6 ml, and was found to have a concentration of 3.3 M, as determined by titration with 2,5-dimethoxybenzyl alcohol.

It was found that this method was superior to other methods involving reaction of either dibutylmercury or 1-bromobutane with lithium. The butyllithium prepared by either of these methods was found to be difficult to separate from the inorganic residues.

4.5 Alkylation Reactions

0.12 M Solutions of lithiated imines were alkylated in 10mm NMR tubes by addition of 1.2 equivalents of iodomethane. Methyl iodide was cooled to near its freezing point (-64°C) and then a portion of it was repeatedly drawn into a syringe in order to cool the syringe. An appropriate amount of methyl iodide was withdrawn into the syringe and was added dropwise to a septum-capped NMR tube containing the lithiated imine at -78°C, accompanied by agitation of the NMR tube. The NMR tube was then sealed with Parafilm[®] and immediately (<3 minutes) transferred to the NMR probe at -78°C for NMR spectral acquisition.

0.67 M Solutions of lithiated imines were lithiated as described above except that the reactions were conducted in flasks accompanied by vigorous stirring and then were transferred via a cannulus to the precooled NMR tube. The NMR tube was then sealed with Parafilm[®] and immediately (<3 minutes) transferred to the NMR probe at -78°C for NMR spectral acquisition.

4.6 General NMR Methods

All NMR measurements were conducted using a Varian XL-300 instrument, using the parameters listed in Table 11.

Except for lithiated imine samples, proton spectra were referenced to the residual ¹H signal of CDCl₃ (δ 7.24 ppm) and ¹³C spectra were referenced to CDCl₃ (δ 77.0 ppm). For lithiated imines the spectra were referenced to THF (¹H_(C1) δ 3.58 ppm; ¹³C_(C1) δ 69

ppm). ^6Li Spectra were referenced externally to 1M LiCl (δ 0 ppm) in D_2O at 20°C, and ^{15}N spectra were referenced externally to ^{15}N -aniline (δ 0 ppm) at 20°C. ^{31}P Spectra were referenced externally to 85% H_3PO_4 (δ 0 ppm) in D_2O .

Table 11

NMR Acquisition Parameters

<u>Nucleus</u>	<u>Decoupling</u>	<u>Sweep Width</u>	<u>Pulse Width</u>	<u>AT*</u>	<u>FRT†</u>
^1H	none	4000Hz	30°	1s	1s
^{13}C	{ ^1H }	16500Hz	30°	0.9s	0.9s
^6Li	{ ^1H }	2200Hz	30°	6.6s	6.6s
^{15}N	{ ^1H }§	15000Hz	30°	1s	2s
^{31}P	{ ^1H }	10000Hz	30°	1s	1s

* acquisition time † repetition rate

§ decoupling during acquisition only

Determination of peak areas was done either by standard integration or by using a curve-fitting program available from the spectrometer software¹²³. In general, the relative peak areas for all ^1H , ^{31}P and ^{15}N spectra, and ^{13}C spectra exhibiting only sharp anion signals were determined using standard integration, while for all ^6Li spectra and ^{13}C spectra exhibiting broad signals, curve fitting was

used. Typical 0.67 M anion samples in 10mm NMR tubes required 512 or 1024 transients to obtain an acceptable signal/noise ratio in the ^{13}C spectrum. ^6Li samples required 32 or 64 transients to obtain a signal/noise ratio of 50. ^{15}N spectra required about 1024 transients and ^{31}P spectra required 32.

^{13}C spectra were Fourier transformed with 1 Hz line-broadening, and no line-broadening was used for other nuclei. Typical solvent linewidths in ^{13}C spectra at -80°C , with line-broadening added, were in the range of 3 to 5 Hz. Similar line-widths were measured for typical sharp ^6Li NMR signals.

The temperature of the NMR probe was regulated using the internal temperature controller of the instrument, and each probe was calibrated using an iron constantin thermocouple placed in an acetone-filled NMR tube in the probe and referenced to 0°C . The solvent-filled tube was meant to approximate the NMR sample. The temperature was allowed to equilibrate 10 minutes, with the proton decoupler activated when calibrating probes other than the proton probe. An uncertainty whose magnitude is not known in both the accuracy and precision of the calibration may arise from temperature gradients within the sample. A further uncertainty in the precision of the temperature calibration due to the instability of the temperature controller can be estimated to be $\pm 1^\circ\text{C}$. Low temperature samples were not allowed to spin, since the spinning rate was found to be irregular at low temperature due to accumulated condensation and ice.

NOE-Difference spectra were acquired by irradiation of one set of protons during the pre-acquisition period, following standard

methods described in the NMR instrument manual^{114,146}. The pre-aquisition period was set at 30s. Samples of lithiated imine used for the NOE-difference experiments were prepared in the usual manner, but in a flask, then the solution was evaporated to dryness under vacuum and pumped for 1 hr at + 20°C in an attempt to remove as much of the solvent and di-*iso*-propylamine as possible. The lithiated imine was then redissolved in THF-D₈ (MSD Isotopes 99.8% D) and transferred via a cannula to the NMR tube. Samples of imines used for the NOE-difference experiments were prepared as ~5% solutions in CDCl₃ (MSD Isotopes 99.8% D) and were degassed by a series of freeze-thaw cycles at 1 mmHg.

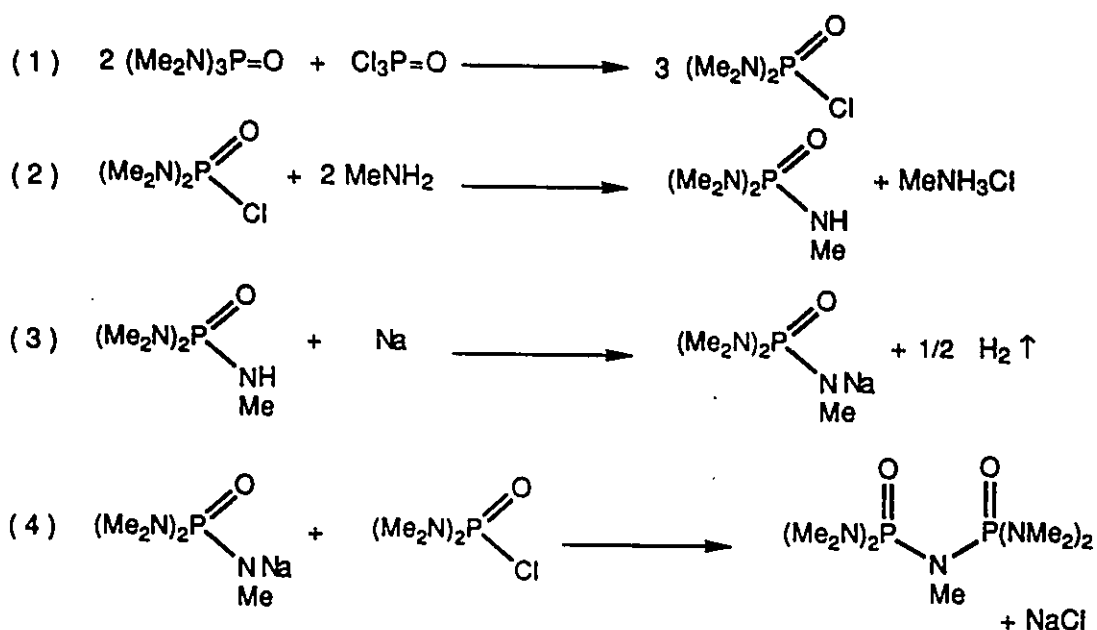
Relaxation times of ¹³C nuclei were measured using the inversion-recovery (180°-τ-90°-t) method^{122,146}. At least nine τ-values were selected, and the T₁ was calculated using a three parameter curve-fitting program supplied with the XL-300 software. NOE Measurements were conducted according to the gated coupling method^{122,146} by comparing signal heights of spectra acquired with NOE enhancement to those acquired with NOE suppression. During either the T₁ or the NOE experiment, acquisition of the series of spectra required for the experiment was done using an interleaving of the acquisitions.

Uncertainty in the T₁ measurements arises from the uncertainty in determining signal heights at each of the τ values and from the uncertainty arising from the three-parameter curve-fitting performed by the computer. The uncertainty of the curve-fit is determined by the computer and reported in its output. The uncertainty in peak heights is not taken into consideration by the

computer program, so the uncertainty in peak heights must be estimated: it was arbitrarily set at $\pm 10\%$.

4.7 Synthesis of "NIPA" Ligand

Nonamethylimidodiphosphoramidate (NIPA) was synthesized by the method partially described by Delpuech et al.¹³⁷. The sequence of reactions for the preparation of NIPA is shown below.



Reaction (1)¹⁴⁷

In a round bottom flask 110g (0.61 moles) of hexamethylphosphoramidate (HMPA) was heated to 100°C under an argon atmosphere, then 46g (0.30 moles) of phosphorusoxychloride (POCl_3)

was added rapidly with vigorous stirring with a magnetic stir-bar and the vessel was fitted with a reflux condenser. Initially a solid yellow-orange product was formed, but as the reaction was heated to 150°C the solid melted. Heating at 150°C was continued for 18 hours, and then the product was fractionally distilled at 2 mmHg pressure. The initial distillate was a mixture of HMPA and POCl₃, having boiling points below 100°C at this pressure. The product, bis(dimethylamino)phosphorusoxychloride (PCl), distilled as a colourless liquid having a boiling range of 100-120°C at 2-5 mmHg (lit. 110°C at 20mmHg)¹⁴⁷ Yield: 123g (78%); ¹H NMR: δ 2.71 (d) J_{P-H} = 12.8 Hz; M.S. (m/z): M⁺ = 172, 170

Reaction (2)

A sample of 85g (0.5 moles) of PCl was dissolved in 1l of anhydrous diethylether, and methylamine was bubbled through the solution. The methylamine was generated by reaction of methylaminehydrochloride (100g, 0.5 moles) with a two-fold excess of KOH in 500 ml pyridine. The methylamine was evolved with the aid of mild heating (~40°C) and forced to pass through the solution of PCl by a gentle flow of argon. The reaction was allowed to continue for 24 hours, after which time no more bubbles were evolving from the methylamine source and a white precipitate (presumably NaCl) was deposited in the flask containing the ether solution of PCl. The precipitate was rapidly removed by filtration through cotton wool in an ambient atmosphere. The ether was distilled out of the vessel under argon, the residue transferred to a smaller flask and fractionally distilled at 0.1 mmHg. Initial fractions containing PCl

were discarded, and the desired product, pentamethylphosphoramidate (PN) was distilled as a viscous, colourless oil at 110-120°C. Yield: 70g (84%), $^1\text{H NMR}$: δ 2.46 ppm (d) $J_{\text{P-H}} = 9.2$ Hz, M.S. (m/z): $M^+ = 165$ (calc.=165 M.U.)

Reactions (3) & (4)

A sample of 24g (0.15 moles) of PN was dissolved in 700ml dry petroleum ether (boiling range: 100-120°C, (BDH)) in a 1l round bottom flask under an atmosphere of argon. To this solution was added 3.6g (0.16 moles) of sodium metal (reaction 3). The reaction was heated to reflux, at which point the sodium was molten and finely divided by vigorous stirring with a magnetic stir-bar. Reflux was continued for 48 hours, during which time all but 0.5g (.02 moles) of sodium was consumed. The unreacted sodium was removed using tweezers, then the solution was cooled to 0°C, resulting in solidification of the mixture as a white gel. To the cool gel was added 25g (0.15 moles) of PCl during 5 minutes (reaction 4). A fairly vigorous exothermic reaction was immediately apparent during the addition of PCl. The reaction was left to stir at 20°C for 24 hours, then the solvent was removed by distillation under argon followed by pumping at 0.1 mmHg at 20°C. The desired product was the second fraction obtained by fractional distillation at 0.1 mmHg, the first fraction being a mixture of solvent and reactants. The product, nonamethylimidodi-phosphoramidate (NIPA) was distilled as a pale yellow oil (b.p. 120-140°C at 0.1 mmHg: lit. 124-126°C at 0.1 mmHg^{135,148}) which solidified upon cooling. The product was then recrystallized from cyclohexane to yield waxy white flakes, m.p.

63.8-65.2°C (lit. 58°C^{135,148}). NIPA is extremely deliquescent and must be manipulated in a dry, inert atmosphere, and should be considered highly toxic and carcinogenic. The ¹H NMR spectrum showed only traces of residual cyclohexane and no water. Yield: 15g (35%); ¹H NMR: δ 2.73 t (J=9.7 Hz) 3H, δ 2.66 d (J=9.6 Hz) 24H [lit. δ 2.76 t (J=9.62 Hz), δ 2.69 d (J=9.55 Hz)¹⁴⁹] ; M.S. (m/z): exact mass= 299.165 ± .003 (calc=299.164).

References

- 1) K.A. Lutomski, A.I. Meyers, in *Asymmetric Synthesis*, p. 263 ff., vol.3, J.D. Morrison, ed., Academic Press, New York (1984)
- 2) K. Tomioka, K. Koga, in *Asymmetric Synthesis*, p. 202 ff., vol.2, J.D. Morrison, ed., Academic Press, New York (1984)
- 3) An example of an enolate equivalent other than those possessing C=N are α -haloeneamines: L. Ghosez in *Organic Synthesis*, B.M. Trost, C.R. Hutchinson, eds., Pergamon Press, Oxford, p 145 ff, (1980)
- 4) R.R. Fraser, in *Comprehensive Carbanion Chemistry*, p. 65 ff., E. Bunce, T. Durst, ed., Elsevier (1984)
- 5) H.O. House, B.M. Trost, *J. Org. Chem.*, **30**, 1341 (1965)
- 6) H.O. House, M. Gall, H.D. Olmstead, *J. Org. Chem.*, **36**, 2361 (1971)
- 7) R.R. Fraser, N. Chuaqui-Offermanns, *Can. J. Chem.*, **59**, 3007 (1981)
- 8) J.K. Smith, D.E. Bergbreiter, M. Newcomb, *J. Am. Chem. Soc.*, **105**, 4396 (1983)
- 9) J.K. Smith, D.E. Bergbreiter, M. Newcomb, *J. Org. Chem.*, **46**, 3157 (1981)
- 10) J.W. Ludwig, M. Newcomb, D.E. Bergbreiter, *J. Org. Chem.*, **45**, 4666 (1980)
- 11) R.R. Fraser, J. Banville, *J. Chem. Soc. Chem. Comm.*, 47 (1979)

- 12) R.R. Fraser, F. Akiyama, J. Banville, *Tetrahedron Lett.*, 3929 (1979)
- 13) R. Amstutz, W.B. Schweizer, D. Seebach, J.D. Dunitz, *Helv. Chim. Acta*, **64**, 2617 (1981)
- 14) D. Seebach, R. Amstutz, J.D. Dunitz, *Helv. Chim. Acta*, **64**, 2622 (1981)
- 15) L.M. Jackman, B.C. Lange, *J. Am. Chem. Soc.*, **103**, 4494 (1981)
- 16) G. Fraenkel, W.R. Winchester, *J. Am. Chem. Soc.*, **111**, 3794 (1989)
- 17) T.F. Bates, M.T. Clarke, R.D. Thomas, *J. Am. Chem. Soc.*, **110**, 5109 (1988)
- 18) W. Bauer, W.R. Winchester, P. v. R. Schleyer, *Organometallics*, **6**, 2371 (1987)
- 19) W. Bauer, D. Seebach, *Helv. Chim. Acta*, **67**, 1972 (1984)
- 20) (a) H. Günther, D. Moskau, P. Bast, D. Schmalz, *Angew. Chem. Int. Ed. Eng.*, **26**, 1212 (1987); (b) P.v.R. Schleyer, *Pure and App. Chem.*, **56**, 151 (1984)
- 21) (a) W. Moene, M. Vos, F.J.J de Kauter, G.W. Klumpp, A.L. Spek, *J. Am. Chem. Soc.*, **111**, 3463 (1989); (b) M. Vos, F.J.J. de Kanter, M. Schakel, N.J.R. van Eikma Hommes, G.W. Klumpp, *J. Am. Chem. Soc.*, **109**, 2178 (1989)
- 22) T. Thoennes, E. Weiss, *Chem. Ber.*, **111**, 3157 (1978)
- 23) S. Brownstein, S. Bywater, D.J. Worsfold, *J. Organometallic Chem.*, **199**, 1 (1980)
- 24) J. Heinzer, J.F.M. Oth, D. Seebach, *Helv. Chim. Acta*, **68**, 1848 (1985)

- 25) R.D. Thomas, M.T. Clarke, R.M. Jensen, T.C. Young,
Organometallics, **5**, 1851 (1986)
- 26) G. Fraenkel, M. Henrichs, J.M. Hewitt, B.M. Su, M.J. Geckle, J. Am.
Chem. Soc., **102**, 3345 (1980)
- 27) G. Fraenkel, M.P. Hallden-Abberton, J. Am. Chem. Soc., **103**,
5657 (1981)
- 28) L.M. Jackman, R.C. Haddon, J. Am. Chem. Soc., **95**, 3687 (1973)
- 29) J.Q. Wen, J.B. Grützner, J. Org. Chem., **51**, 4220 (1986)
- 30) T. Laube, J.D. Dunitz, D. Seebach, Helv. Chim. Acta, **68**, 147,
(1985)
- 31) L.M. Jackman, N.M. Szeverenyi, J. Am. Chem. Soc., **99**, 4954
(1977)
- 32) H.O. House, A.V. Prabhu, W.V. Phillips, J. Org. Chem., **41**, 1209
(1976)
- 33) P. Strazewski, C. Tamm, Helv. Chim. Acta, **69**, 1041 (1986)
- 34) D. Barr, W. Clegg, R.E. Mulvey, R. Snaith, J. Chem. Soc. Chem.
Comm., 285 (1984)
- 35) D. Reed, D. Barr, R.E. Mulvey, R. Snaith, J. Chem. Soc. Dalton
Trans., 557 (1986)
- 36) A.S. Galiano-Roth, E.M. Michaelides, D.B. Collum, J. Am. Chem.
Soc., **110**, 2658 (1988)
- 37) J.S. DePue, D.B. Collum, J. Am. Chem. Soc., **110**, 5518 (1988)
- 38) A.S. Galiano-Roth, D.B. Collum, J. Am. Chem. Soc., **111**, 6772
(1989)
- 39) L.M. Jackman, L.M. Scaramoutzos, J. Am. Chem. Soc., **109**, 5348
(1987)

- 40) L.M. Jackman, L.M. Scaramoutzos, W. Porter, *J. Am. Chem. Soc.*, **109**, 6524 (1987)
- 41) R.A. Wanat, D.B. Collum, G. Van Duyne, J. Clardy, R.T. DePue, *J. Am. Chem. Soc.*, **108**, 3415 (1986)
- 42) N. Kallman, D.B. Collum, *J. Am. Chem. Soc.*, **109**, 7466 (1987)
- 43) H. Dietrich, W. Mahdi, R. Knorr, *J. Am. Chem. Soc.*, **108**, 2462 (1986)
- 44) R. Benken, H. Günther, *Helv. Chim. Acta*, **71**, 694 (1988)
- 45) S. Buchholz, K. Harms, M. Marsch, W. Massa, G. Boche, *Angew. Chem. Int. Ed. Eng.*, **28**, 72 (1989)
- 46) S. Harder, J. Boersma, L. Brandsma, J.A. Kanters, W. Bauer, P.v. R. Schleyer, *Organometallics*, **8**, 1698 (1989)
- 47) T. Maetzke, D. Seebach, *Helv. Chim. Acta*, **72**, 624 (1989)
- 48) R.A. Wanat, D.B. Collum, *J. Am. Chem. Soc.*, **107**, 2078 (1985)
- 49) G. Boche, *Angew. Chem. Int. Ed. Eng.*, **28**, 277 (1989)
- 50) D. Barr, W. Clegg, R.E. Mulvey, R. Snaith, K. Wade, *J. Chem. Soc. Chem. Comm.*, 295 (1986)
- 51) D. Barr, W. Clegg, R.E. Mulvey, R. Snaith, *J. Chem. Soc. Chem. Comm.*, 226 (1984)
- 52) T. Fjeldberg, P.B. Hitchcock, M.F. Lappert, A.J. Thorne, *J. Chem. Soc. Chem. Comm.*, 822 (1984)
- 53) L.M. Jackman, C.W. DeBrosse, *J. Am. Chem. Soc.*, **105**, 4177 (1983)
- 54) D. Enders, G. Bachstädter, K.A.M. Kremer, M. Marsch, K. Harms, G. Boche, *Angew. Chem. Int. Ed. Eng.*, **27**, 1552 (1988)
- 55) A.S. Galiano-Roth, D.B. Collum, *J. Am. Chem. Soc.*, **110**, 3546 (1988)

- 56) L.M. Englehardt, A.S. May, C.L. Raston, A.H. White, J. Chem. Soc. Dalton Trans., 1671 (1983)
- 57) D. Seebach, W. Bauer, J. Hansen, T. Laube, W.B. Schweizer, J.D. Dunitz, J. Chem. Soc. Chem. Comm., 853 (1984)
- 58) G. Boche, M. Marsch, K. Harms, Angew. Chem. Int. Ed. Eng., **25**, 373 (1986)
- 59) D. Barr, W. Clegg, R.E. Mulvey, R. Snaith, J. Chem. Soc. Chem. Comm., 79 (1984)
- 60) D. Colgan, R.I. Papasergio, C.L. Raston, A.H. White, J. Chem. Soc. Chem. Comm., 1708 (1984)
- 61) D. Barr, W. Clegg, R.E. Mulvey, R. Snaith, J. Chem. Soc. Chem. Comm., 469 (1984)
- 62) D. Barr, W. Clegg, R.E. Mulvey, R. Snaith, K. Wade, J. Chem. Soc. Chem. Comm., 700 (1984)
- 63) G. Wilkinson, ed., *Comprehensive Organometallic Chemistry*, Vol.1, Chapter 2, Pergamon Press, Oxford, (1982)
- 64) G. Fraenkel, W.R. Winchester, J. Am. Chem. Soc., **111**, 3794 (1989)
- 65) J.S. DePue, D.B. Collum, J. Am. Chem. Soc., **110**, 5524 (1988)
- 66) M.J. Kaufman, A.J. Streitwieser, Jr., J. Am. Chem. Soc., **109**, 6092 (1987)
- 67) D.R. Armstrong, D. Barr, W. Clegg, R.E. Mulvey, D. Reed, R. Snaith, J. Chem. Soc. Chem. Comm., 869 (1986)
- 68) D. Barr, M.J. Doyle, R.E. Mulvey, P.R. Raithby, D. Reed, R. Snaith, D.S. Wright, J. Chem. Soc. Chem. Comm., 318 (1989)
- 69) G. Boche, K. Harms, M. Marsch, J. Am. Chem. Soc., **110**, 6925 (1988)

- 70) R. Hacker, E. Kaumann. P.v. R. Schleyer, W. Mahdi, H. Dietrich, *Chem. Ber.*, **120**, 1533 (1987)
- 71) D.B. Collum, D. Kahne, S.A. Gut, R.T. DePue, F. Mohamadi, R.A. Wanat, J. Clardy, G. Van Duyne, *J. Am. Chem. Soc.*, **106**, 4865 (1985)
- 72) D.R. Armstrong, D. Barr, W. Clegg, S.M. Hodgson, R.E. Mulvey, D. Reed, R. Snaith, D.S. Wright, *J. Am. Chem. Soc.*, **111**, 4719 (1989)
- 73) D.R. Armstrong, D. Barr, R. Snaith, W. Clegg, R.E. Mulvey, K. Wade, D. Reed, *J. Chem. Soc. Dalton Trans.*, 1071 (1987)
- 74) H. Normant, *Angew. Chem. Int. Ed. Eng.*, **6**, 1046 (1967)
- 75) T. Maetzke, D. Seebach, *Helv. Chim. Acta*, **72**, 624 (1989)
- 76) D. Barr, R. Snaith, W. Clegg, R.E. Mulvey, K. Wade, D. Reed, *J. Chem. Soc. Dalton Trans.*, 2141 (1987)
- 77) R. Snaith, Cambridge University, personal communication
- 78) B. Centinkaya, P.B. Hitchcock, M.F. Lappert, M.C. Misra, A.J. Thorne, *J. Chem. Soc. Chem. Comm.*, 149 (1983)
- 79) S.M. Bachrach, J.P. Ritchie, *J. Am. Chem. Soc.*, **111**, 3134 (1989)
- 80) M.E. Jung, T.J. Shaw, *Tetrahedron Lett.*, 3305 (1977)
- 81) M. Jung, T.J. Shaw, R.R. Fraser, J. Banville, K. Taymaz, *Tetrahedron Lett.*, 4149 (1979)
- 82) A. Hosomi, Y. Araki, H. Sakurai, *J. Am. Chem. Soc.*, **104**, 2081 (1982)
- 83) R.R. Fraser, J. Banville, K.L. Dhawan, *J. Am. Chem. Soc.*, **100**, 7999 (1978)
- 84) D. Wurmb-Gerlich, F. Vogtle, A. Mannschreck, H.A. Staab, *Justus Liebigs Ann. Chem.*, **708**, 36 (1967)

- 85) N.P. Marullo, E.H. Wagener, *Tetrahedron Lett.*, 2559 (1969)
- 86) W.B. Jennings, D.R. Boyd, *J. Am. Chem. Soc.*, **94**, 7187 (1972)
- 87) C.G. McCarty, in *Chemistry of the Carbon-Nitrogen Double Bond*, Chapter 9, Saul Patai, ed., Wiley-Interscience, U.K., (1970)
- 88) R.R. Fraser, J. Banville, F. Akiyama, N. Chuaqui-Offermans, *Can. J. Chem.*, **59**, 705 (1981)
- 89) R.R. Fraser, M. Bresse, N. Chuaqui-Offermans, K.N. Houk, N.G. Rondan, *Can. J. Chem.*, **61**, 2729 (1983)
- 90) J.Y. Lee, T.J. Lynch, D.T. Mao, D.E. Bergbreiter, M. Newcomb, *J. Am. Chem. Soc.*, **103**, 6215 (1981)
- 91) (a) H. Winnerström, S. Forsén, Björn Roos, *J. Phys. Chem.*, **76**, 2430 (1972); (b) G.I.L. Jones, D.G. Lister, N.L. Owen, M.C.L. Gerry, P. Palmieri, *J. Mol. Spect.*, **60**, 348 (1976)
- 92) P. Salomaa, P. Nissi, *Acta Chim. Scand.*, **21**, 1386 (1967)
- 93) M. Schlosser, J. Hartmann, *J. Am. Chem. Soc.*, **98**, 4674 (1976)
- 94) P.v. R. Schleyer, J.D. Dill, J.A. Pople, W.J. Hehre, *Tetrahedron Lett.*, 2497 (1977)
- 95) (a) S. Bank, *J. Am. Chem. Soc.*, **87**, 3245 (1965); (b) S. Bank, A. Schriesheim, C.A. Rowe, Jr., *J. Am. Chem. Soc.*, **87**, 3244 (1965)
- 96) J.R. Larson, N.D. Epiotis, F. Bernardi, *J. Am. Chem. Soc.*, **100**, 5713 (1978)
- 97) N.D. Epiotis, D. Bjorkquist, L. Bjorkquist, S. Sarkanen, *J. Am. Chem. Soc.*, **95**, 7558 (1973)
- 98) R.R. Fraser, K.L. Dhawan, *J. Chem. Soc. Chem. Comm.*, 674 (1976)
- 99) K.N. Houk, R.W. Strozier, N.G. Rondan, R.R. Fraser, N. Chuaqui-Offermans, *J. Am. Chem. Soc.*, **102**, 1426 (1980)

- 100) R.J. Elliot, W.G. Richards, *J. Chem. Soc. Perkin Trans. II*, 1005 (1982)
- 101) R. Glaser, A. Streitwieser Jr., *J. Am. Chem. Soc.*, **111**, 7340 (1989)
- 102) R.R. Fraser, N. Chuaqui-Offermanns, K.N. Houk, N.G. Rondan, *J. Organometallic Chem.*, **206**, 131 (1981)
- 103) G. Fraenkel, W.R. Winchester, *J. Am. Chem. Soc.*, **110**, 8720 (1988)
- 104) E.D. Becker, *High Resolution NMR*, Academic Press, New York, (1980)
- 105) E. Breitmaier, W. Voelter, *Carbon-13 NMR Spectroscopy*, VCH Verlagsgesellschaft, Weinheim, (1987)
- 106) A. Steigel in *Dynamic NMR Spectroscopy (NMR: Basic Principles and Progress, vol.15)*, P. Diehl, E. Fluck, R. Kosfeld, eds., Springer-Verlag, Berlin, (1978)
- 107) A.E. Derome, *Modern NMR Techniques for Chemistry Research*, Pergamon Press, Oxford, (1987)
- 108) H. Kessler, *Angew. Chem. Int. Ed. Eng.*, **9**, 219 (1970)
- 109) R.R. Fraser, J.-L. A. Roustan, J.R. Mahajan, *Can. J. Chem.*, **57**, 2239 (1979); For another semi-empirical treatment see H. Shanan-Atidi, K.H. Bar-Eli, *J. Phys. Chem.*, **74**, 961 (1970)
- 110) G.C. Levy, *Acc. Chem. Res.*, **6**, 161 (1973)
- 111) T.D. Alger, D.M Grant, J.R. Lyeria, *J. Phys. Chem.*, **75**, 2539 (1971)
- 112) R.K. Harris, *Nuclear Magnetic Resonance Spectroscopy*, Longman Scientific and Technical, U.K., (1986)

- 113) R.A. Bell, J.K. Saunders, in *Topics in Stereochemistry*, N.L. Allinger, E.L. Eliel, eds., Vol. 7, p.1ff, Wiley-Interscience, New York, 1973
- 114) L.D. Hall, J.K.M. Sanders, *J. Am. Chem. Soc.*, **102**, 5703 (1980)
- 115) A.I. Meyers, D.R. Williams, G.W. Ericson, S. White, M. Druelinger, *J. Am. Chem. Soc.*, **103**, 3081 (1981)
- 116) Thanks to Professor Edgar Anderson, Imperial College, London for suggesting the mixed lithiated imine experiment.
- 117) V. Gutmann, *The Donor-Acceptor Approach to Molecular Interactions*, Plenum, London (1972); Selected donor numbers: benzene, 0.1; acetone, 17.0; water, 18.0; diethyl ether, 19.2; THF, 20.0; pyridine, 33.1; HMPA, 38.8.
- 118) Ruddick, Bunger, Sakano, *Purification of Organic Solvents, in Techniques in Organic Chemistry*, Interscience, New York (1976)
- 119) R.C. Weast, ed., *Handbook of Chemistry and Physics*, 60th Ed., CRC Press, Boca Raton, (1980)
- 120) H.J. Reich, D.P. Green, N.H. Phillips, *J. Am. Chem. Soc.*, **111**, 3444 (1989)
- 121) The estimated rates at -80°C are based on the measured ΔG^{\ddagger} of $12.5 \text{ kcal mole}^{-1}$ at 266 K for exchange between **1a** and **1b** and a variety of entropy values. Based on $\Delta S^{\ddagger} = 20 \text{ cal mole}^{-1} \text{ K}^{-1}$, $\tau_{\text{ex}} = 300\text{s}$; based on $\Delta S^{\ddagger} = 0 \text{ cal mole}^{-1} \text{ K}^{-1}$, $\tau_{\text{ex}} = 7\text{s}$; based on $\Delta S^{\ddagger} = -30 \text{ cal mole}^{-1} \text{ K}^{-1}$, $\tau_{\text{ex}} = 0.02\text{s}$ at -80°C .
- 122) C. Brevard, P. Granger, *Handbook of High Resolution Multinuclear NMR*, Wiley-Interscience, New York, (1981)

- 123) The curve-fitting program is not standard to the XL-300 software. This Pascal program for Lorentzian line-shape analysis was written for Varian 4000 series spectrometers, and generates Lorentzian curves whose intensity, frequency and line-width can be adjusted to fit the measured spectrum. It was developed by Mr. R. Boyko and Dr. B.D. Sykes, Dept. of Biochemistry, University of Alberta, Edmonton, Alberta.
- 124) D. Barr, W. Clegg, R.E. Mulvey, R. Snaith, *J. Chem. Soc. Chem. Comm.*, 287 (1984)
- 125) R.D. Rogers, J.L. Atwood, R. Gruning, *J. Organomet. Chem.*, **157**, 229 (1978)
- 126) D. Mootz, A. Zinnius, B. Bottcher, *Angew. Chem. Int. Ed. Eng.*, **8**, 378 (1969)
- 127) M.F. Lappert, M.J. Slade, A. Singh, J.L. Atwood, R.D. Rogers, R. Shakir, *J. Am. Chem. Soc.*, **105**, 302 (1983)
- 128) J.B. Grutzner, J.M. Lawlor, L.M. Jackman, *J. Am. Chem. Soc.*, **94**, 2306 (1972)
- 129) L.M. Jackman, L.M. Scaramoutzos, C.W. DeBrosse, *J. Am. Chem. Soc.*, **109**, 5355 (1987)
- 130) N.L. Allinger, Quantum Chemistry Program Exchange, 1982
- 131) U. Burkert, N.L. Allinger, *Molecular Mechanics*, American Chemical Society, Washington D.C., (1982)
- 132) R.R. Fraser, J. Banville, unpublished results
- 133) R.R. Fraser, T.S. Mansour, S. Savard, *J. Org. Chem.*, **50**, 3232 (1985)
- 134) K.P. Lannert, M.D. Joesten, *Inorg. Chem.*, **7**, 2048 (1968)

- 135) M.W.G. DeBolster, W.L. Groenveld, *Rec. Trav. Chim.*, **90**, 687 (1971)
- 136) P.T. Miller, P.G. Lenhert, M.D. Joesten, *Inorg. Chem.*, **11**, 2221 (1972)
- 137) P.R. Rubini, L. Rodehüser, J.-J. Delpuech, *Inorg. Chem.*, **18**, 2962 (1979)
- 138) K. Boloko, A. Courtois, J.-J. Delpuech, E. Elkaim, J. Protas, D. Rinaldi, L. Rodehüser, P.R. Rubini, *J. Am. Chem. Soc.*, **106**, 6333 (1984)
- 139) M. Cossentini, T. Strzalko, J. Seyden-Penne, *Bull. Chim. Soc. Fr.*, 531 (1987)
- 140) R. Knorr, A. Weiss, P. Löw, E. Räßple, *Chem. Ber.*, **113**, 2462 (1980)
- 141) R.R. Fraser, T.S. Mansour, *Tetrahedron Lett.*, 331 (1986)
- 142) (a) J.F. McGarrity, J. Prodolliet, T. Smyth, *Org. Magn. Res.*, **17**, 59 (1981); (b) J.F. McGarrity, C.A. Ogle *J. Am. Chem. Soc.*, **107**, 1805 (1985); (c) J.F. McGarrity, C.A. Ogle, Z. Brich, H.-R. Loosli, *J. Am. Chem. Soc.*, **107**, 1810 (1985)
- 143) T. Strzalko, J. Seyden-Penne, F. Fromet, J. Corset, M.-P. Simonnin, *Can. J. Chem.*, **66**, 391 (1988)
- 144) M.R. Winkle, J.M. Lansinger, R.C. Ronald, *J. Chem. Soc. Chem. Comm.*, 87 (1980)
- 145) E.H. Amonoo-Neizer, R.A. Shaw, D.O. Skovlin, B.C. Smith, *Inorganic Syntheses*, **8**, 20 (1966)
- 146) *XL-Series NMR Spectrometer System: Advanced Operation*, Publication No. 87-146056, Revision B1084, Varian Associates

Inc., Palo Alto, California (1984)

- 147) P.Lester, Chem. Abs., 49 6300g (1955)
- 148) A. Debo, Chem. Abs., 54 24397 (1960)
- 149) G. Hägele, R.K. Harris, M.I.M. Wazeer, R. Keat, J. Chem. Soc. Dalton Trans., 1985 (1974)

Vita

Name: Philip A. Carson

Place of Birth: London, Ontario

Year of Birth: 1961

**Post-Secondary
Education and Degrees:**

The University of Western Ontario
London, Ontario
1979-1984 B.Sc. (Honours Chemistry)

The University of Western Ontario
London, Ontario
1984-1986 M.Sc. (Chemistry)

The University of Ottawa
Ottawa, Ontario
1986-1989 Ph.D. (Chemistry)

Publications:

Philip A. Carson, Paul de Mayo, "Surface Photochemistry: Semiconductor mediated reactions of some 1,2-diarylcyclopropanes.", *Canadian Journal of Chemistry*, **65**, 976 (1987)

Philip A. Carson, Robert R. Fraser, "Aggregation of some lithiated imines.", presented at the Canadian Chemical Conference, June 1989, Victoria, B.C.